2010

Protocol design and optimization for QoS provisioning in wireless mesh networks

Wei Zhou
Iowa State University

Protocol design and optimization for QoS provisioning in wireless mesh networks

by

Wei Zhou

A dissertation submitted to the graduate faculty

in partial fulfillment of the requirements for the degree of

DOCTOR OF PHILOSOPHY

Major: Computer Engineering

Program of Study Committee:
Daji Qiao, Major Professor
Manimaran Govindarasu
Ahmed E. Kamal
Aditya Ramamoorthy
Wensheng Zhang

Iowa State University

Ames, Iowa

2010

TABLE OF CONTENTS

LIST OF TABLES vi

LIST OF FIGURES vii

ACKNOWLEDGMENTS ix

ABSTRACT x

CHAPTER 1. INTRODUCTION AND RESEARCH GOALS 1

1.1 Introduction 1

1.2 Problem statement and research goals 3

1.2.1 High throughput routing metric 3

1.2.2 Fairness provisioning among clients in WMNs 4

1.2.3 Wireless mesh network testbed 5

1.2.4 Network design and capacity optimization 6

1.3 Summary and organization 7

CHAPTER 2. DESIGN OF ROUTING METRIC FOR MRMC WMNs 8

2.1 Introduction and motivation 8

2.2 Problem definition and assumption 9

2.3 Proposed routing metric 9

2.3.1 Adjusted expected transfer delay (AETD) 10

2.3.2 Calculations of ETD and EIA 11

2.3.3 Case study 13

2.4 Performance evaluation 14

2.4.1 Simulation setup 14

2.4.2 Random deployment without obstacles . . . 15
2.4.3 Random deployment with obstacles . . . 20
2.4.4 Summary . . . 20
2.5 Conclusion . . . 21

CHAPTER 3. FAIRNESS PROVISIONING AMONG CLIENTS IN WMNs . . . 23

3.1 Introduction . . . 23
3.2 Issues of the existing fairness notions . . . 26
3.2.1 Limitation of BbF . . . 26
3.2.2 Limitation of TbF . . . 27
3.3 Problem definition . . . 28
3.4 Proposed fairness notion . . . 29
3.4.1 Fulfillment-based fairness (FbF) . . . 29
3.4.2 Examples revisited . . . 29
3.4.3 Optimization algorithms . . . 30
3.5 Performance evaluation . . . 31
3.5.1 Simulation setup . . . 31
3.5.2 Small-scale networks . . . 33
3.5.3 Large-scale networks . . . 34
3.5.4 Summary . . . 35
3.6 Conclusion . . . 35

CHAPTER 4. CYMESH: WIRELESS MESH NETWORK TESTBED AT ISU . . . 37

4.1 Motivation . . . 37
4.2 Related work . . . 38
4.2.1 SRSC testbeds . . . 38
4.2.2 MRMC testbeds . . . 39
4.2.3 Network management in WMNs . . . 40
4.3 Design goals . . . 42
4.4 Design and implementation . . . 43

4.4.1 Overview of CyMesh . . . 43
4.4.2 Platform selection . . . 43
4.4.3 Hardware components . . . 44
4.4.4 Software components . . . 45
4.5 Experimental results, observations and experiences . . . 52
4.5.1 Baseline experiments . . . 52
4.5.2 Deployment and link measurement . . . 57
4.5.3 Routing metric in MRMC networks . . . 60
4.6 Conclusions . . . 63
CHAPTER 5. NETWORK DESIGN AND CAPACITY OPTIMIZATION FOR WMNs . . 65
5.1 Literature survey . . . 65
5.2 Motivation . . . 66
5.3 System models . . . 66
5.3.1 Network architecture . . . 66
5.3.2 Directional antenna and interference model . . . 67
5.4 Problem statement . . . 69
5.4.1 Design objectives . . . 69
5.4.2 Dual-path routing and one-to-one AP-GN association . . . 69
5.5 Joint routing and channel assignment . . . 70
5.5.1 Constructing the auxiliary graph . . . 71
5.5.2 MIP formulation . . . 72
5.6 Performance evaluation . . . 75
5.6.1 Simulation setup . . . 75
5.6.2 Effect of antenna directionality and channel diversity . . . 76
5.6.3 Grid topology . . . 77
5.6.4 Random topology . . . 80
5.7 A heuristic approach to the joint routing and channel assignment problem . . . 82
5.7.1 Distributed algorithm 1 . . . 82

5.7.2 Distributed algorithm 2 84
5.7.3 Performance evaluation 85
5.8 Conclusion 87
CHAPTER 6. SUMMARY 89
BIBLIOGRAPHY 91

LIST OF TABLES

Table 2.1 Route selections with different routing metrics 14

Table 3.1 Bandwidth of different client-AP association plans in Example I 27

Table 3.2 Bandwidth and timeshare allocations with different client-AP association plans in Example II 28

Table 3.3 Example I revisited with FbF 30

Table 3.4 Example II revisited with FbF 30

Table 4.1 MAC layer parameters 53

Table 5.1 Additional notations used in the MIP Formulation 72

Table 5.2 Summary of the two heuristic algorithms 83

LIST OF FIGURES

Figure 1.1 Illustration of WMN and problems studied in this dissertation 2

Figure 2.1 Problem with the hop-distance-based interference model 12
Figure 2.2 An example network topology 13
Figure 2.3 Comparison of WCETT with various β 16
Figure 2.4 Comparison of AETD with various α 17
Figure 2.5 Throughput comparison with various node densities 17
Figure 2.6 Throughput comparison with various network sizes 19
Figure 2.7 Throughput comparison with various numbers of available channels 20
Figure 2.8 An example network topology with obstacles 21
Figure 2.9 Throughput comparison in networks with obstacles (30 scenarios) 22

Figure 3.1 Example I to illustrate performance anomaly with BbF 27
Figure 3.2 Example II to illustrate association anomaly with TbF 28
Figure 3.3 Pseudo-code of the Simple_maxmin algorithm 31
Figure 3.4 Pseudo-code of the RS_maxmin algorithm 32
Figure 3.5 Results of small-scale networks 33
Figure 3.6 Results of large-scale networks 35

Figure 4.1 MCL functions as a layer 2.5 protocol 46
Figure 4.2 Software architecture of CyMesh 48
Figure 4.3 CyMesh network topology in the ECpE building at ISU Campus 49
Figure 4.4 Snapshots of the CyMesh GUI 50
Figure 4.5 A snapshot of the JPerf utility 51

Figure 4.6 A snapshot of the JPerf bandwidth analysis 52
Figure 4.7 Single-hop link: effect of packet size on TCP throughput 54
Figure 4.8 A two-hop topology 55
Figure 4.9 Enabling parallel transmissions on forwarding node 56
Figure 4.10 Link capacity measurement 59
Figure 4.11 Effect of number of radios and channel diversity on TCP throughput 61
Figure 4.12 Effect of routing metric and path length on delay and throughput 62

Figure 5.1 Directional antenna and interference model 68
Figure 5.2 An example network graph G and its auxiliary graph G' 71
Figure 5.3 The formulated MIP problem 73
Figure 5.4 Effect of antenna directionality and channel diversity 76
Figure 5.5 The grid-topology network with 49 nodes 78
Figure 5.6 Comparison of system throughput in grid-topology networks 79
Figure 5.7 Results of 10 simulated scenarios in the grid-topology network 79
Figure 5.8 Random-topology networks with 49 nodes 80
Figure 5.9 Comparison of system throughput in random-topology networks 81
Figure 5.10 Results of 10 simulated scenarios in random-topology networks 81
Figure 5.11 Performance comparison of heuristic algorithms and MIP 86
Figure 5.12 Impact of traffic load and number of channels on system throughput 87
Figure 5.13 Impact of traffic load and number of channels on fairness 87

ACKNOWLEDGMENTS

I would like to take this opportunity to express my thanks to those who helped me with various aspects of conducting research and the writing of this dissertation.

I wish to express my thanks to my advisor, Dr. Daji Qiao, for his inspiration, guidance and support throughout this research and the writing of this dissertation. My thanks are due to all my committee members for their efforts and contributions to this work.

I would also like to thank my wife, Fei Huang, and my parents. The work presented in this dissertation would not have been possible without their constant loving support.

ABSTRACT

Wireless Mesh Network (WMN) has been recognized as a promising step towards the goal of ubiquitous broadband wireless Internet access. By exploiting the state-of-the-art radio and multi-hop networking technologies, mesh nodes in WMN collaboratively form a stationary wireless communication backbone. Data between clients and the Internet is routed through a series of mesh nodes via one or multiple paths. Such a mesh structure enables WMN to provide clients high-speed Internet access services with a less expensive and easier-to-deployment wireless infrastructure comparing to the wired counterparts.

Due to the unique characteristics of WMN, existing protocols and schemes designed for other well-studied wireless networks, such as Wi-Fi and Mobile Ad-hoc Network (MANET), are not suitable for WMN and hence cannot be applied to WMN directly. Therefore, novel protocols specifically designed and optimized for WMN are highly desired to fully exploit the mesh architecture. The goal is to provide high-level Quality-of-Service (QoS) to WMN clients to enable a rich portfolio of wireless and mobile applications and scenarios.

This dissertation investigates the following important issues related to QoS provisioning in WMN: high throughput routing between WMN clients and the Internet, fairness provisioning among WMN clients and network-level capacity optimization. We propose innovative solutions to address these issues and improve the performance, scalability and reliability of WMN. In addition, we develop CyMesh, a multi-radio multi-channel (MRMC) wireless mesh network testbed, to evaluate the capacity and performance of WMN in real world environments. Extensive simulation (using the QualNet simulator) and experimental (over the CyMesh testbed) results demonstrate the effectiveness of the designed protocols. In particular, we learn that the system capacity of WMN can be improved significantly by exploiting the MRMC network architecture and the antenna directionality of radios equipped on mesh

nodes, and our proposed fulfillment based fairness is a reasonable notion for fair service provisioning among WMN clients. Moreover, we report the encountered problems, key observations and learned lessons during the design and deployment of CyMesh, which may serve as a valuable resource for future MRMC WMN implementations.

CHAPTER 1. INTRODUCTION AND RESEARCH GOALS

1.1 Introduction

The tremendous growth of Internet and wireless communication technologies such as cellular networks and Wi-Fi networks is revolutionizing the way people communicate with each other. Cellular networks offer wide coverage and keep us stay in touch when we are away from home and office. However, even with today's 3G networks, wireless data service remains expensive and slow. In comparison, Wi-Fi offers significantly higher speed wireless data services but its coverage is limited. The gap between cellular and Wi-Fi networks is limiting the popularization of numerous wireless and mobile applications. In order to satisfy the growing demand for fast and affordable Internet access, novel solutions that offer high data rates and wide area coverage are becoming increasingly desirable.

Wireless Mesh Network (WMN) has emerged as a promising solution to bridge the gap between cellular and Wi-Fi networks and offer last-mile wireless Internet access with guaranteed Quality of Service (QoS). As shown in Fig. 1.1, a typical WMN consists of a collection of wireless mesh nodes including Gateway Nodes (GNs), Mesh Routers (MRs) and Access Points (APs).

- AP – mesh node which has Access Point functionality and provides last-hop access services to clients within its coverage area;
- GN – mesh node which connects to the Internet through the wired link with much higher bandwidth than the wireless links between mesh nodes;
- MR – mesh node which relays traffic between APs and GNs.

By exploiting state-of-the-art radio technology, these mesh nodes collaboratively form a stationary wireless communication backbone. In WMN, data (primarily between clients and the Internet) is routed

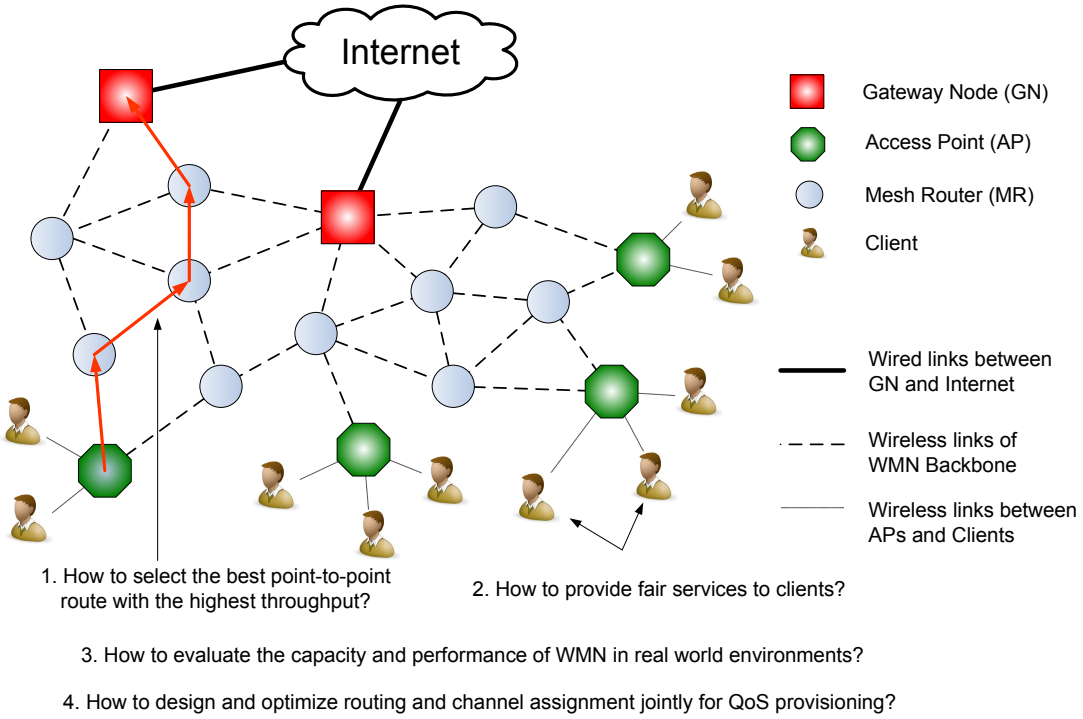

Figure 1.1 Illustration of WMN and problems studied in this dissertation

through a series of mesh nodes via one or multiple paths. Such a mesh structure enables WMN to (1) provide clients high-speed Internet access services with a less expensive and easier-to-deploy wireless infrastructure compared to the wired counterparts; and (2) significantly extend the coverage area of traditional Wi-Fi networks and provide wide-area coverage for Internet-based mobile applications.

Due to the unique characteristics of WMN, existing protocols and schemes designed for other well-studied wireless networks architectures, such as Wi-Fi and MANET (Mobile Ad-hoc Network), are not suitable for WMN and hence cannot be applied to WMN directly. For example, WMN differs from the traditional Wi-Fi in that each node in WMN may be equipped with multiple radios instead of a single radio, while end-to-end communication usually involves multi-hop transmissions. Compared to MANET, the mesh nodes in WMN are mostly stationary and have no energy constraints. Promising but challenging, creating a seamless wireless mesh environment involves research in many aspects such as capacity enhancement, multi-hop routing and service fairness. Therefore, careful system-level network planning, management and optimization are needed to fully exploit the mesh architecture.

1.2 Problem statement and research goals

In this dissertation, we study the following important issues related to QoS provisioning in WMN: high throughput routing, fairness provisioning among WMN clients and network-level capacity optimization with consideration of practical limitations. Further, we design and implement a multi-radio multi-channel (MRMC) WMN testbed to evaluate the capacity and performance of WMN in real world environments. We aim to identify the critical issues that affect the QoS in current-generation wireless networks and propose innovative solutions that can offer better performance, scalability and reliability for WMNs.

1.2.1 High throughput routing metric

With the increasing bandwidth demand of Internet applications, high throughput provisioning becomes more and more challenging especially for large-scale wireless networks considering the interference and scalability issues. Despite the fact that multiple non-interfering frequency channels are available to IEEE 802.11 devices [1], most existing 802.11-based multi-hop wireless networks follow the single-radio single-channel (SRSC) paradigm, where each node is equipped with a single radio interface and all radio interfaces operate on the same frequency channel at any given time. Such system often suffers low channel utilization and poor system throughput.

Recently, the MRMC network architecture has been recognized as one of the promising approaches to improve the system throughput of 802.11-based multi-hop wireless networks. In comparison to the traditional SRSC network architecture, each node is now equipped with multiple radio interfaces and each radio interface may operate on one of multiple available non-interfering frequency channels. Moreover, the rate adaptation capability [2, 3] of an 802.11 device allows it to adjust its transmission rate dynamically to the varying link quality between itself and the receiving node.

On the other hand, the MRMC network architecture has presented many new research challenges, such as optimal channel assignment, coordination among neighboring nodes, high throughput routing, etc. In the first part of this dissertation, we focus on the routing problem in MRMC networks. We study existing popular routing metrics and find that the desired routing metric for MRMC networks should account for three fundamental factors: transmission rate, link quality, and channel diversity.

Unfortunately, none of the existing routing metrics considers all of the three factors thus cannot make correct decision on high throughput route selection. Our goal is to propose a new routing metric with the following considerations:

1. The proposed routing metric must take into account all the factors that may affect the end-to-end throughput of a multi-hop route in MRMC WMNs, including link quality, transmission rate and channel diversity.

2. Design of the routing metric should take the advantage of multiple available channels in the network to minimize co-channel interference and optimize spectrum and spatial reuse.

3. The proposed routing metric should be light-weight in terms of computational complexity, so one can easily apply it to existing routing protocols.

1.2.2 Fairness provisioning among clients in WMNs

Fair allocation of system resource among clients is one of the critical issues that affects the QoS in WMNs. Although there has been significant research on the fairness issues in both wired and wireless networks, there is little research on resource allocation in WMNs. Fairness provisioning and throughput optimization are both desired in WMNs, unfortunately, they are two imperative issues and hence difficult to be achieved simultaneously. For example, maximizing the total system bandwidth optimizes for the overall usage of network resources. However, this criterion may starve a client in favor of several other clients. Max-min bandwidth fairness is proposed to address such issues when there is resource requirement conflict. The goal of max-min fairness is to maximize the bandwidth allocated to the client which receives least bandwidth. However, if two clients are demanding distinct resources and there are no conflicts between their requirements, then a guarantee on the minimum assigned bandwidth may lead to waste on the system resource. Therefore, a well-defined fairness objective function and the corresponding service provisioning schemes are critical to address these issues.

In the second part of this dissertation, we study the problem of fair service provisioning among the clients in WMNs. Typically, a WMN consists of multiple APs, while a client may associate with one of them according to certain criteria. For example, each client selects the AP with the strongest signal

strength as in today's WLANs. Without a well-defined fairness notion and provisioning mechanism, such un-planned association scheme may lead to significant performance degradation. Ideally, the network resource should be allocated to each client in an egalitarian manner to avoid starving one client while allocating all resources to others. The problem we study in this part can be considered as a multi-AP WLAN where the APs collaborate with each other and have controls over all AP-clients association. The objectives of this study are to: (1) define an appropriate fairness notion for achieving a balance between fairness and throughput optimization in systematic way, and (2) develop the corresponding schemes to implement it.

Two fairness notions have been proposed based on max-min criterion for such multi-AP WLANs: Bandwidth-based Fairness (*BbF*) and Timeshare-based Fairness (*TbF*). Unfortunately, our studies show that both of them could lead to serious system throughput degradation. Specifically, we identify the *performance anomaly* problem inherited with Bandwidth-based fairness *BbF* and the *association anomaly* problem inherited with Timeshare-based fairness *TbF*. Our investigation motivates the need for defining a more fitting fairness notion to address the problems associated with *BbF* and *TbF*, and developing efficient algorithms for implementing it.

1.2.3 Wireless mesh network testbed

In most wireless network research, performance evaluation has been addressed through numerical analysis and simulations. Although simulation offers a convenient combination of flexibility and controllability, there exists significant evidence that simulation results could be difficult to transfer into reality. The main reason is that most simulations are based on simplistic assumptions or abstracted models which neglect many factors that could affect the performance of real world networks. To study the potential capability and performance of WMNs in real world, experimentation is probably the most reliable method. Therefore, it is highly desired to build a WMN testbed to create a proof-of-concept prototyping platform to facilitate a broad range of experimental research in WMN. This could help us to test the effectiveness and efficiency of our proposed schemes and verify the theocratical analysis as well as simulation results. In the third part of this dissertation, we describe the design and implementation of a MRMC WMN testbed with the following design goals:

- Reliability and Robustness: to maintain network connectivity with unmanned operation.
- Flexibility: for easy tuning of basic network parameters and implementation of new routing components.
- Scalability and Efficiency: to minimize the induced overhead and keep the network scalable.
- Reproducibility: to produce similar results with similar environments and configurations.
- Visualization and Monitoring: to understand the network topology and monitor node/link conditions in real-time.
- Remote Configuration and Management: to allow users to remotely manage or configure the network and carry out experiments.
- Cost-efficiency: to keep cost reasonably low without compromising the desired capabilities and functionalities.

1.2.4 Network design and capacity optimization

Our simulation and experimental results from previous studies indicate that: (1) network-level design and capacity optimization are critical to achieve efficient radio resource usage in MRMC WMNs; (2) with omni-directional antennas used on most IEEE 802.11 devices and limited number of non-overlapping channels in 802.11, system capacity of multi-hop WMNs is inevitably affected by the interference between multiple simultaneous transmissions. It has been well known that interference among transmissions operating on the same frequency channel could be alleviated by using multiple radios on each mesh node and by assigning different channels to each radio, thus enabling more concurrent transmissions using directional antennas on each mesh node could further improve the system throughput via alleviating the interference between nearby nodes thus allowing more concurrent transmissions in the network.

In the fourth part of this dissertation, we propose a joint routing and channel assignment algorithm for multi-hop WMNs with directional antennas, which is designed to enhance both spatial and

frequency reuse for optimizing the performance of WMNs. Moreover, the design of the proposed algorithm take into account practical constraints to enable feasible implementation.

1.3 Summary and organization

Despite the numerous advantages and promising future of WMN, there are many research challenges that remain unresolved and require considerable research effort. In this dissertation, we focus our research on QoS provisioning in WMNs and approach related problems with both theoretical and experimental methodologies. Our research goal is to make WMN reach its full potential and become a robust and viable wireless Internet access technology.

The rest of the dissertation is organized as follows. In Chapter 2, we present our research on routing metric design for MRMC WMNs. A new fairness metric addressing the anomalies inherent with the existing fairness notions is proposed in Chapter 3. In order to evaluate the proposed schemes in real world environments, we have developed and deployed CyMesh, a multi-hop WMN testbed using off-the-shelf IEEE 802.11 devices, which is described in detail in Chapter 4. In Chapter 5, we present a network-level design and optimization framework for capacity optimization in WMNs with directional antennas. We summarize our research contributions and conclude the dissertation in Chapter 6.

CHAPTER 2. DESIGN OF ROUTING METRIC FOR MRMC WMNs

2.1 Introduction and motivation

MRMC network architecture enables potential capacity improvement in multi-hop wireless networks. It has also presented many new research challenges such as optimal channel assignment, coordination among neighboring nodes, high-throughput routing, etc. In this chapter, we study the routing problems for high-throughput in MRMC wireless networks.

Routing in multi-hop wireless networks has received a lot of attention from the various points of view. The authors of [4,5] propose an MCR (Multi-Channel Routing) scheme that includes an interface assignment strategy and a routing protocol to utilize all available channels effectively in multi-channel multi-interface wireless networks. The routing metric used in MCR accounts for channel diversity and interface-switching cost, however, it cannot fully exploit the MRMC feature because: (1) link quality and bandwidth are not jointly considered in the MCR routing metric; and (2) MCR is based on the hop-distance-based channel interference model and, hence, may suffer from the zigzag-route issues. There are several recent work [6, 7] that perform theoretical analysis on joint optimization of channel assignment and routing in MRMC wireless networks, which is different from the issues we address in this work.

We start the investigation by examining the existing routing metrics in MRMC wireless networks. There are three fundamental factors to be considered when designing a routing metric for such networks: transmission rate, link quality, and channel diversity. The popular hop-count routing metric (HOP) does not perform well in MRMC wireless networks. The reason is that HOP does not consider any of the three fundamental factors. In [8], the authors propose a routing metric for SRSC wireless networks, called the cumulative expected transmission count (ETX), which takes into account the link quality factor. In [9], WCETT (weighted cumulative expected transmission time) routing metric is pro-

posed specifically for MRMC wireless networks. It calculates the ETT (expected transmission time) of each hop and makes the routing decision based on the cumulative ETT (CETT) along with the channel diversity of each candidate route. However, channel diversity is characterized indirectly by the sum of ETTs of hops operating at the bottleneck frequency channel (BETT). The tradeoff between CETT and BETT is indicated by a weight β:

$$\text{WCETT} = (1 - \beta) \cdot \text{CETT} + \beta \cdot \text{BETT}. \tag{2.1}$$

Unfortunately, WCETT metric may not be adequate to reflect the actual channel-diversity level of a route. Under certain circumstances, two candidate routes with different channel-diversity patterns may have the same WCETT value and WCETT cannot differentiate them.

The inherent drawbacks of existing routing metrics motivate us to design a new routing metric which considers all three fundamental factors aforementioned when making routing decision and achieve high throughput.

2.2 Problem definition and assumption

The problem is formulated as follows. Given (1) a pair of source and sink nodes in a MRMC WMNs, (2) link quality information of all links, and (3) predetermined channel assignment information, the goal is to design a routing metric to achieve high end-to-end route throughput. Moreover, we assume that if the two radios on the same node operate on different frequency channels, then they can transmit or receive simultaneously without interfering each other.

2.3 Proposed routing metric

In this work, we propose a new routing metric called AETD (adjusted expected transfer delay) for high throughput route selection in MRMC WMNs. The work is inspired by the following observation: by selecting a route on which hops operating on the same frequency channel are separated as far as possible, the interference and channel contention may be minimized, hence improving the system throughput. The key idea of AETD is to make the routing decision based on the expected end-to-end transfer delay of a single packet as well as the expected interval between consecutive packet arrivals,

which serves as a good indicator of the channel-diversity level. As a result, AETD is able to identify the routes with better channel diversity and make the appropriate routing decision.

2.3.1 Adjusted expected transfer delay (AETD)

When a sequence of packets are transmitted from a source node to a destination node, the achieved throughput is determined by the following features of the selected route:

- ETD: the expected end-to-end transfer delay of a single packet;
- EIA: the lower bound of the expected interval between consecutive packets arrivals at the destination node.[1]

Apparently, an ideal route shall have a small ETD as well as a small EIA.

ETD is affected by the following: (1) the hop count of the route; and (2) the bandwidth and link quality of each hop along the route that determine the per-hop transmission rate and transmission time. A shorter route (measured in hops) does not necessarily yield a smaller end-to-end transfer delay. It is likely that a smaller hop count implies a longer average hop distance and, consequently, lower transmission rates and larger overall transfer delay. On the other hand, a route with a larger hop count but shorter average hop distance may instead yield a smaller end-to-end transfer delay.

EIA is affected by the following: (1) the channel diversity of the route; and (2) the bandwidth and link quality of each hop along the route that determine the per-hop transmission rate and transmission time. A more channel-diverse route experiences less interference as packet transmissions on different channels do not interfere with each other. In the extreme case when the route is perfectly channel-diverse, i.e., when packet transmissions on any two hops along the route do not interfere with each other — either because they are far apart from each other or because they operate on different frequency channels, packet transmissions on each hop may proceed successfully at the same time without encountering any channel contention and the consequent contention resolution procedure. Hence, a very short interval between consecutive packet arrivals is expected under such scenario, which equals the maximum single-hop transmission time along the route.

[1]EIA is obtained by assuming perfect contention resolution among contending stations. We choose not to include the contention resolution time in EIA as this would depend on the implementation details of the underlying MAC layer protocol.

2.3.2 Calculations of ETD and EIA

Let $\mathcal{N}_r = \{0, 1, \cdots, k\}$ denote the node sequence along route r of k hops from the source node 0 to the destination node k. Let $\mathcal{H}_r = \{h_1, h_2, \cdots, h_k\}$ denote the corresponding hop sequence along route r, and let h_i represent the hop between nodes $(i-1)$ and i. For each hop h_i, let C_{h_i} denote the frequency channel nodes $(i-1)$ and i use to communicate with each other, and let ETT_{h_i} denote the expected packet transmission time over hop h_i.

Then, ETD_r, the expected end-to-end transfer delay of a single packet over route r is simply

$$\text{ETD}_r = \sum_{h_i \in \mathcal{H}_r} \text{ETT}_{h_i}. \tag{2.2}$$

The calculation of EIA_r, the lower bound of the expected interval between consecutive packet arrivals over route r, varies with the interference model. There are two types of interference models: *physical-distance-based interference model* and *hop-distance-based interference model*. The physical-distance-based interference model reflects the actual interference phenomenon in the network, while the hop-distance-based interference model makes the following assumptions to simplify the modeling of the interference:

- Packet transmissions may only interfere with each other if they operate on the same frequency channel and are within the interference distance;
- The interference distance is measured in hops and is calculated as:

$$\text{interference distance} = \left\lceil \frac{\text{interference range}}{\text{average hop distance}} \right\rceil. \tag{2.3}$$

Unfortunately, these assumptions may not hold under certain circumstances. Next, we explain this problem by comparing two routes shown in Fig. 2.1(a).

The interference range of packet transmissions from nodes 3 to 4 is shown as the dashed circles in Fig. 2.1(a). Then, according to the hop-distance-based interference model, the interference distance is 2 hops. Clearly, the 2-hop interference distance holds in Fig. 5.1(a) with a straight-line route while in Fig. 5.1(b), due to the zigzag nature of the route, packet transmissions from nodes 0 to 1 are interfered by packet transmissions from nodes 3 to 4 although they are 3 hops apart.

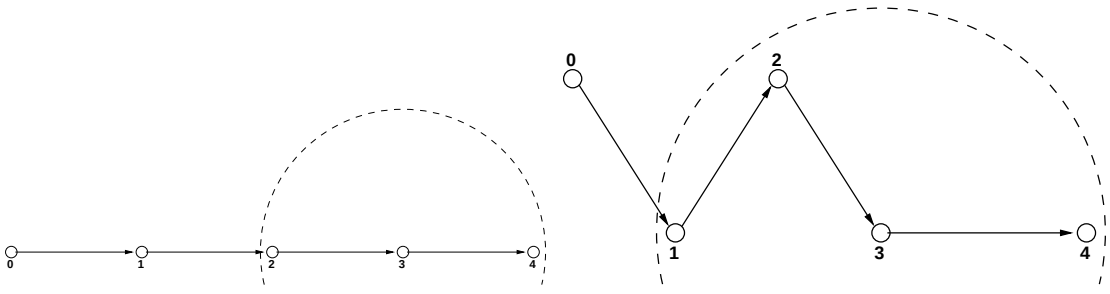

(a) a straight-line route (b) a zigzag route

Figure 2.1 Problem with the hop-distance-based interference model

In general, it is not trivial to incorporate the physical-distance-based interference model into the routing metric, since it requires complicated message exchanges between neighboring nodes and more traffic flow information maintained at each node. In this study, our calculation of EIA_r is based on the hop-distance-based interference model with special considerations to counter the above-described problem associated with the hop-distance-based interference model. The calculation details of EIA_r are as follows.

Firstly, we define $\text{EIA}_{r(i)}$ as the expected interval between consecutive packet arrivals from node i to destination node k ($k > i$) along route r, which may be calculated recursively as follows:

$$\text{EIA}_{r(i)} = \begin{cases} \text{ETT}_{h_k} & \text{if } i = k-1, \\ \text{ETT}_{h_{i+1}} + \text{EIA}_{r(i+1)} & \text{if } \exists\, i+1 < j \leqslant \min\{i+m+1,\ k\} \\ & \text{such that } C_{h_{i+1}} = C_{h_j}, \\ \max\left\{\text{ETT}_{h_{i+1}},\ \text{EIA}_{r(i+1)}\right\} & \text{else,} \end{cases} \tag{2.4}$$

where m is the interference distance (measured in hops) in the hop-distance-based interference model. The "+" operation in Eq. (2.4) accounts for the fact that, when some packet transmissions from node $(i+1)$ to the destination interfere with the packet transmission over hop h_{i+1}, both transmissions may not succeed at the same time. On the other hand, the "max" operation in Eq. (2.4) corresponds to the perfect pipelining between packet transmissions over hop h_{i+1} and from node $(i+1)$ to the destination when they do not interfere with each other. Then, EIA_r is simply a special case of $\text{EIA}_{r(i)}$ when $i = 0$:

$$\text{EIA}_r = \text{EIA}_{r(0)}. \tag{2.5}$$

Note that, given two routes with the same ETD, the one with better channel diversity or with a better

channel-diversity pattern shall have a smaller EIA.

Based on the above analysis, we propose a new routing metric, called AETD (adjusted expected transfer delay), that combines ETD and EIA:

$$\text{AETD} = (1 - \alpha) \times \text{ETD} + \alpha \times \text{EIA} \tag{2.6}$$

where α is a tunable parameter between 0 and 1. The α value in ATED shall be kept small. The reason is that with a small α value, only the routes with fairly small end-to-end transfer delay may be selected, meaning that the selected route has few hops and is less zigzag. Consequently, the problem associated with the hop-distance-based interference model could be alleviated.

2.3.3 Case study

We use a simple example to illustrate different route selections with different routing metrics, including HOP, ETX, WCETT, and AETD. Fig. 2.2 shows the network topology and each communication link in the network is characterized by its operating frequency channel (C), the expected transmission count (etx), and the expected transmission time (ETT) over the link. Assume that the interference distance is two hops, meaning that, if packet transmissions are within two hops from each other, they interfere and cannot succeed at the same time.

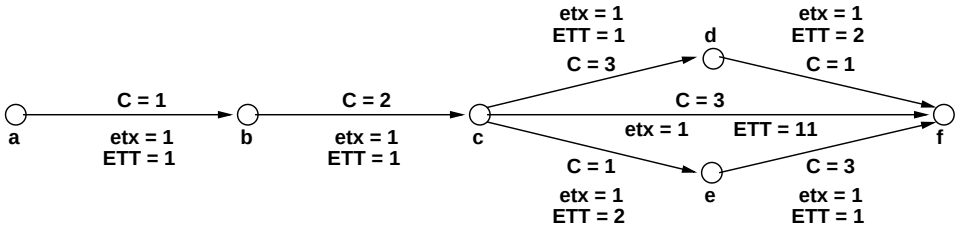

Figure 2.2 An example network topology

Table 2.1 lists three possible routes from nodes a to f: [a-b-c-f], [a-b-c-d-f], and [a-b-c-e-f], and compares their respective routing metric values under different routing schemes. Both HOP and ETX select the shortest route [a-b-c-f] but with the largest end-to-end transfer delay of 13.

Unfortunately, WCETT is unable to distinguish between routes [a-b-c-d-f] and [a-b-c-e-f], regardless of the β value, although these two routes show different channel-diversity patterns. Note that route

Table 2.1 Route selections with different routing metrics

available routes	routing metrics			
	HOP	ETX	WCETT	AETD
[a-b-c-f]	3	3	$(1-\beta)\cdot 13+\beta\cdot 11$	$(1-\alpha)\cdot 13+\alpha\cdot 11$
[a-b-c-d-f]	4	4	$(1-\beta)\cdot 5+\beta\cdot 3$	$(1-\alpha)\cdot 5+\alpha\cdot 2$
[a-b-c-e-f]	4	4	$(1-\beta)\cdot 5+\beta\cdot 3$	$(1-\alpha)\cdot 5+\alpha\cdot 3$
route selection	[a-b-c-f]	[a-b-c-f]	[a-b-c-d-f] or [a-b-c-e-f]	[a-b-c-d-f]

[a-b-c-d-f] has the perfect channel-diversity pattern: two hops operating on the same frequency channel of C = 1 are placed at the opposite ends of the route. Hence, packet transmissions along this route do not interfere with each other and the perfect pipelining of packet transmissions may be achieved. On the other hand, along the route [a-b-c-e-f], packet transmissions from nodes a to b and from nodes c to e interfere with each other since they operate on the same frequency channel and are within the interference distance.

In comparison, the proposed AETD routing metric considers explicitly the channel-diversity pattern of a given route and, hence, is able to select the more channel-diverse route if available. As shown in the example, AETD recognizes the better channel diversity-pattern of route [a-b-c-d-f] and makes the right route selection.

2.4 Performance evaluation

We evaluate the effectiveness of the proposed AETD routing metric using the QualNet simulator [10].

2.4.1 Simulation setup

The simulated network is a square flat area with wireless nodes uniform-randomly deployed inside the network. All nodes are static. The source and destination nodes sit at the lower-left and upper-right corners of the network. Each simulated node is equipped with two IEEE 802.11b [3] radio interfaces. The operation of the radio interfaces conform to the following rules:

- A link-quality-based rate adaptation scheme is employed at each radio interface so that it may

operate at one of the four available 802.11b transmission rates: 1 Mbps, 2 Mbps, 5.5 Mbps, and 11 Mbps; the corresponding maximum transmission ranges for different rates are 249 m, 161 m, 146 m, and 103 m, respectively;

- Each pair of radio interfaces on neighboring nodes may communicate with each other via one of multiple available non-interfering frequency channels, and the channel assignment is random.

We evaluate and compare the throughput performance of the following routing metrics: (1) hop count (HOP); (2) cumulative expected transmission count (ETX); (3) cumulative expected transmission time (CETT); (4) weighted cumulative expected transmission time (WCETT) with β = 0.2, 0.4, 0.6, 0.8, and 1.0, respectively; and (5) the proposed AETD routing metric with α = 0.025, 0.05, 0.1, 0.2, 0.4, 0.8, and 1.0, respectively. Note that CETT is equivalent to WCETT with β = 0.0 and AETD with α = 0.0.

We conduct the simulation with various node densities, network sizes, numbers of available channels, and node deployment patterns. In each simulation run, the source node sends 1000 UDP packets to the destination node. The source data rate is set high enough to saturate the network and, in order to have a fair comparison of the testing schemes, the queue size of each wireless node inside the network is set to infinite to avoid packet dropping caused by queue overflow. The packet size is 1024 octets.

2.4.2 Random deployment without obstacles

In the first part of the simulation, we compare the testing schemes when there are no obstacles inside the network. Each point in the figures is averaged over 100 simulation runs.

2.4.2.1 Effects of β in WCETT

We first evaluate the effects of the β parameter in WCETT and show the results in Fig. 2.3. The node density is fixed at 200 nodes/km^2 and the number of available channels is three. The network size varies from (125 m $\times$ 125 m) to (2 km $\times$ 2 km), which correspond to the average path length of 2.6, 4.8, 10.3, 20.5, and 40 hops, respectively.

As shown in the figure, when the network size is small, WCETT shows throughput improvement over CETT. However, when the network size increases and the average path length becomes large, the

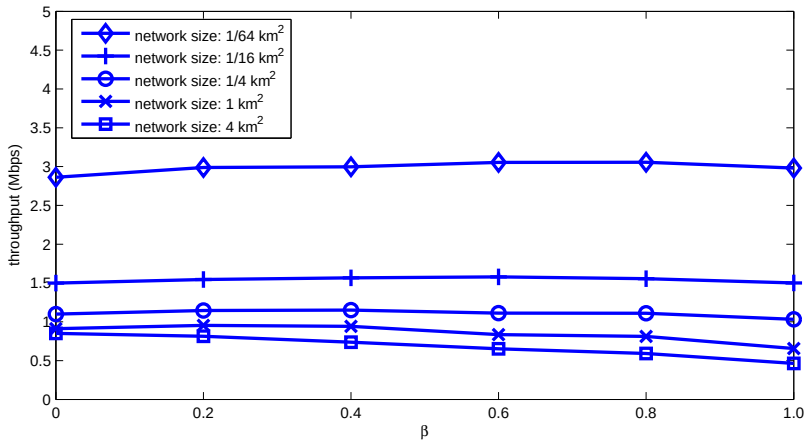

Figure 2.3 Comparison of WCETT with various β

throughput performance of WCETT (with a non-zero β value) is comparable or even worse than that of CETT, which is consistent with the observations in [9]. In the following simulation runs, we fix the β value to 0.2.

2.4.2.2 Effects of α in AETD

We also study the effects of the α parameter in the proposed AETD routing metric. The node density is fixed at 200 nodes/km^2 and the network size is fixed to be (2 km $\times$ 2 km). The number of available channels is three. Simulation results are plotted in Fig. 2.4.

In general, AETD metrics with smaller α values yield higher throughput than CETT, and the highest throughput is achieved when $\alpha = 0.05$. On the other hand, the AETD throughput starts decreasing when $\alpha \geqslant 0.1$ and reaches the lowest point when $\alpha = 1.0$. This is because, with a larger α value, AETD is more concerned about the channel diversity along the route and, as a result, a zigzag route may be selected. This observation supports our earlier statement that choosing a small α value is critical to counter the inherent problem associated with the hop-distance-based interference model by avoiding zigzag routes.

We have also noticed similar trends with various node densities, network sizes, and numbers of available channels. The only difference is that, with different network configuration, the highest AETD throughput may be achieved with different small α values. Overall, $\alpha = 0.05$ seems to be a good choice

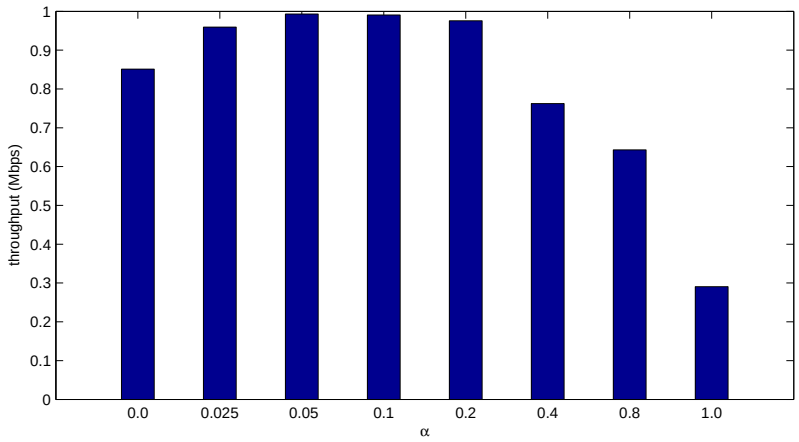

Figure 2.4 Comparison of AETD with various α

and hence will be used in all following AETD simulation runs.

2.4.2.3 Effects of Node Density

In this set of simulation runs, we vary the node density in the network from 50 nodes/km^2 to 200 nodes/km^2. The network size is (2 km $\times$ 2 km) and the number of available channels is three. Simulation results are plotted in Fig. 2.5.

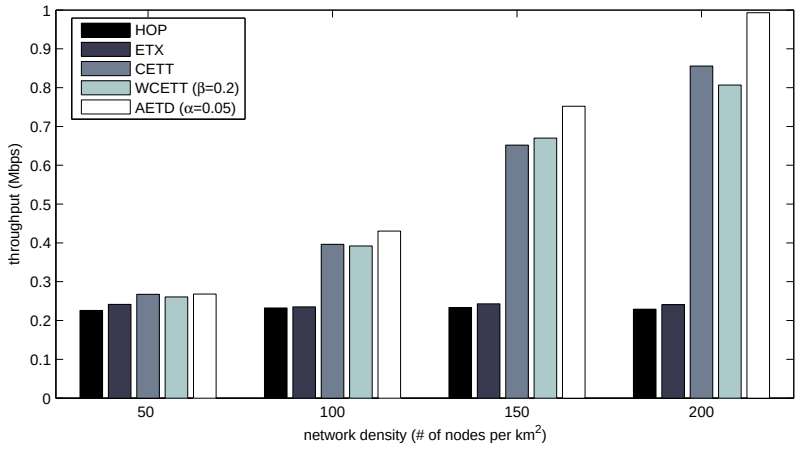

Figure 2.5 Throughput comparison with various node densities

It is interesting to see that the throughput of HOP does not change with the node density. This is

simply because the HOP metric always selects the route with minimum number of hops even when the nodes are densely-deployed in the network. We have a similiar observation on ETX but with different rationale behind it. Since each node has the rate-adaptation capability, it can always lower its transmission rate, whenever necessary, to communicate with a far-away neighboring node in a sparse network, while maintaining a similar transmission count. For this reason, the node density in the network has minimum impact on the route selection by ETX.

As expected, AETD has the best throughput performance with each simulated node density and the performance improvement of AETD over CETT and WCETT becomes more significant as the node density increases. This is because, with more nodes deployed in the network, there are more routes available between the source and the destination nodes. Hence, it is more likely for AETD to find a route (1) with similar end-to-end transfer delay as that of the route selected by CETT or WCETT, and (2) with much better channel diversity. As shown in the figure, AETD outperforms CETT by 15.4% and 16.7%, and outperforms WCETT by 12.3% and 22.1%, when the node density increases to 150 and 200 nodes/km^2, respectively.

2.4.2.4 Effects of Network Size

Fig. 2.6 shows the simulation results with various network sizes: (125 m $\times$ 125 m), (250 m $\times$ 250 m), (500 m $\times$ 500 m), (1 km $\times$ 1 km), and (2 km $\times$ 2 km). The node density is fixed at 200 nodes/km^2 and the number of available channels is three.

In general, as the network size increases, the throughput decreases for all testing schemes. This is because the increasing distance between the source and destination nodes requires more packet relays in the network and creates potentially more interferences and channel contentions along the route. Note, however, that the throughput performance of AETD is least affected by the increasing network size, because the AETD metric favors the routes with good channel diversity, which may ameliorate the channel contention problem caused by the increased route length.

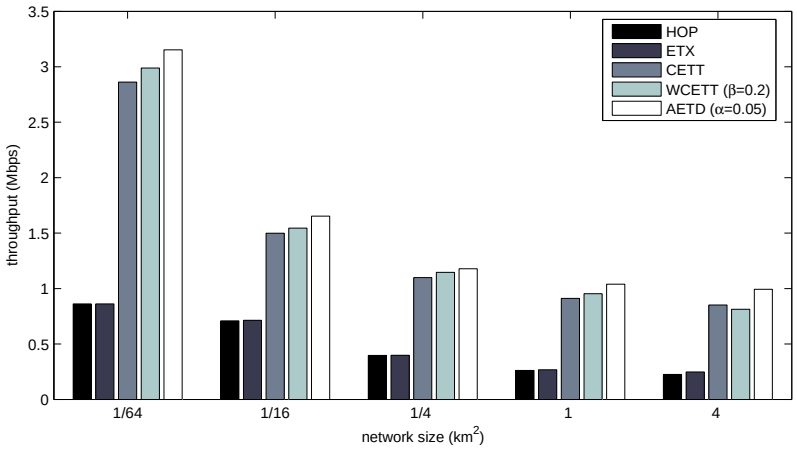

Figure 2.6 Throughput comparison with various network sizes

2.4.2.5 Effects of Number of Available Channels

Fig. 2.7 shows the simulation results with various numbers of available channels. The network size is (2 km $\times$ 2 km) with the node density of 200 nodes/km^2.

We have two observations. First, since neither HOP nor ETX considers channel diversity when making the routing decisions, both of them show marginal, if any, performance improvement when more communication channels are available for assignment in the network.

Secondly, when all the radio interfaces operate on the same frequency channel, i.e., when the number of available channels is one, AETD, CETT, and WCETT are equivalent. As the number of available channels increases, AETD, CETT, and WCETT all show significant performance improvement but due to different reasons. Recall that the communication channels between neighboring nodes are randomly assigned in our simulation. Therefore, with more channels assigned randomly in the network, the route selected by CETT may have better channel diversity. In other words, CETT benefits implicitly from the increasing number of available channels. WCETT takes into consideration the channel diversity in its routing metric, however, indirectly through its BETT component. In comparison, channel diversity is considered explicitly in the AETD metric, which allows AETD to take full advantage of the increasing number of available channels and achieve more performance improvement. As shown in the figure, the throughput improvement for AETD is 18.5% in comparison to 14.7% for CETT and 16.0% for WCETT when the number of available channels increases from three to five.

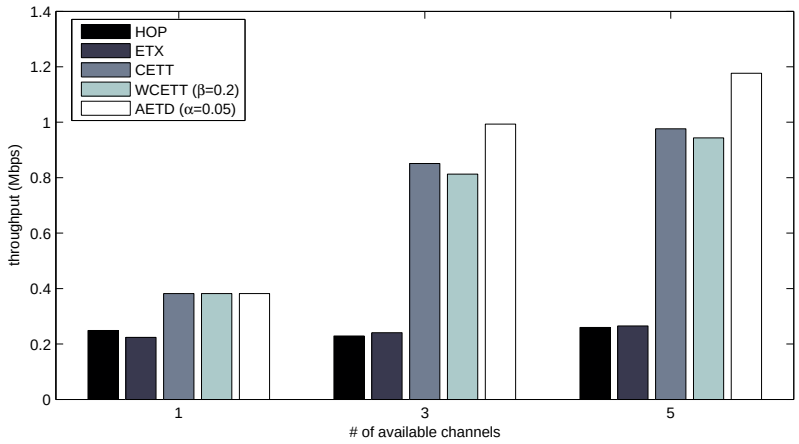

Figure 2.7 Throughput comparison with various numbers of available channels

2.4.3 Random deployment with obstacles

In the second part of the simulation, we compare the testing schemes when there are some obstacles inside the network. Fig. 2.8 shows an example topology of such network: the blank areas correspond to obstacles where nodes are uniform-randomly deployed around them. We simulate 30 different scenarios and the results are plotted in Fig. 2.9.

As shown in Fig. 2.8, all routes are forced to detour around the obstacles. The routes selected by AETD, CETT, and WCETT are longer (measured in hops) than those selected by HOP and ETX, but with much shorter expected interval and/or delay performances. Therefore, as shown in Fig. 2.9, AETD, CETT, and WCETT all achieve significantly higher throughput than HOP and ETX in each simulated network topology. Moreover, because of better channel diversity in the AETD routes, AETD yields a higher throughput than CETT and WCETT in most of the simulated scenarios (shown in Fig. 2.9).

2.4.4 Summary

Based on the observations from the simulation results, we summarize the effectiveness of AETD as follows:

- AETD considers explicitly the channel diversity when making the routing decision. For this rea-

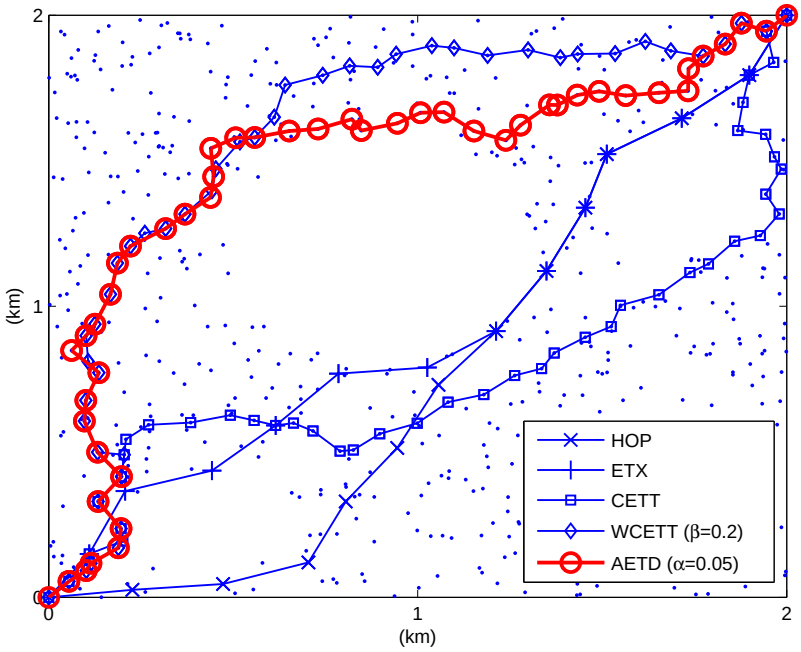

Figure 2.8 An example network topology with obstacles

son, it achieves significantly higher throughput than HOP and ETX while outperforming CETT and WCETT in most simulated scenarios;

- It is critical to choose a small α value in AETD;
- AETD is most suitable for routing in wireless networks with high node densities and/or large numbers of available channels;
- With a well-planned channel assignment, AETD may achieve even higher throughput enhancement over other routing metrics.

2.5 Conclusion

In this chapter, we investigate the routing issues in MRMC WMNs. A new AETD (adjusted expected transfer delay) routing metric is proposed to take into account the expected end-to-end transfer delay of a single packet as well as the expected interval between consecutive packet arrivals. Both

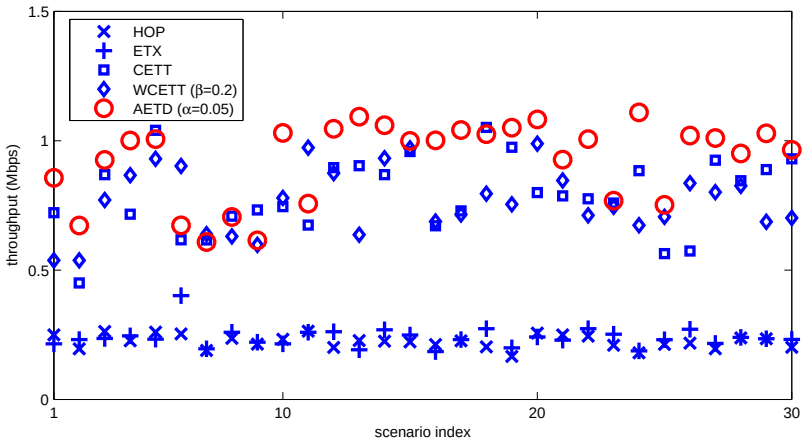

Figure 2.9 Throughput comparison in networks with obstacles (30 scenarios)

analysis and simulation results suggest that the expected interval between consecutive packet arrivals is a good indicator of the actual channel-diversity level of a given route.

We compare the throughput performance of AETD via simulation against four well-known routing metrics: HOP (hop count), ETX (cumulative expected transmission count), CETT (cumulative expected transmission time), and WCETT (weighted cumulative expected transmission time). Simulation runs are conducted under various node densities, network sizes, numbers of available channels, and node deployment patterns, and results show that AETD consistently outperforms other routing metrics in term of throughput provisioning.

Possible extension includes using statistical link quality estimation and considering inter-flow interference in multi-flow scenarios. It is also desirable to incorporate an effective channel assignment scheme to work with AETD to minimize the impact of interference and improve throughput.

CHAPTER 3. FAIRNESS PROVISIONING AMONG CLIENTS IN WMNs

3.1 Introduction

In computer networks, fairness has been used as a criterion to guide the design of resource allocation scheme and traffic controls. The notion of fairness has evolved over time, from simple equality to a form of equality modulated by the user's need. However, it is difficult to judge if a fairness notion itself is "fair" or not. For example, in current widely deployed protocols like weighted fair queuing, TCP congestion control and TCP-friendly rate control, "flow rate fairness" is employed for fair resource allocation [11–14], which subjects fairness congestion control on a per-flow basis. On the other hand, some researchers [15] argue that comparing flow rates (i.e. flow rate fairness) should not be used for claims of fairness in wireless networks. Instead, one should judge fairness mechanisms on how they share out the "cost" of each user's actions on others.

In this study, we investigate the fair service provisioning and intelligent association problems in the "last-hop" connections of WMNs. As shown in Fig. 1.1, a typical WMN consists of multiple access points (APs), and a client may associate with one of the APs to access the Internet throughput the mesh backhaul. Since the association decision is made at each client independently, it is possible that multiple clients associate with the same AP, which may lead to significant performance degradation. Our objective is to provide intelligent association control between the clients and APs in order to efficiently utilize the system resource while maintaining a certain level fairness among clients. We assume that the setup of the mesh backhaul is perfect such that each AP operates as it is directly connected to the Internet[1]. Therefore, the scenario we study can be considered as a multi-AP WLAN, and our goal is to find an appropriate fairness notion and develop feasible schemes to implement the fairness notion. In the rest of this Chapter, we use "multi-AP WLANs" to refer to the "last-hop" part

[1]This assumption can be easily extended and adopted to WMNs with bandwidth limitations on each AP.

of WMNs for simplicity.

In such multi-AP WLANs, maximum system throughput could be achieved if each AP is assigned a non-interfering frequency channel[2] and serves a single client with the highest data rate (among all clients that are associated with this AP) while other clients are starved. The IEEE 802.11 standard multi-access protocol attempts to achieve long-term max-min bandwidth fairness. Such Bandwidth-based Fairness (BbF) has been studied jointly with maximization of system throughput by many researchers [16–19]. In fact, these two goals create inherent conflicts between them. Moreover, nodes in WLANs may transmit at different rate because: (1) the IEEE 802.11 "auto-rate" mechanism will select "appropriate rate" for a node based on distance, channel condition and other factors; and (2) different technologies offer difference maximum transmitting rate (e.g. 11 Mbps for 802.11b and 54 Mbps for 802.11a). When data rates diversity exists, the node transmitting at lower data rates will consume more air time. Obviously, such max-min bandwidth fairness does not translate to max-min timeshare fairness, and may cause significant system throughput degradation.

In [20], the author proposes "Proportional Fairness" which seeks a tradeoff between fairness and throughput. The idea is to assign each user sufficient bandwidth without unduly restricting the amount of bandwidth available to other users. Formally, proportional fairness to maximize the weighted sum of the logarithm of the bandwidth allocation. Sadeghi et al. [21] and Tan et al. [22] study the proportional fairness problem for single-AP WLANs. They proposed "Timeshare-based Fairness" (TbF) which assigns the channel access timeshare to each client in a fair manner, regardless of transmitting rate. These schemes can efficiently prevent high-rate users from being "dragged down" by low-rate users in single-AP scenario. Furthermore, Jiang [23] et al. have shown that proportional fairness in bandwidth usage is equivalent or close to max-min fairness in air-time usage. That is, given a fixed number of clients (ignoring the all the protocol overhead), the throughput of one client is independent of the data rates used by other clients, if proportional fairness is achieved. They also investigate approaches to achieving proportional fairness in both WLANs and ad hoc networks.

Unfortunately, the work mentioned above do not consider the problem of network-wide proportional fairness in multi-AP scenarios. A generalized proportional fairness problem is formulated in [24]

[2]In this scenario, each AP operates on an administrator-assigned frequency channel and each client typically associates with an AP. All communications between an AP and its associated clients occur on the channel assigned to the AP.

for 3G wireless data networks, but the proposed mechanism cannot be easily applied to WLANs. Recent work [25] studies the proportional fairness problem in multi-rate multi-AP WLANs. Two approximation algorithms are proposed which yield tight worst-case guarantee for the NP-hard problem. Unfortunately, since most commercial WLAN devices do not allow modification in the protocol, it's technically challenging to implement "Proportional Fairness" or "Timeshare-based Fairness" in practice. On the other hand, in IEEE 802.11e based networks, it is possible to assign equal TXOP length in each clients or adjusting initial contention windows of different clients. However IEEE 802.11e may not be adequate for guaranteeing QoS in large-scale enterprise environments [26]. Therefore, more control mechanisms will have to reside in centralized servers to ensure fairness.

Once a fairness objective function is determined, the next question is how to achieve such fairness in real networks. Numerous approaches have been proposed to achieve different fairness notions and provide fair service to clients. In multi-AP WLANs, a common approach is load balancing (intelligent association). With the default 802.11 setting, a client always associates with an AP with the strongest RSSI (Received Signal Strength Indicator), i.e., Strongest Signal First (SsF). Clearly, this may lead to unevenly distributed loads among APs and hence potential degradation in aggregate system throughput [26–28]. To address this problem, an effective solution is to consider more parameters in addition to RSSI when making the client-AP association decisions, such as load information of APs, channel variation and interference. Such techniques have been proposed in [29–31].

Another type of approaches is to use the cell breathing technique [32, 33], which allows APs to adjust their coverage areas via varying the transmit power of beacon frames. In [34], the authors proposed an efficient client-based approach for frequency assignment and load balancing in 802.11 WLANs that leads to better usage of the wireless spectrum. The authors of [35] proposed a load balancing algorithm by carefully planning client-AP association to balance load among APs. It has been shown in [35] that, in the fractional association case, a max-min load-balanced association plan results in a max-min fair bandwidth allocation among clients and vice versa. Note that the aforementioned schemes were all designed with fair bandwidth allocation as the target fairness criterion, we expect that our proposed fairness notion could be able to incorporate with these schemes seamlessly.

3.2 Issues of the existing fairness notions

The observation of existing research works motivates us to explore appropriate fairness notions and the corresponding implementation schemes to provide fair services among the clients in WMNs. We model the the "last-hop" part of WMNs as a multi-AP WLAN with assumption of unlimited bandwidth on APs to the Internet. The goal is to seek efficient approaches to achieve them. We begin our research by conducting detailed investigation on the limitations of two aforementioned fairness notions in multi-AP WLANs: Bandwidth-based Fairness (*BbF*) and Timeshare-based Fairness (*TbF*).

3.2.1 Limitation of BbF

Given a client-AP association plan, bandwidth allocations of clients are calculated using the simple load calculation model specified in [35], which ignores the transmission overheads such as contention window and backoff time periods. Specifically, let C be the client of our interest and let A_C denote the AP that C is associated with. Furthermore, let $\{A_C\}$ denote the set of clients that are associated with A_C. Then the bandwidth allocated to C can be calculated by

$$B_C = \frac{1}{\sum_{C' \in \{A_C\}} \frac{1}{R_{C',A_C}}}, \tag{3.1}$$

where R is the data rate between two stations. Consider the multi-AP WLAN shown in Fig. 3.1. Two 802.11a [2] APs (A_1 and A_2) operate on non-interfering frequency channels and two clients, C_1 and C_2, may be associated with either AP. All stations are running the basic 802.11 DCF. Circles represent APs' coverage areas with radius of *r*. Each line represents a possible client-AP association and the number near the line represents the data rate (in Mbps) of the corresponding wireless link.

Possible client-AP association plans and the corresponding bandwidth allocations are compared in Table 3.1. Clearly, the best association plan to achieve max-min BbF is to associate C_1 with A_1, and C_2 with A_2, respectively. Unfortunately, it results in a system throughput of 21 Mbps, which is only 35% of the maximum possible 60 Mbps. This example clearly shows the performance anomaly with BbF in multi-AP WLANs, where bandwidth allocation to the high-rate client C_1 is affected by the low-rate client C_2.

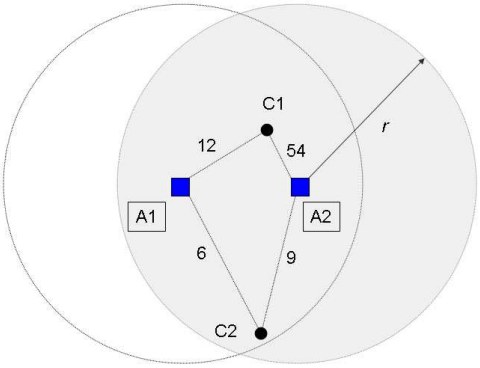

Figure 3.1 Example I to illustrate performance anomaly with BbF

Table 3.1 Bandwidth of different client-AP association plans in Example I

Client-AP Association Plan	B_{C_1}	B_{C_2}	B_{sys}	BbF Decision
$\{C_1 \leftrightarrow A_1, C_2 \leftrightarrow A_2\}$	12	**9**	21	$\surd$
$\{C_1 \leftrightarrow A_2, C_2 \leftrightarrow A_1\}$	54	**6**	60*	
$\{C_1 \leftrightarrow A_1, C_2 \leftrightarrow A_1\}$	**4**	**4**	8	
$\{C_1 \leftrightarrow A_2, C_2 \leftrightarrow A_2\}$	**7.7**	**7.7**	15.4	

3.2.2 Limitation of TbF

TbF was proposed to address the BbF-caused performance anomaly in single-AP WLAN. Rather than allocating fair bandwidth to clients, the goal of TbF is to assign equal channel access time to all clients such that high-rate clients could transmit more data than low-rate clients during the same time period, thus yielding higher system throughput.

Consider the WLAN shown in Fig. 3.2. Two 802.11a APs (A_1 and A_2) operate on non-interfering frequency channels and there are three clients in the network. C_2 may be associated with either AP, but C_1 can only be associated with A_1, and C_3 with A_2 respectively. Clients such as C_1 and C_3 are called *1-AP clients*, because they are only able to communicate with a single AP. Similar to the calculation of bandwidth allocation for BbF, timeshare allocated to a client C can be calculated by

$$T_C = \frac{\frac{1}{R_{C,A_C}}}{\sum_{C' \in \{A_C\}} \frac{1}{R_{C',A_C}}}. \tag{3.2}$$

where R is the data rate between two stations. Possible client-AP association plans and the corresponding bandwidth and timeshare allocations are compared in Table 3.2. The best plan to achieve max-min

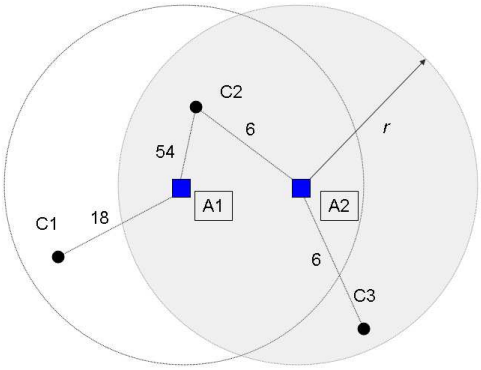

Figure 3.2 Example II to illustrate association anomaly with TbF

TbF fairness is to associate C_1 with A_1, while C_2 and C_3 with A_2. The resulting system throughput is 24 Mbps, which is significantly lower than the maximum possible 33 Mbps. In this example, association anomaly occurs to C_2 as it chooses to communicate with A_2 at the low 6 Mbps rather than communicating with A_1 at the high 54 Mbps, which is caused by the low-rate 1-AP client C_3. In general, the presence of low-rate 1-AP clients is one of the main reasons to cause association anomaly.

Table 3.2 Bandwidth and timeshare allocations with different client-AP association plans in Example II

Client-AP Association Plan	B_{C_1}	B_{C_2}	B_{C_3}	B_{sys}	T_{C_1}	T_{C_2}	T_{C_3}	TbF Decision
$\{C_1 \leftrightarrow A_1, C_2 \leftrightarrow A_1, C_3 \leftrightarrow A_2\}$	13.5	13.5	6	33*	0.75	**0.25**	1	
$\{C_1 \leftrightarrow A_1, C_2 \leftrightarrow A_2, C_3 \leftrightarrow A_2\}$	18	3	3	24	1	**0.5**	**0.5**	$\surd$

3.3 Problem definition

The observed limitations of BbF and TbF motivate the need for defining a more fitting fairness notion for such multi-AP WLANs scenarios in WMNs. The new fairness notion should (1) address the identified performance anomaly as well as association anomaly issues in multi-rate multi-AP WLANs; and (2) achieve balance between overall system capacity and fair resource allocation among all clients.

3.4 Proposed fairness notion

3.4.1 Fulfillment-based fairness (FbF)

We propose a new fairness notion called the Fulfillment-based Fairness (FbF) for multi-AP WLANs. The goal of FbF is to address both performance anomaly and association anomaly in multi-AP WLANs. FbF takes into consideration clients' maximum transmission rates as well as their association options to different APs. It emphasizes fair bandwidth fulfillment among clients rather than fair allocation of the absolute bandwidth or the access time. A client's *bandwidth fulfillment level* is a new concept. Formally, it is defined as the ratio of a client's actual bandwidth allocation to its *maximum attainable bandwidth allocation*, which is achieved with the most favorable (with respect to this client) association plan that (1) reduces as much as possible the load of the AP this client is associated with, while (2) guaranteeing that each client is served by one of the APs. Note that A client's maximum attainable bandwidth allocation could be different from its maximum transmission rate. Next, we will revisit the previous examples and describe how FbF address the performance anomaly and association anomaly issues.

3.4.2 Examples revisited

Let's first revisit Example I with FbF. Since the most favorable association plans for C_1 and C_2 are $\{C_1 \leftrightarrow A_2, C_2 \leftrightarrow A_1\}$ and $\{C_1 \leftrightarrow A_1, C_2 \leftrightarrow A_2\}$, respectively, their maximum attainable bandwidth allocations are 54 Mbps and 9 Mbps, respectively, which happen to be the same as their maximum transmission rates. Possible client-AP association plans and the corresponding bandwidth allocations and fulfillment levels (denoted as F) are compared in Table 3.3. Results show that the association plan to achieve max-min FbF indeed results in the highest system throughput, thanks to the fact that a client's bandwidth fulfillment level reflects not only its maximum transmission rate but also its available association options.

We now revisit Example II. From the comparison results shown in Table 3.4, we can see that max-min FbF and maximum system throughput are, again, achieved simultaneously. In this example, the most favorable association plans for C_1, C_2, and C_3 are $\{C_1 \leftrightarrow A_1, C_2 \leftrightarrow A_2, C_3 \leftrightarrow A_2\}$,

Table 3.3 Example I revisited with FbF

Association Plan	B_{C_1}	B_{C_2}	B_{sys}	F_{C_1}	F_{C_2}	FbF
$\{C_1 \leftrightarrow A_1, C_2 \leftrightarrow A_2\}$	12	9	21	**0.22**	1	
$\{C_1 \leftrightarrow A_2, C_2 \leftrightarrow A_1\}$	54	6	60*	1	**0.67**	$\surd$
$\{C_1 \leftrightarrow A_1, C_2 \leftrightarrow A_1\}$	4	4	8	**0.07**	0.44	
$\{C_1 \leftrightarrow A_2, C_2 \leftrightarrow A_2\}$	7.7	7.7	15.4	**0.14**	0.86	

$\{C_1 \leftrightarrow A_1, C_2 \leftrightarrow A_1, C_3 \leftrightarrow A_2\}$, and $\{C_1 \leftrightarrow A_1, C_2 \leftrightarrow A_1, C_3 \leftrightarrow A_2\}$, respectively. Hence, their maximum attainable bandwidth allocations are 18 Mbps, 13.5 Mbps, and 6 Mbps, respectively. Notice the difference between C_2's maximum attainable bandwidth allocation of 13.5 Mbps and its maximum transmission rate of 54 Mbps. This is because, even with the most favorable association plan, C_2 still has to contend with C_1 to communicate with A_1. In fact, maximum attainable bandwidth allocations vary with the percentage of 1-AP clients in the network and their maximum transmission rates. In general, the differences between maximum attainable bandwidth allocations and maximum transmission rates become less significant with smaller number of 1-AP clients present in the network. In the extreme case when there are no 1-AP clients in the network, i.e., each client can communicate with at least two APs, maximum attainable bandwidth allocations are the same as maximum transmission rates.

Table 3.4 Example II revisited with FbF

Client-AP Association Plan	B_{C_1}	B_{C_2}	B_{C_3}	B_{sys}	F_{C_1}	F_{C_2}	F_{C_3}	FbF Decision
$\{C_1 \leftrightarrow A_1, C_2 \leftrightarrow A_1, C_3 \leftrightarrow A_2\}$	13.5	13.5	6	33*	**0.75**	1	1	$\surd$
$\{C_1 \leftrightarrow A_1, C_2 \leftrightarrow A_2, C_3 \leftrightarrow A_2\}$	18	3	3	24	1	**0.22**	0.5	

3.4.3 Optimization algorithms

The authors of [35] showed that it is an NP-hard problem to find client-AP association plans to achieve max-min fairness in practical multi-AP WLANs. We present two algorithms to calculate the optimal association plan based on the proposed fulfillment-based fairness notion: (1) the **Simple_maxmin** algorithm to find optimal client-AP association plans to achieve max-min fairness in small-scale networks via simple permutation test, and the pseudo code of this algorithm is shown in Fig. 3.3; (2) the

RS_maxmin algorithm to find client-AP association plans to achieve approximate max-min fairness in large-scale networks via random shuffle.

Algorithm 1 Simple_maxmin(A, C)

A : set of access points $\{a\}$
C : set of clients $\{c\}$
X : client-AP association plan $\{c \leftrightarrow a\}$
$\vec{S}$: resource allocation vector sorted in non-decreasing order

1: $\vec{S}_{maxmin} = \vec{0}$;
2: $X_{maxmin} = null$;
3: **for** $(\forall X)$ {
4: $\vec{S}_X = \vec{0}$;
5: Assign client-AP associations according to X;
6: **for** $(\forall c \in C)$
7: Calculate c's allocated resource s_c;
8: **if** $(\vec{S}_X > \vec{S}_{maxmin})$ {
9: $\vec{S}_{maxmin} = \vec{S}_X$; $X_{maxmin} = X$;
10: }
11: }
12: **return** X_{maxmin}

Figure 3.3 Pseudo-code of the Simple_maxmin algorithm

The pseudo code of **RS_maxmin** is shown in Fig. 3.4. During each random shuffle, each client in the network is assigned with a random number and the client list is then sorted according to the random numbers. Starting from the client with the smallest number, each client determines its AP association that improves the resource allocation vector the most. This process continues and loops around the client list until the resource allocation vector stops improving. We repeat random shuffles for a certain number of times and record the one that results in the best resource allocation vector.

3.5 Performance evaluation

We carry out extensive simulations to study the performance of FbF, BbF and TbF under various scenarios.

3.5.1 Simulation setup

In our simulation, we assume that:

Algorithm 2 RS_maxmin(A, C)

$A, C, X, \vec{S}$: same as those in **Simple_maxmin**

1: $\vec{S}_{maxmin} = \vec{0}$;
2: $X_{maxmin} = null$;
3: **while** ($n <$ *num_shuffle*){
4: $\vec{S'}_{maxmin} = \vec{S'} = \vec{0}$;
5: $X'_{maxmin} = X' = null$;
6: Let C' be a random permutation of C;
7: **while** TRUE{
8: **for** ($\forall c \in C$) {
9: **for** ($\forall a \in A$) {
10: **if** (c associating with a improves $\vec{S'}$)
11 Associate c with a in X';
12: }
13: }
14: **if** ($\vec{S'} > \vec{S'}_{maxmin}$) {
15: $\vec{S'}_{maxmin} = \vec{S'}$; $X'_{maxmin} = X'$;
16: }
17: **else** break;
18: **if** ($\vec{S'}_{maxmin} > \vec{S}_{maxmin}$) {
19: $\vec{S}_{maxmin} = \vec{S'}_{maxmin}$; $X_{maxmin} = X'_{maxmin}$;
20: }
21: }
22: n++;
23: }
24: **return** X_{maxmin}

Figure 3.4 Pseudo-code of the RS_maxmin algorithm

- All clients and APs are static;
- The setup of the WMN backhaul is perfect such that each AP operates as it is directly connected to the Internet. The bandwidth between APs and the Internet is much higher than the that of the links between clients and APs.
- Each station is equipped with an IEEE 802.11a interface that may transmit at one of the eight available rates: 6, 9, 12, 18, 24, 36, 48, and 54 Mbps;
- MAC protocol is the basic 802.11 DCF;
- The reachability and the maximum transmission rate between a client and an AP is determined by the distance between them;

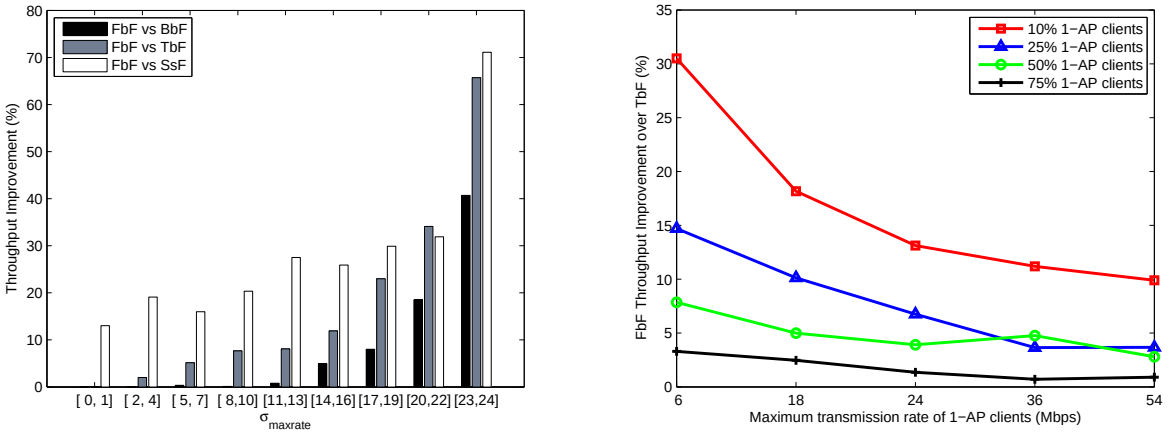

(a) Comparison of all testing schemes under various rate diversity among clients

(b) Comparison of FbF and TbF under various percentage of 1-AP clients and various maximum transmission rate of such 1-AP clients

Figure 3.5 Results of small-scale networks

- Rate adaptation is disabled;
- All APs operate on non-interfering frequency channels.

We simulate two types of network scenarios: (1) small-scale networks with 3 APs and 10 clients, where optimal client-AP association plans to achieve max-min fairness are determined by the **Simple_maxmin** algorithm; (2) large-scale networks with 10 APs and 40 clients, where client-AP association plans to achieve approximate max-min fairness are determined by the **RS_maxmin** algorithm.

We compare the performances of client-AP association plans corresponding to Fulfillment-based Fairness (FbF), Bandwidth-based Fairness (BbF), and Timeshare-based Fairness (TbF), as well as the naive Strongest Signal First (SsF) association plan. Performance metric is the aggregate system throughput. In each simulation run, clients send CBR flows to their associated APs. Data rates are set high enough to saturate the channel. Each point in the figures is averaged over 100 simulation runs.

3.5.2 Small-scale networks

We first compare the performances of testing schemes when there are no 1-AP clients in the networks. Simulation results are shown in Fig. 3.5(a).

Note that Y-axis is not the absolute bandwidth measurement but the throughput improvement (in

percentage) of FbF over other testing schemes. X-axis represents the standard deviation of the maximum transmission rates among all clients, denoted by $\sigma_{maxrate}$, which we use to characterize the transmission rate diversity among clients. In 802.11a networks, $\sigma_{maxrate}$ can be as large as 24 Mbps since the maximum difference between available transmission rates is 48 Mbps.

We have the following observations: (1) In general, FbF outperforms other testing schemes, and when the rate diversity is high, the performance improvements of FbF over other schemes become more significant; (2) When the rate diversity is low, BbF and FbF show comparable performances; this is because the inherent performance anomaly with BbF is less likely to occur when most stations transmit at similar data rates; on the other hand, when the rate diversity is high, most likely BbF will exhibit performance anomaly; as shown in the figure, when $\sigma_{maxrate}$ is between 23 and 24 Mbps, FbF outperforms BbF by more than 40%; (3) TbF does not perform well because of its inherent association anomaly while the poor performance of SsF is most likely due to the unbalanced loads among APs.

Fig. 3.5(b) compares the throughput improvement of FbF over TbF with various percentages of 1-AP clients in the network and various maximum transmission rates of such 1-AP clients. As shown in the figure, with a fixed percentage of 1-AP clients in the network, the improvement of FbF over TbF increases as the maximum transmission rate of 1-AP clients decreases. This confirms our earlier discussion that the presence of low-rate 1-AP clients is one of the main reasons to cause association anomaly. On the other hand, with the fixed maximum transmission rate of 1-AP clients, the improvement of FbF over TbF decreases with more 1-AP clients present in the network. This makes sense because, with more 1-AP clients, fewer clients in the network are able to adjust their associations, and consequently, the benefit of applying intelligent association control becomes less salient. In fact, when the percentage of 1-AP clients reaches 100%, each client can only communication with a single AP, i.e., the client-AP associations have already been determined; hence all fairness notions are equivalent.

3.5.3 Large-scale networks

We repeat the above simulations for large-scale networks and the number of random shuffles in the **RS_maxmin** algorithm was set to 1000. Simulation results are plotted in Figs. 3.6(a) and 3.6(b). Similar trends can be observed in large-scale networks as those in small-scale networks, while the

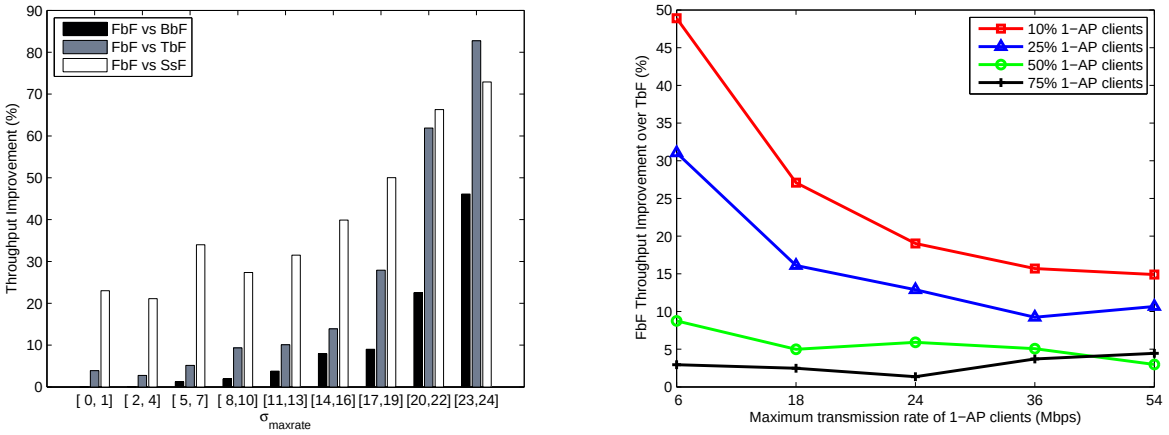

(a) Comparison of all testing schemes under various rate diversity among clients

(b) Comparison of FbF and TbF under various percentage of 1-AP clients and various maximum transmission rate of such 1-AP clients

Figure 3.6 Results of large-scale networks

throughput improvement of FbF over other testing schemes becomes even more significant. This is because larger-scale networks offer more options for client-AP associations and hence more room for performance enhancement.

3.5.4 Summary

Simulation results show that FbF leads to vastly improved system throughput in the presence of high transmission rate diversity among clients and/or low-rate 1-AP clients that can only communicate with a single AP at low transmission rates, which can be often observed in practical WMNs. Hence, we conclude that FbF seems to be an attractive fairness notion when designing and managing the "last-hop" connections in WMNs.

3.6 Conclusion

We investigate the fair service provisioning problem in the client-AP association control in WMNs. We present a new fairness notion Fulfillment-based Fairness (FbF) based on the identified issues. Fairness is, of course, a subjective notion, and we don't claim that the proposed FbF is "fairer" than others. In comparison to existing fairness notions, such as Bandwidth-based Fairness (BbF) and Timeshare-based Fairness (TbF), the key idea of FbF is to allocate bandwidth to clients in proportion to their

respective maximum attainable bandwidth allocations, which takes into consideration not only clients' maximum transmission rates but also their association options. As a result, FbF does not suffer anomalies inherent with existing fairness notions for multi-AP WLANs scenarios. Moreover, our work can be easily extended to study the scenarios where each AP has a pre-determined bandwidth limit to the Internet.

In this work, we assume that all clients have the same weight, however it can be extended to scenarios with heterogenous client weights. Future work includes considering FbF jointly with channel assignment to APs and studying relevant problems, e.g., how to determine clients' bandwidth allocations and fulfillment levels when APs operate on overlapping or partially-overlapping frequency channels. Moreover, if reducing computation time and the gap between approximation and optimization solutions are critical, the performance of the proposed heuristic algorithm could be improved by using LP-based approximation algorithms for network optimization.

CHAPTER 4. CYMESH: WIRELESS MESH NETWORK TESTBED AT ISU

4.1 Motivation

In most wireless network research, performance evaluation has been addressed through numerical analysis and simulations. Although simulation offers a convenient combination of flexibility and controllability, there exists significant evidence that simulation results could be difficult to transfer into reality. The main reason is that most simulations are based on simplistic assumptions or abstracted models which neglect many factors that could affect the performance of real world networks. To study the potential capability and performance of WMNs in real world, experimentation is probably the most reliable method. We have deployed CyMesh, a multi-radio multi-channel (MRMC) wireless mesh network testbed using off-the-shelf IEEE 802.11 equipments in the Electrical and Computer Engineering and Computer Science department buildings at Iowa State University. The main objects of CyMesh are to evaluate the algorithms and schemes we proposed in previous chapters and to build an extendable platform for future research in WMNs.

In this chapter, we first describe our experiences on the design and implementation of CyMesh. We also deliberate the hardware and software components and deployment details of the testbed. We then present our experimental results and discuss the encountered issues, observations and learned lessons. Our main contributions are: (1) reporting on the encountered problems, key observations and proposed solutions in the design and deployment of an MRMC wireless mesh network testbed; (2) evaluating the performance of our proposed schemes, AETD, as discussed in Chapter 2.

4.2 Related work

A number of wireless testbeds with various design goals have been built in academia and industry. The meritorious characteristic spectrum of these testbeds is wide with overlapping and non-overlapping features. In this section, we present a survey on the works that are most relevant to the design components of CyMesh. We present a review of the testbeds that are compliant with IEEE 802.11 standards and share the similar research objectives with CyMesh. From hardware point of view, we group them in two categories: single-radio single-channel (SRSC) architecture and MRMC architecture. We also review a number of different approaches in network management. We highlight their advantages and techniques used to address the core design issues, and compare them with CyMesh in the related aspects.

4.2.1 SRSC testbeds

Most earlier wireless network testbeds use a SRSC platform for evaluating wireless protocols. MIT RoofNet [36] is one of the pioneer testbed implementations using readily available IEEE 802.11-compliant hardware. RoofNet consists of over 40 active nodes as in 2007. By providing broadband Internet access to users near the MIT campus, Roofnet aims to conduct 802.11 measurement experiments, and study the problems of high-throughput routing, adaptive bit-rate selection and unplanned mesh architecture. The Broadband and Wireless Network (BWN) Lab at Georgia Institute of Technology has built BWN-Mesh [37], a WMN testbed consisting of 15 IEEE 802.11b/g based mesh routers, several of which are connected to the Internet. The research is focused on adaptive protocols for transport, routing and MAC layer design. The experiments demonstrate that the existing protocols (i.e., TCP, AODV, and 802.11 as transport, routing and MAC layer protocols) do not perform well in terms of end-to-end delay and throughput in WMNs. The ORBIT (Open Access Research Testbed for Next-Generation Wireless Networks) [38] system is a wireless network testbed with a two-tier architecture that has been deployed at Rutgers University. In ORBIT, every node is always connected to a wired backbone to make experiments easier to monitor and manage, so their management is realized entirely through the wired infrastructure. ORBIT is available to researchers for remotely controlled experiments. CyMesh uses the similar approaches as ORBIT and offers functionalities of remote management and configuration.

A mesh network has been deployed in the under-resourced community at Houston's East End by Rice University and Technology For All (TFA) [39]. The network consists of 18 nodes spanning approximately 3 square kilometers and provides Internet access services to over 4,000 users as of 2007. Extensive measurements are performed to characterize the propagation environment and correlate received signal strength with application layer throughput. They demonstrate that by careful placement of the Internet gateway and router nodes, the network performance improves by up to 50 percent with respect to both throughput and reliability.

4.2.2 MRMC testbeds

Since single-radio based networks operate on the same frequency channel, performance is inevitably impacted by interference. Researchers have studied using multiple radios to alleviate interference and improve system capacity. The University of California, Santa Barbara Mesh Testbed [40] is an experimental wireless mesh network deployed on five floors of the Engineering building of UCSB. The network consists of 15 nodes, and each node is equipped with multiple IEEE 802.11a/b/g wireless cards. Their research focuses on designing protocols and systems for robust operation of multi-hop wireless networks. MAP [41] is an experimental wireless mesh network testbed at Purdue University that contains 32 nodes, including laptops and PDAs with IEEE 802.11a/b/g wireless cards. They study how to exploit the multi-radio feature of WMNs and provide satisfactory Internet access services to mobile users. A WMN testbed using Intel IXP425 series XScale network processors as routers and iPAQ PDA as clients has been built at Carleton University [42]. Two wireless LAN cards are installed on the mini-PCI slots at each mesh node. One of them is an IEEE 802.11a/g compliant radio, which is the backbone traffic carrier. Another is an IEEE 802.11b radio, which provides access to wireless clients. Such setup enables higher bandwidth transmission in the backbone; however, such setup lacks flexibility in network planning and the capacities of the links between clients and mesh routers are also limited.

Researchers at Intel have deployed a multi-radio mesh network testbed designed for home use and its characteristics have been studied in [43]. One of their key observations is that even slightest adjustment in the position of the nodes or the alignment of the antennas could lead to significant changes

in performance results [44], thus realtime monitoring could give users feedback on how to configure and deploy a wireless mesh network for better performance. We have similar observations on node configuration and antenna setup during the deployment of CyMesh. Another indoor testbed is deployed by Microsoft Research to study the routing problem in MRMC networks. They have developed a mesh layer module called MCL (Mesh Connectivity Layer) [45], which uses WCETT as the routing metric. CyMesh is built on MCL and extended to support multiple routing metrics and provide more functionalities for network management and configuration.

There are also a variety of wireless testbeds built to serve other research purposes. For example, to eliminate the effect of interference from other devices operating in the ISM bands, iWWT (Illinois Wireless Wind Tunnel) [46] is proposed to be implemented in an electromagnetic anechoic chamber at the University of Illinois at Urbana-Champaign. The goal of iWWT is to build a repeatable experimental environment and study the effect of various parameters in the presence of interference. A number of testbeds have been built to study the capacity degradation problem in multihop wireless networks [47–49]. In addition, some researchers proposed to use cross-layer schemes for interference-aware channel selection while some others focus on intelligent scheduling for packet transmissions [50, 51].

4.2.3 Network management in WMNs

Network management is an important component of WMNs for performance monitoring, parameters configuration and software distribution. Simple Network Management Protocol (SNMP) [52] is a popular network management protocol. It is originally designed for wired networks using a centralized design. In SNMP, each network device maintains minimal states in the form of counters and variables. The SNMP protocol allows periodic polling of variables that are triggered by network events. A Network Management System (NMS) periodically polls each device from a central server and presents the information to an administrator. SNMP serves as a monitoring tool and leaves the task of analysis and management to humans or other software tools. Several commercial mesh systems are bundled with SNMP-based or proprietary centralized management solutions [53, 54]. The working philosophy of MCL is similar to SNMP; however, MCL works in a distributed manner without centralized control,

and hence MCL does not rely on a "centralized" server.

The aforementioned mesh testbed at UCSB is managed by a set of interconnected components called MeshMan (for management and configuration), MeshMon (for parameter monitoring), and MeshViz (for topology visualization) [108]. Most of the mesh nodes use a wired back-haul for information management and easier control of experiments in the testbed. SCUBA [55] is an interactive visualization framework designed to assist in the diagnosis of large-scale wireless mesh networks, which is implemented on a 15-node mesh testbed at UCSB. Various metrics from the network are collected in a central database through a gateway node. SCUBA queries the database to drive its interactive visualization tools. SCUBA in its present form has limited diagnostic capabilities, but could potentially be used as a complementary tool for MeshMon to help the system administrator visualize the network. Our approaches share some similarities with them; however, network management and update distribution in CyMesh can be performed either by the wired connection or mesh network itself. In most cases, wired connection is used only for debugging and fault diagnosis. Furthermore, CyMesh does not rely on the wired back-haul for monitoring and visualization. Instead, we exploit the MCL proactive link update information which has very limited impact on user traffic.

The Distributed Ad hoc Monitoring Network (DAMON) [56, 57] developed at UCSB is another distributed system for monitoring ad hoc and sensor networks. It monitors network behavior and sends collected measurements to data repositories or sinks. DAMON is designed for evaluating AODV but it also supports monitoring of a range of protocols, devices and network parameters. JANUS [58] is a framework for distributed monitoring of WMNs. Their proposed approach uses Pastry to retrieve network information that is collected at different layers of the stack, which is available at all nodes in the system. Pastry is an early work in peer-to-peer overlay network [59]. They test the initial prototype of JANUS system on Windows platform. Similiar to CyMesh, nodes in JANUS also use the Link Quality Source Routing (LQSR) protocol implemented in MCL [45].

In this section, we have reviewed the current and previous works on to wireless network testbeds, which provide us an useful guidance in the design of CyMesh in many aspects such as hardware and software selections, functionality, extendability and cost efficiency. In the following section, we present the design and implementation details of CyMesh.

4.3 Design goals

Our goal is to build a wireless platform for development and evaluation of new protocols in WMNs. The testbed should possess the following characteristics:

- Reliability and Robustness: It is desired that the testbed can maintain network connectivity with unmanned operation, and can deal with software and hardware failures robustly with self-healing and fast reconfiguration capabilities. This is important for WMNs to handle interruptions such as broken links, failed nodes, human's interventions or physical obstructions.

- Flexibility: It is critical that users of the testbed can easily tune the basic network parameters and implement new routing components.

- Scalability and Efficiency: The mesh routing protocols used in the testbed should induce low overhead to keep the network scalable with increasing number of nodes. The impact of control overhead on user traffic should be kept to the minimum level.

- Reproducibility: The testbed should be able to produce similar results with similar environments and configurations.

- Visualization and Monitoring: A graphic representation of the network is essential to understand the network topology and node/link conditions. Monitoring the status of many nodes in a scalable manner is a challenging task. It is important that the management and monitoring related traffics do not affect the user traffic yet be frequent enough to be meaningful and adaptive to changing network conditions.

- Remote Configuration and Management: The testbed should allow users to remotely manage or configure the network, carry out experiments, and preferably distribute update to all nodes with zero-on-site operation. In addition, the testbed should also be accessible for researchers from anywhere in the world.

- Cost-efficiency: The cost of the testbed should be kept reasonably low but without compromising the desired capabilities and functionalities.

The design of CyMesh is primarily motivated by the above factors. In the next section, we will describe various options to build CyMesh and discuss how our choices of hardware and software components meet the design goals.

4.4 Design and implementation

4.4.1 Overview of CyMesh

Currently, CyMesh consists of 9 stationary nodes (desktop PC) deployed in Coover Hall (Department of Electrical and Computer Engineering) and the Atsantoff Hall (Department of Computer Science) at Iowa State University. In addition, 3 mobile nodes, including one laptop and two PDAs, are used to provide flexibility in topology management. The stationary nodes together form a topology with over 12 wireless links covering a variety of link conditions such as indoor and outdoor, line-of-sight (LOS) and none-line-of-sight (NLOS). All PCs and laptops operate on Windows XP Professional and all PDAs operate on Windows Mobile 5.0 operating system (O.S.). We employ the MCL (Mesh Connectivity Layer) in conjunction with MR-LQSR (Multi-Radio Link Quality Source Routing) [45] as the mesh control and routing module for CyMesh. Furthermore, a set of customized software have been developed using Java and script language for the purposes of network visualization, management, configuration and remote experiment setup. We now describe the design and implementation of CyMesh in detail.

4.4.2 Platform selection

There exist numerous options for the architecture of our testbed: from PCs to GNU Software Radio as hardware platforms, and from Windows to Linux as O.S.. Each solution has different advantages and disadvantages. To select one that fits our design requirements best, we have performed extensive research with the considerations discussed in Chapter 4.3. In addition, the hardware should offer flexibility to support multiple wireless interfaces and extendability for future upgrade. Remote access should be available at all stationary nodes, allowing easy configuration and diagnosis. Users should be able to carry out experiments from virtually anywhere through the Internet. Moreover, the hardware should be widely available and cost-efficient.

After thorough search and comparison, we select PC and MCL (Mesh Connectivity Layer) [45] as the hardware and software platforms of CyMesh for the following reasons. Firstly, the overall performance of different platforms could vary considerably due to the difference in computing power and bandwidth among several interfaces (e.g., PCI, USB, serial port, etc). Most PC platforms have the general CPU with high clock and bus speed and therefore are superior to the embedded ones in computing power. This is important to implement various complex protocols on mesh nodes and allow future growth in application and protocol complexity. Secondly, the hardware must have the capability to support multiple IEEE 802.11 wireless cards (adapters). PC platform offers high speed interfaces including PCI, USB, PCMCIA, IEEE 1394 and so on. In addition, using PC allows us to equip each desktop node with a PCI and a USB wireless adapter with necessary physical separation to avoid the radiation leakage. Thirdly, the Windows XP O.S. provides us a powerful platform for developing custom-built softwares including network visualization, monitoring, configuration, diagnosis and remote experimentation. Finally, all the desktop nodes used in CyMesh are 2-3 years old workstation PCs recycled from a hardware upgrade of a ECpE department teaching lab. Even though these workstations are not the newest model, they are more powerful than most embedded platforms and also significantly lower the cost of the testbed. In summary, this platform setup is flexible, cost-efficient and powerful enough to meet our design goals, which allows us to easily implement new network protocols and quickly deploy for practical experiments.

4.4.3 Hardware components

CyMesh's hardware components include: (1) nine Dell Precision 360 workstations running Windows XP SP2, which allows up to four wireless interfaces (adapters); (2) one Dell D400 Laptop running Windows XP SP2 as mobile node; and (3) two HP iPAQ PDAs running Windows Mobile 5.0 which function as clients only. To enable remote access, all stationary nodes are connected to the Internet.

Each desktop and laptop is equipped with two IEEE 802.11 adapters to create an MRMC environment. To avoid the effect of electromagnetic waves between two closely-located adapters (cards), we install one PCI and one USB card on each desktop node. We test the following four adapters to evaluate the possible performance difference between the cards of different models and manufacturers, they are

Netgear MA311 802.11b PCI, Trendnet TEW-423PI 802.11b/g PCI, LinkSys WPC55AG 802.11a/b/g PCMCIA and LinkSys WUSB55AG USB card. The default antenna gain on these cards is about 2 dBi; however, the Netgear MA311 and Trendnet TEW-423PI cards provide an option to connect to an external antenna, which enables us to increase the transmission range of these cards with higher gain antennas. The laptop has two wireless interfaces (including the built-in wireless card and a PCMCIA or USB card) while each PDA is equipped with only one wireless interface in Compact Flash format. In addition, we have some other equipments with specific purposes:

- USB extension cable: The PCI slots in most motherboards are very closely placed to each other, and two parallel wireless PCI cards may suffer severe signal leakage no matter what frequency channels they operate on [38, 60]. Therefore, we use USB extension cables to provide the necessary separation between the PCI card's antenna and the USB card. Our initial experiments clearly verify that such setup is a flexible way to measure and reduce the effect of leakage radiation.

- High gain antenna: Due to the deployment environment, some NLOS or outdoor links have poor link quality. These links are unstable when using the default antenna on the wireless adapters. Such poor quality links could significantly disrupt the routing protocol and make it difficult to repeat the experiments. Therefore, we employ high gain antennas and custom-made signal reflectors to improve the quality of such links.

- Custom-made signal reflector: We install the custom-made signal reflector to some adapters which cannot only boost the signal strength in certain direction but also function as attenuator to reduce interference from other directions.

4.4.4 Software components

Software architecture plays an important role in the implementation of wireless network testbeds. Mature software platform and proper configuration ensure a stable experiment environment, while minimizing the effects of unexpected node failure, software malfunction and interruption. When making decisions on software components, we consider the following factors. Firstly, we want to have the ability of modifying many aspects of the software, both in terms of implementation and parameter tuning.

Open-source software that allows for network-customized modifications is highly desired, especially for the mesh control and routing protocols. Otherwise, it will be very difficult to reflect users' intentions and evaluate the effectiveness of new protocols. Secondly, the O.S. should not consume a large portion of system resources, so it can support the mesh control software and a large variety of software tools for debugging, monitoring and measurement. Thirdly, software uniformity is necessary to support frequent software updates and modifications.

4.4.4.1 MCL: Mesh connectivity layer

MCL (Mesh Connectivity Layer) [45] is an open source WMN implementation developed by Microsoft Research. It is essentially a virtual adapter that Windows applications can use just like any other network interface. It comes with a configuration and diagnostic utility, as well as a link statistics and performance analyzer called ttcp. As show in Fig. 4.1, architecturally, MCL is a layer 2.5 protocol which fits between the network and link layers. MCL is transparent to the protocols running on top of it (e.g., TCP/IP), as well as those running beneath it (e.g., 802.11 MAC). Specifically, to higher layer applications, MCL appears to be just another Ethernet link, albeit a virtual link. To lower layer protocols, MCL appears to be just another protocol running over the physical link. There is hence no need to change these technologies in order to work with MCL.

As its routing protocol, MCL uses a modified version of Dynamic Source Routing [61], called Link Quality Source Routing (LQSR) that assigns relative weights to the links among the nodes. More in detail, information such as the channel, bandwidth, and loss are determined for every possible link and sent to all nodes. By exploiting these information, LQSR defines the best path for the data trans-

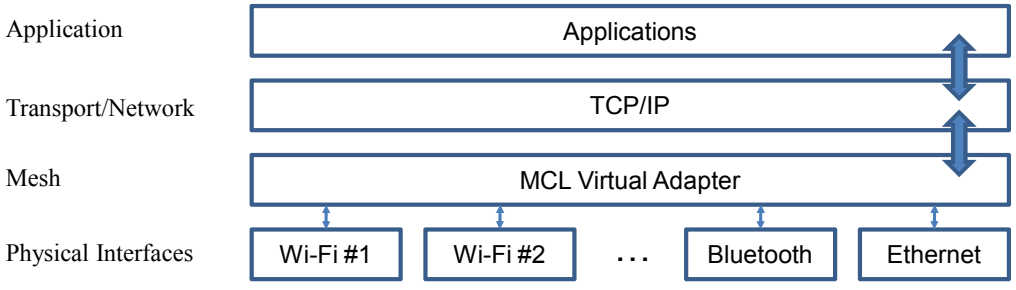

Figure 4.1 MCL functions as a layer 2.5 protocol

mission from a given source to a given destination. The utilized routing metric is known as Weighted Cumulative Expected Transmission Time (WCETT). If the optimum path between a particular source and the corresponding destination changes, LQSR updates the routing tables on the relevant nodes and modifies the route accordingly.

In summary, we choose MCL as the mesh network management module for CyMesh because: (1) MCL allows developers to test and compare various routing metrics by replacing the default WCETT with new metrics; (2) MCL provides seamless support to routing in MRMC networks, which is a key component of our research; during our experiments, we make changes in the routing stack of MCL source code, generate new executables, and then distribute them to all mesh nodes without modifying any other software components; (3) In Windows XP, we are able to use the Windows DDK (Driver Development Kit) and the Windows SDK (Software Development Kit) which provide powerful development environments for extending the capabilities of MCL.

4.4.4.2 CyMesh utility programs

We have developed a set of utility programs and automation scripts for network visualization, management and remote configuration. The software architecture of CyMesh and its interfaces to MCL are shown in Fig. 4.2.

Visualization and Monitoring The need to visualize the network is essential to implement wireless mesh networks. A graphic representation of the network is necessary to better understand how the network is deployed and how the nodes are interacting. Moreover, since the node and link conditions in wireless networks could vary and be unstable over time, the visualization system must be dynamic on a real time level. Finally, the ability to display the entire network from any mesh node would make the program much more portable.

With these considerations in mind, we have developed the CyMesh Utility GUI for network visualization, monitoring and management. As shown in Fig. 4.2, the visualization and monitoring module of CyMesh consists of four classes and one data structure. The main class, GUI, displays the graphical user interface. The GUI calls the Parser class at a fixed interval to obtain the most updated network information from MCL, and stores it in a data structure called Host. When a user clicks on a node

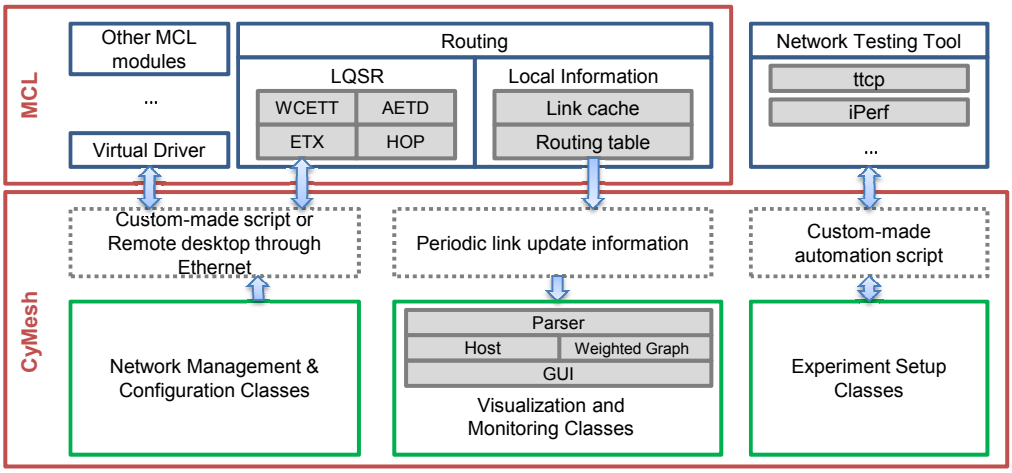

Figure 4.2 Software architecture of CyMesh

in the GUI, the routing table is calculated using the WeightedGraph class to help calculate the route information. WeightedGraph class is used to hold the network information as a weighted graph to make calculations easier. Finally, the Parser uses the current routing metric when calculating the information to store in Host. More specifically, in order to gather information of the mesh network, the CyMesh utility uses the MCL command, *mcl lc*. The *mcl lc* command displays the contents, plus information and statistics of the link cache. We then parse the output to obtain the information needed. For displaying the topology and calculate the routing table of each node, we require the following information: MAC address of the virtual adapter, the frequency channel it operates on, neighbor nodes of the virtual adapter and the Expected Transmission Time (ETT) values of each links. These values are stored in the Host data structure. The GUI then uses that to display the topology of the network.

This approach is favorable for this program since it allows all of the network information to be obtained from one node. A key feature of the CyMesh visualization tool is that it exploits the periodical link update information to visualize network topology, displays the most updated network conditions, and enables users to monitor link conditions, node status and routing tables in real time without introducing additional traffic to the network. Fig. 4.3 is a snapshot of the CyMesh GUI that depicts the network topology in Coover Hall. Note that the three desktop nodes in Atsantoff Hall are not shown in the GUI since the link between the two buildings is temporarily unavailable due to office relocation.

Network Management and Configuration The CyMesh GUI provides interfaces for network man-

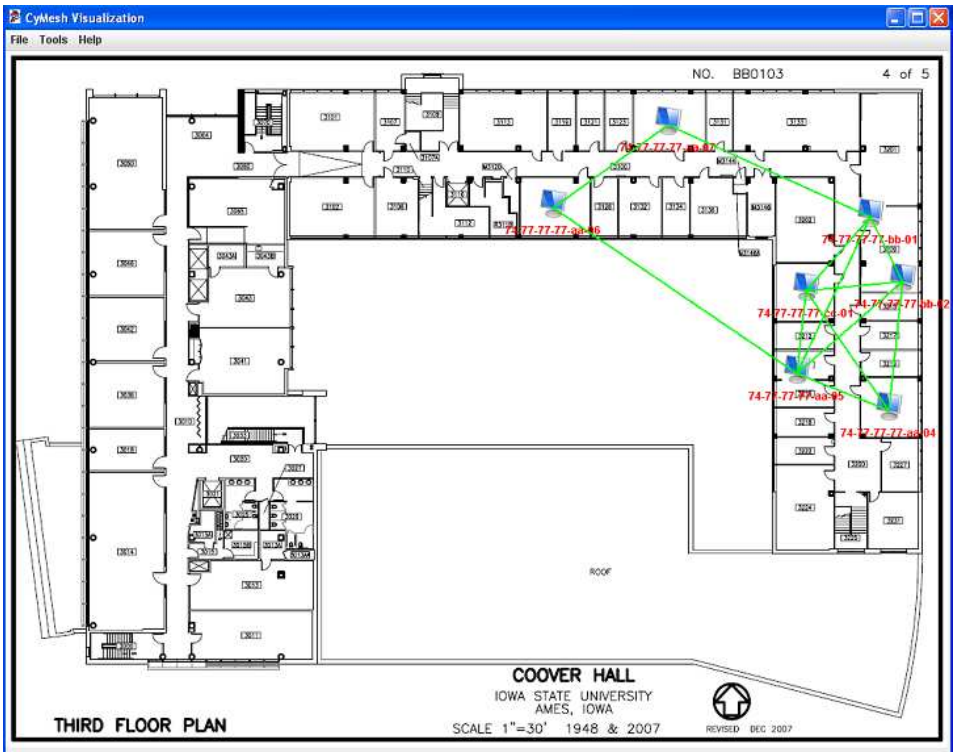

Figure 4.3 CyMesh network topology in the ECpE building at ISU Campus

agement and configuration. This is implemented by distributing MCL commands over Telnet connection using automation scripts. When users try to execute commands on remote nodes, the script will automatically establish a Telnet connection between the local host and the remote node in order to send commands and check results. For example, to implement the function of flushing the routing table and neighbor information cache of a node locally or remotely, we generate and store a VBScript (vbs) file on each node which will be executed by commands sent by local or remote users. A snapshot of the flush menu is shown in Fig. 4.4(c). Moreover, in order to evaluate different routing metrics and compare their performance with the default WCETT metric, we extend the LQSR module of MCL to support AETD, ETX and HOP routing metric, as discussed in Chapter 2. In order to switch between different routing metrics, one needs to change the source code in LQSR and recompile the entire MCL project to generate a set of new MCL executables. To simplify such time-consuming and inefficient process, we generate the MCL executables for all routing metrics and store them on each node, along with a VBScript file that can automatically change the routing metrics. As shown in Fig. 4.4(b), this

(a) Function menu

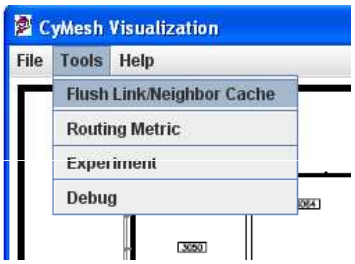

(b) Routing metric

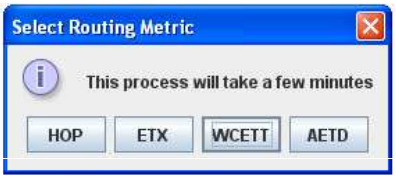

(c) Flush routing table & link cache

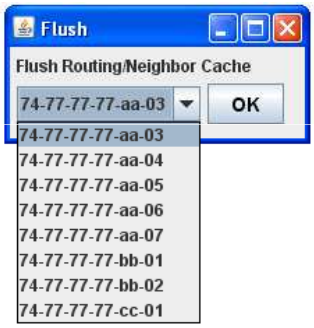

(d) Experiment setup

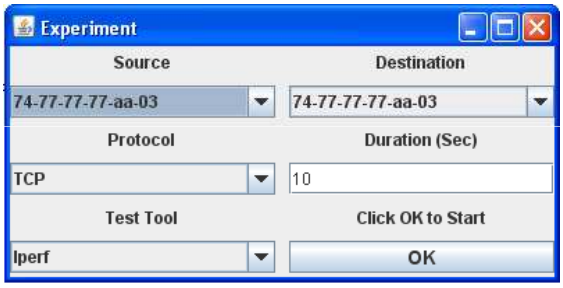

Figure 4.4 Snapshots of the CyMesh GUI

script can be executed locally or remotely through Telnet connection.

Carrying Out Experiment An important feature of CyMesh is allowing user to carry out network experiments easily through the CyMesh GUI. To realize this, we have installed ttcp and iPerf on all PC nodes for network performance testing, while ttcp is installed on all PDAs. Fig. 4.4(d) shows the experiment setup interface in the CyMesh GUI. Users can setup experiments from any mesh node with zero-on-site operation, which can greatly reduces the time spent in network experiments especially for large-size networks deployed in multiple buildings. Moreover, all these functionalities are available to researchers outside Iowa State University through the Internet. It should be noted that other network performance testing tools can be easily integrated in CyMesh in order to evaluate more web applications such as VoIP and video streaming.

iPerf operates in a client server manner, generating traffic between two devices and measuring key network criteria. It provides feedback in easy to understand tables and graphs, showing throughput, packet loss and jitter between the client and server. iPerf can be run from a command line or a GUI

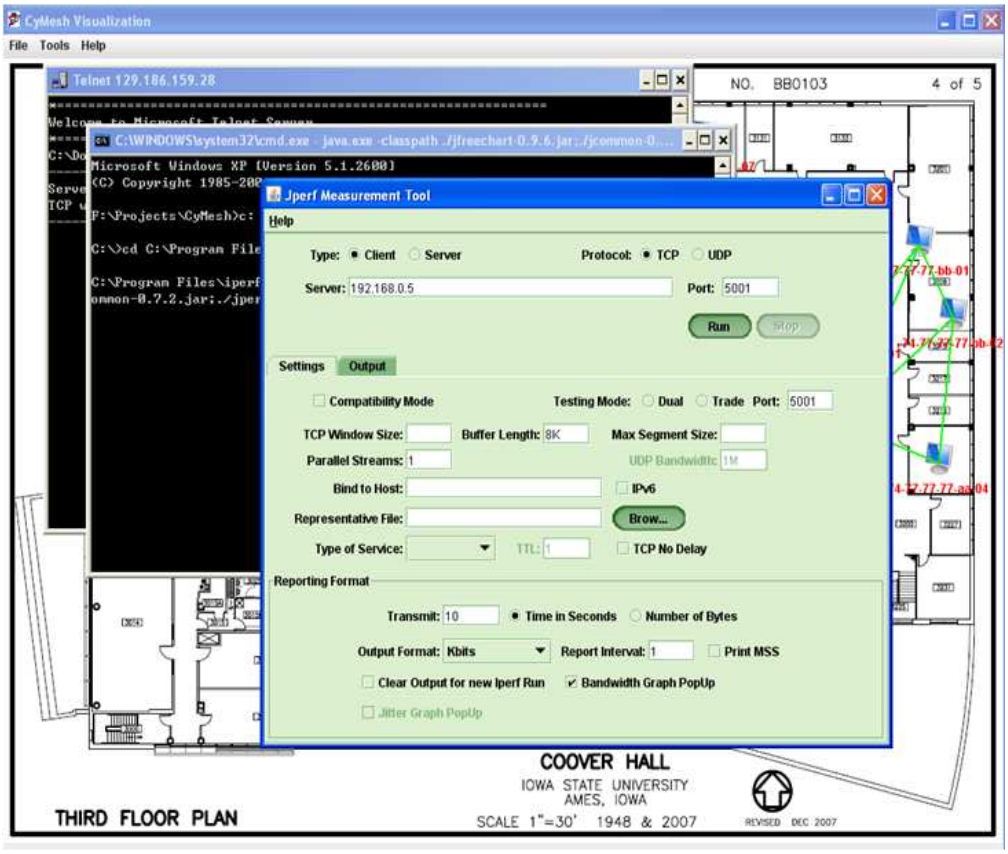

Figure 4.5 A snapshot of the JPerf utility

interface, called JPerf. We have integrated JPerf into CyMesh to measure communication channel characteristics, and provide statistics (e.g., bandwidth, jitter and packet loss) about the network links in CyMesh. Fig. 4.5 and Fig. 4.6 show the JPerf experiment setup interface and bandwidth analysis interface respectively.

With such a flexible software platform, we are able to conveniently and visually manage the whole CyMesh testbed from any mesh node or through the Internet. More importantly, the capabilities of CyMesh can be easily extended for other design purposes.

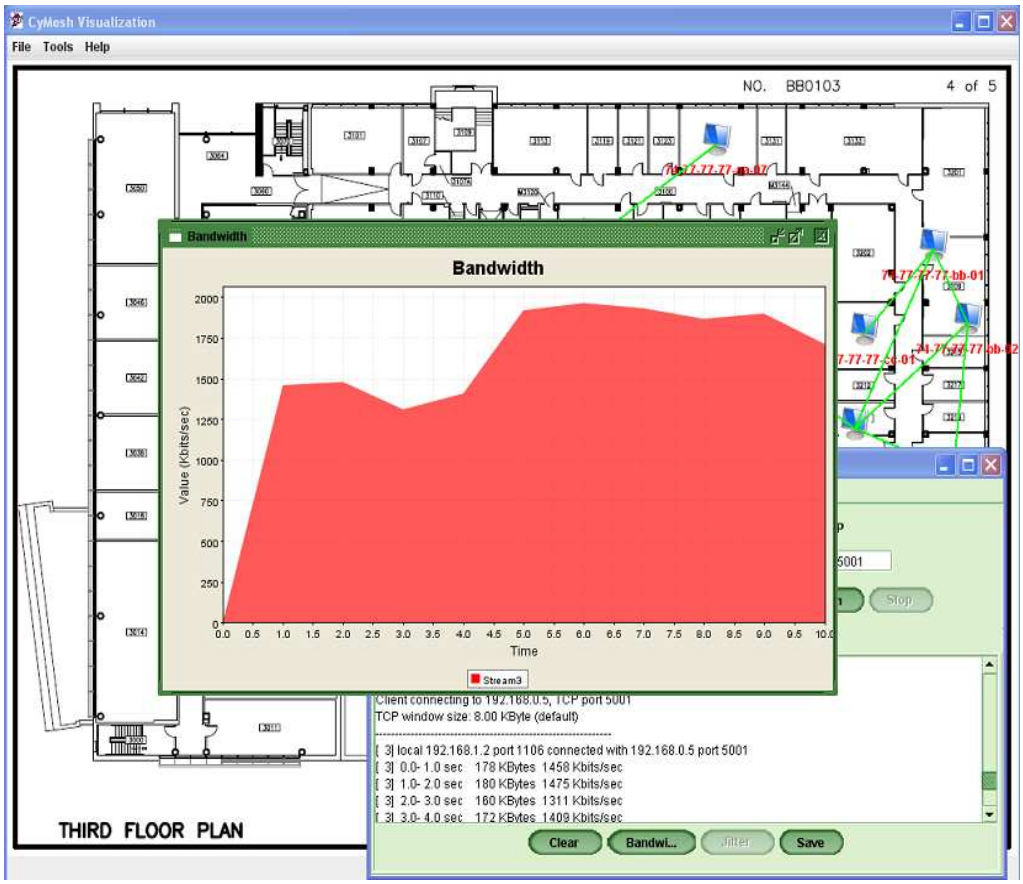

Figure 4.6 A snapshot of the JPerf bandwidth analysis

4.5 Experimental results, observations and experiences

4.5.1 Baseline experiments

We begin by conducting a series of simple but important baseline experiments in order to: (1) provide a single-hop link performance baseline against which we can compare the performance of multi-hop links; (2) verify the conditions to validate the assumptions we make in MRMC networks; (3) define the default configuration of experimental parameters.

4.5.1.1 Single-hop link

We first perform a series of single-hop wireless link experiments and compare the experiment results with the simulation results from QualNet simulator. Two desktop nodes are placed 4 meters apart

Table 4.1 MAC layer parameters

Parameter	IEEE 802.11b	IEEE 802.11g	IEEE 802.11a
Slot Time	20 us	9 us	9 us
SIFS (Short Inter-frame Space)	10 us	10 us	16us
DIFS = (2.Slot Time+SIFS)	50 us	28 us	34us
CW_{min}	31	15	15
CW_{max}	1023	1023	1023

to create a typical indoor LOS link. Both nodes are equipped with the same wireless adapters which are configured to operate on the same channel. We study the 2.4 GHz band for 802.11b/g as well as the 5 GHz band for 802.11a. In order to minimize the interference from background noise existing in these unlicensed frequency bands, all the baseline experiments are carried out during nighttime and each experiment is repeated 10 times. Table 4.1 shows the MAC layer characteristics of the three 802.11 modes. We use the power control algorithm provided by the manufacturers to determine the transmit power on each adapter. Because the RTS/CTS handshake mechanism could lead to severe throughput degradation in multi-hop scenarios [62], we disable it in all experiments since our research is mainly focused on multi-hop network instead of infrastructure-based WLAN scenarios.

In 802.11, a MAC Service Data Unit (MSDU) is fragmented into multiple MAC Protocol Data Units (MPDUs) based on the fragmentation threshold. The TCP Maximum Segment Size (MSS) is 1460 bytes, including 20 bytes of encapsulation data. There are 40 bytes of TCP/IP header information, and 36 additional bytes of data will be added in the MAC encapsulation process, resulting in a maximum 802.11 fragment size of 1536 bytes. The throughput achieved by the TCP flow with different packet size is shown in Fig. 4.7, along with the QualNet simulation results for comparison. We observe that the experimental and simulated results match closely to each other with very small differences most likely due to non-ideal channel conditions not modeled in the simulator. As expected, 802.11a and 802.11g yield higher throughput than 802.11b. 802.11g operates in the same 2.4 GHz frequency band as 802.11b but uses OFDM as the modulation scheme, which is more efficient than DSSS. 802.11a also uses OFDM and shares the same timing parameters as 802.11g, but operates in the 5 GHz frequency band. In general, 802.11a has shorter transmission ranges but suffers less interference from other devices.

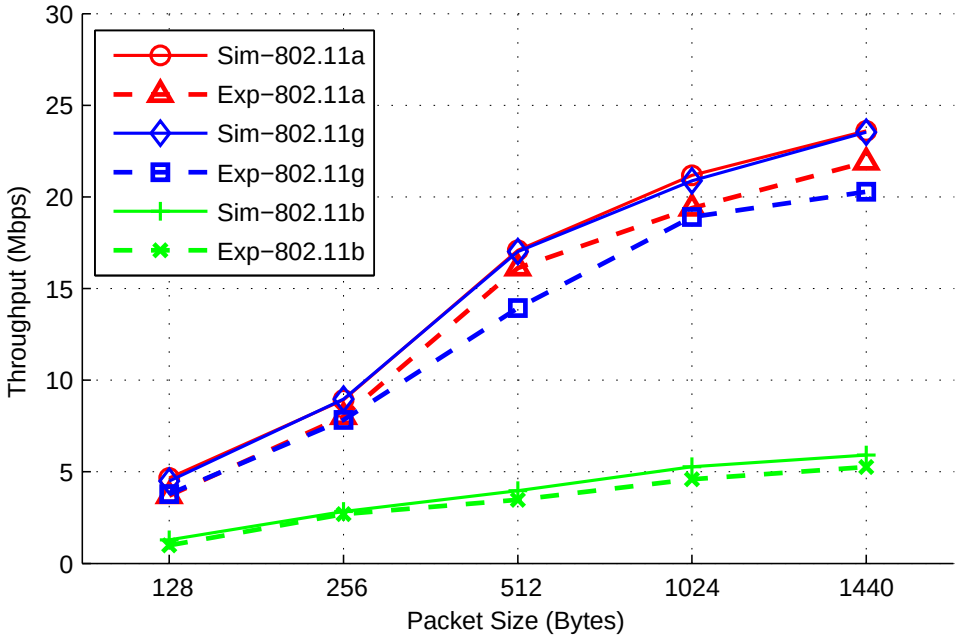

Figure 4.7 Single-hop link: effect of packet size on TCP throughput

Note that across all experiments performed for each packet length, the minimum, average and maximum achieved throughput are very similar although instantaneous rates can vary significantly on occasion. Since packet length has significant effect on throughout, we set the payload size to 1500 bytes in the following experiments and use the single-hop link throughput as the reference throughput upper bound.

4.5.1.2 Impact of closely located wireless adapters and channel separation

Channel diversity is critical to minimize the interference between adjacent links in multi-hop wireless networks. The 2.4 GHz frequency band, shared by devices like 802.11b/g, Bluetooth, cordless phone and microwave ovens, is becoming increasingly crowded and interference is inevitable in typical scenarios such as office, home, and conference center. 802.11a devices operating on the 5 GHz frequency band have a significant advantage over 802.11b/g due to the ability to avoid the congested 2.4 GHz frequency band. Moreover, there are 12 non-overlapping channels in 802.11a compared to only 3 in 802.11b/g.

With the established baseline results obtained from the single-hop experiments, we proceed to

investigate the capacity enhancement by the MRMC feature in WMNs. The basic assumption we made in MRMC networks is that, node with multiple wireless adapters allows parallel transmissions without interfering with each other if they operate on non-overlapping channels. To verify this experimentally, we create a simple 2-hop scenario with 3 desktop nodes, as shown in Fig. 4.8. The distance of each hop is 4 meters. We set up static routes on all nodes such that the traffic between nodes A and B is forced to go through node R.

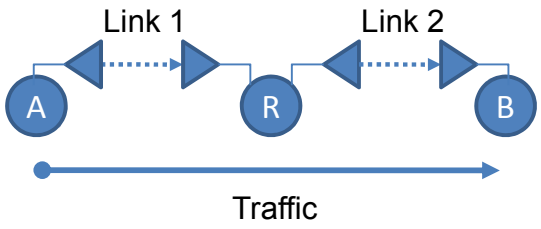

Figure 4.8 A two-hop topology

We begin our experiments by installing two Netgear PCI adapters on node R, which relays the traffic between nodes A and B. When measured independently, the throughput of both links is 4.7 Mbps using 802.11b and 20.3 Mbps using 802.11a. We expect that the end-to-end throughput will only be limited by the bottleneck link if two links are operating on non-overlapping channels. Fig. 4.9 shows the measured throughput in this typical forwarding scenario. Firstly, we observe a significant issue with this setup. When the two PCI adapters installed on node R operate on the same frequency band, regardless of channel assignment, only one adapter is active in most of the time and node R cannot operate properly as a mesh router. By reviewing the related work and careful investigation, we confirm that if two wireless adapters are installed in adjacent PCI slots, radiation leakage is inevitable from wireless adapter's chipset, connectors and antennas, thus may significantly lower the throughput. In order to resolve this issue, we set the default configuration on desktop nodes as follows: one PCI adapter plus one USB adapter. In addition, we use an extension cable to provide necessary physical separation between the two adapters. Specifically, we install a Netgear PCI adapter along with a LinkSys USB adapter on node R, then repeat our experiments and evaluate the throughput by varying the channel separation on the two links, while iteratively increasing the vertical physical distance between two adapters. The results clearly show the impact of physical distance between two radios and the effect of

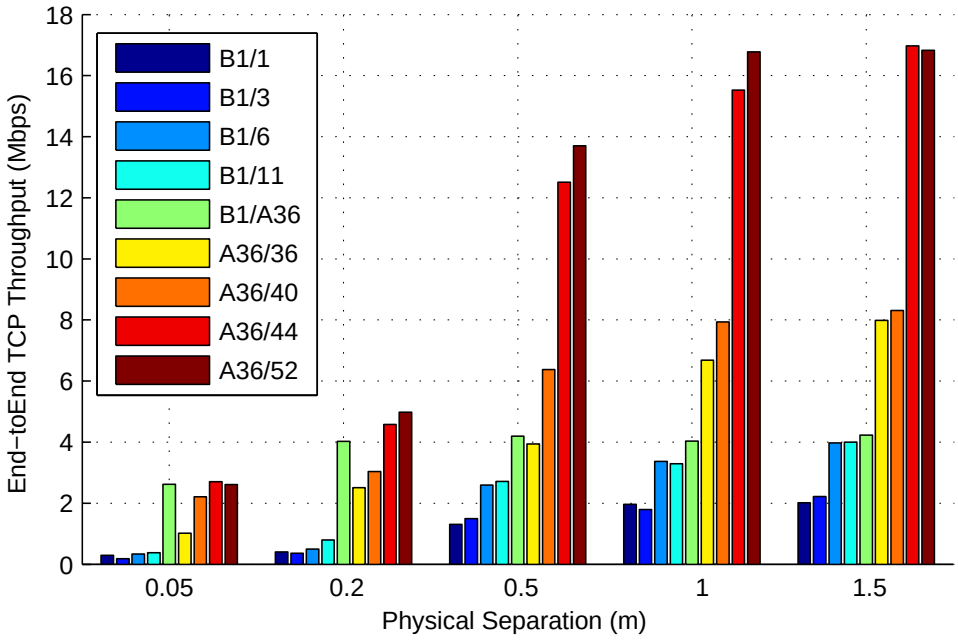

Figure 4.9 Enabling parallel transmissions on forwarding node

channel frequency separation. We have four key observations from these experiments:

- Within a distance of 0.2 meter, throughput is severely degraded due to the interference caused by signal power leakage, even if two radios operate on non-overlapping channels on same band. One possible reason is that the transmitted energy from one radio is strong enough to distort the internal filters and amplifiers in the nearby interface, which prevents them from working properly at the same time [63]. The impact of interference becomes less significant as we increase the distance to 0.5 meter. Beyond a distance of 1 meter, adjacent links on non-overlapping channels can operate independently at full rate without interfering each other. This enables possible parallel transmissions using different radio interfaces on forwarding node, and hence achieves potential throughput improvement of multi-hop flows.

- With sufficient physical separation, both cards attached to the same node are able to work at full speed simultaneously, which shows that significant gain is possible using multiple radios. 3 non-overlapping channels in the 2.4 GHz frequency band and 6 non-overlapping channels in the 5 GHz frequency band are available in our current setup. The combination of these non-overlapping channels can provide maximum channel diversity in our 12-node setup. However, if

the number of non-overlapping channels becomes inadequate due to high node density, intelligent channel assignment mechanism is highly desired to achieve high performance by minimizing the effect of interference.

- We have found that the above interference issue is hardware dependent, which is verified by replacing the Netgear card with TrendNet PCI card and repeating the experiments. A different setup may require different configurations. Using custom hardware or placing physical separation between multiple radios may alleviate the interference problem. Therefore, the number of truly non-overlapping channels must be determined experimentally for forwarding nodes in MRMC networks.

- When evaluating the impact of hardware by combining different adapters, we observe that two adapters (e.g. a PCI and a USB) from the same manufacturer cannot work simultaneously on the same node, possibly due to driver conflict. Such issue is observed on both Netgear and LinkSys adapters. Therefore, we recommend testbed developers to consider using adapters from different manufacturers if a similar problem is observed.

The main conclusion from these experiments is that, in order to evaluate protocols in MRMC mesh networks, designer must carefully select the hardware and determine configurations such as type of hardware, physical separation between radios, channel assignment on mesh router nodes based on extensive experiments. The goal is to exploit the available spectrum as efficiently as possible and achieve the highest bandwidth possible from the existing technologies [63].

4.5.2 Deployment and link measurement

Our testbed deployment is based on non-hierarchical, pure meshing architecture without centralized server or tier-based control. As mentioned earlier, network monitoring, management and configuration can be performed from *any* node in CyMesh or remotely through Internet using custom-made software. This is one of the features that distinguishes CyMesh from other works, which provides great flexibility and convenience to users and developers.

Friendly propagation environment is used in many previous indoor wireless testbed efforts, where experiments are carried out with all wireless nodes in the same room or office lobby. All links are LOS and short distance. However, real world deployment environment for wireless network could be much more complicated due to practical limitations. Therefore, to provide insights on the wireless network performance, it is important to account for the factors such as interference, path loss, shadowing and multi-path effect.

An ideal placement of nodes may provide flexible topologies as desired. However, this task is not trivial due to cost, environment and other practical reasons. With these considerations, we perform careful survey based on our available budget and resources and make the following node placement decision. As shown in Fig. 4.3, 9 stationary nodes (desktop PC) are deployed in the 3rd floor of the Coover Hall and three are deployed in the 1st floor in Atsantoff Hall to form the mesh backbone structure.

Since the ISU infrastructure Wi-Fi (2.4 GHz) co-exists with CyMesh, most experiments are carried out during nighttime in order to avoid interference, and each experiment is repeated several times for accurate measurement. It should be noted that, the source of most interference cannot be controlled. Therefore, one of the goals of wireless network testbeds is to study how to reduce the effect of interference, instead of eliminating interference completely. We consider our current deployment a reasonable solution that accounts for repeatability, easy manageability and extendability.

Upon successful deployment and configuration, we measure the quality of each link independently to create performance reference for multi-hop experiments. Accurate link quality prediction is crucial to routing protocols in wireless networks. Signal to Noise Ratio (SNR) has been used as a measurement for the predicting packet delivery ratio over a wireless link. However, SNR could vary drastically over space and time and it usually requires excessive probing packets. Several previous studies have shown that a simple direct mapping between SNR and delivery ratio values is often inaccurate. Moreover, the IEEE 802.11 standard specifies that link quality should be (for DSSS modulation) calculated from the correlation value obtained when code lock is achieved between the local pseudonoise (PN) code and the incoming PN codes. Most Wi-Fi card vendors use RSSI (Receive Signal Strength Indicator) which is hash of actual signal strength, missed beacons, retransmissions due to collision as the link quality

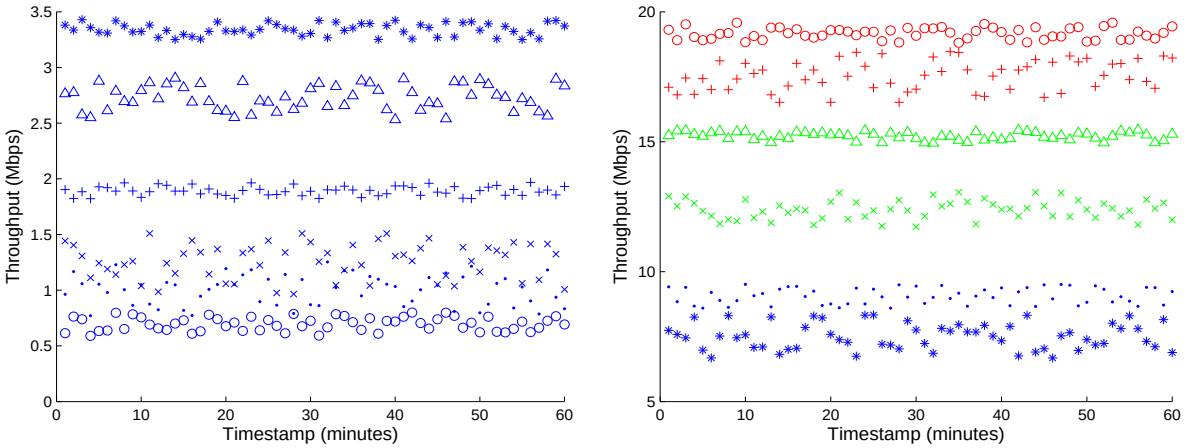

(a) Throughput of the links operating in 802.11b mode (2.4 GHz)

(b) Throughput of the links operating in 802.11g (2.4 GHz) and 802.11a (5 GHz) modes

Figure 4.10 Link capacity measurement

metric [64, 65]. Unfortunately, such RSSI values only provide very limited information to developers since the hash or mapping functions are usually unavailable to clients, and sometimes it is difficult to access the device driver directly and retrieve detailed information. Therefore, we measure the UDP throughput of each link, which is jointly determined by the link's packet loss ratio and bandwidth.

For each link, we use ttcp to generate fully-saturated 1500-byte/packet UDP traffic with a duration of 30 seconds. Each link measurement is repeated 10 times and the average values are recorded. Note that 802.11a operates on a higher carrier frequency (5 GHz), hence its signal is more likely to be absorbed by obstacles and thus cannot penetrate as far as 802.11b, especially in NLOS conditions. For LOS and short distance links, we test both 802.11b/g and 802.11a adapters with link rate adaptation enabled. We record the highest achievable link capacity and use them as the benchmark for the performance of multi-hop routes.

Fig. 4.10 shows the capacity of all the links including those in Atsantoff Hall. Most links can only operate in 802.11b mode due to long distance or the obstacles between the nodes. The current deployment allows three links to use 802.11a or 802.11g with good connectivity and higher throughput. In addition, for some NLOS outdoor links with distances larger than 30 meters, we have installed a 14 dBi high gain antenna and custom-made signal reflector to increase the signal strength and maintain a stable link quality. It is observed that even though both 802.11a and 802.11g use OFDM as the

modulation scheme and have the same theoretical maximum throughput, the measured throughput using 802.11a is slightly higher than 802.11g with lower variance. This is cecause the noise level in the 2.4 GHz frequency band (802.11g) is higher, which results in lower signal to noise ratio (SNR) and hence lower data rate or more packet retries. Since the 5 GHz frequency band is less prone to interference, we decide to set these links to operate in 802.11a mode in the evaluation of the MRMC routing metrics.

4.5.3 Routing metric in MRMC networks

In SRSC wireless networks, throughput of an individual flow may decrease rapidly as node density and number of hops increase mainly because of the following reasons: (1) forwarding nodes cannot send and receive data simultaneously, and (2) due to the omnidirectional transmission nature of most 802.11 devices, if a node is transmitting, all neighbors within its carrier sense range will be prevented from transmission or exposed to interference.

MRMC architecture could significantly improve the network capacity by enabling simultaneous transmission on forwarding nodes, and reduce interference among adjacent links by operating them on different frequency channels. Previous work shows that routing metric plays an important role in such scenarios and has received extensive research efforts [9]. As discussed in Chapter 2, we have proposed AETD, a routing metric that quantifies end-to-end characteristics (link quality, data rate and channel diversity) of a path when making the routing decision. Simulation results show that AETD can provide noticeable throughput gain comparing to other routing metrics. In this section, we evaluate the performance of these routing metrics using CyMesh.

We test four different routing metrics by modifying the routing module in MCL, they are HOP, ETX, WCETT (default in MCL) and AETD. Since the number of links between stationary nodes is limited, we exploit the three mobile nodes to create various network topologies as desired. The reason for creating controlled topologies is that, different routing metrics may select different path (route) for the same source and destination pair, which may be different in bandwidth and link quality and hence yield different end-to-end throughput. Such difference becomes more significant as the network size and density increase, in other words, there are more candidate paths between a source and a destination.

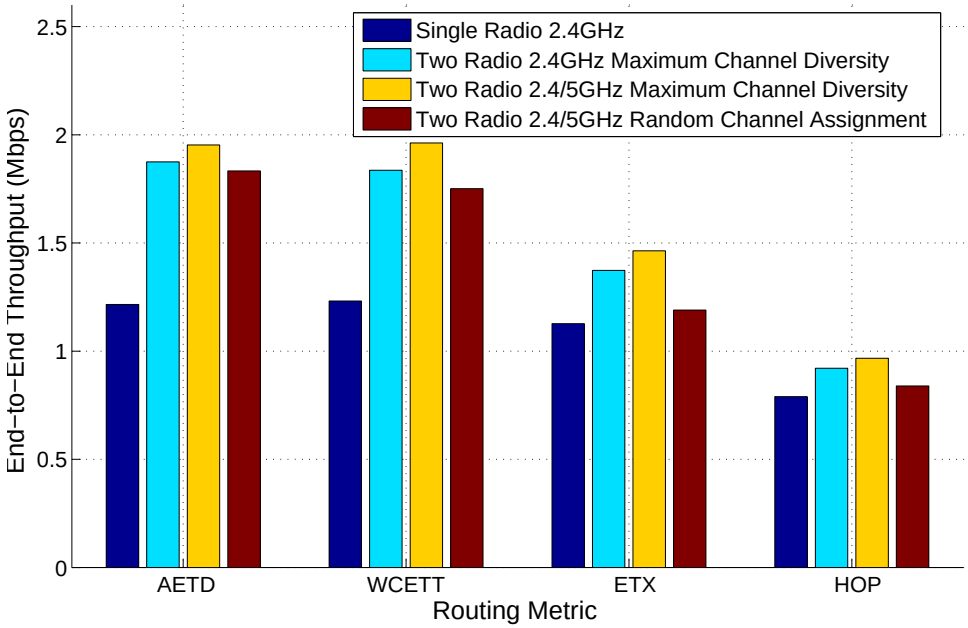

Figure 4.11 Effect of number of radios and channel diversity on TCP throughput

So routing metrics with more considerations in link quality (e.g., bandwidth and channel diversity) may have more options in route selection. For each flow, we measure the performance of the path selected by each routing metric in terms of end-to-end delay and TCP throughput. We use ttcp to generate TCP traffic, and use 56 bytes Ping messages to measure the transmission delay (half the round trip time). There is only one one active flow in the network at any time and each measurement is performed with a duration of 30 seconds.

Firstly, we evaluate the four routing metrics' performance with different number of radios on each node. In the single radio setup, all radios operate on the same channel in the 2.4 GHz frequency band to ensure connectivity. In the two radio setup, we test both 802.11b/g (2.4 GHz) and 802.11a/b/g (2.4/5 GHz Mixed) modes by setting non-overlapping channels to the two radios at the same node (i.e., channel assignment with maximum channel diversity in theory). This allows us to evaluate the impact of channel diversity based the identified truly non-overlapping channels in the 2.4 GHz frequency band from baseline experiments.

Fig. 4.11 shows the average throughput of flows between all source and destination pairs among the nine stationary nodes and the laptop node (74-77-77-77-cc-01 as shown in the middle of the topology

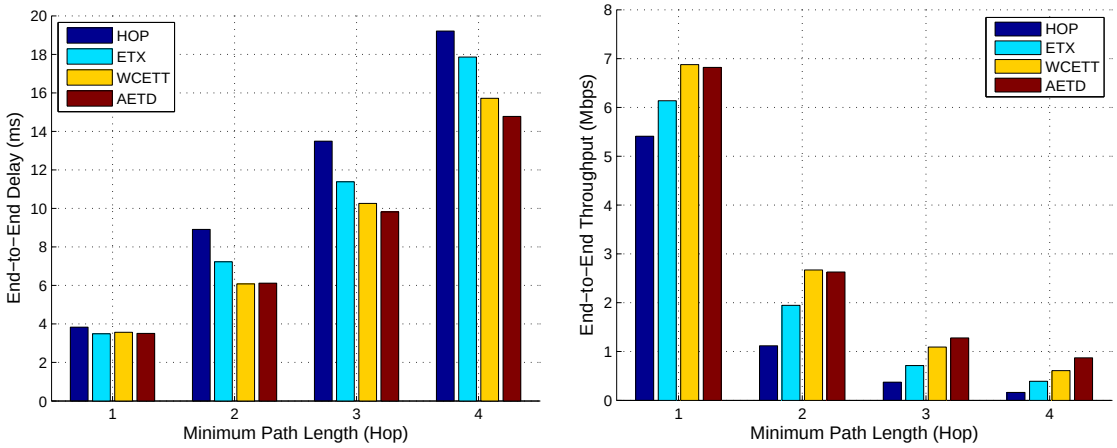

(a) End-to-End delay (2.4 GHz/5 GHz mixed)

(b) End-to-End throughput(2.4 GHz/5 GHz mixed)

Figure 4.12 Effect of routing metric and path length on delay and throughput

in Fig. 4.3). We have three key observations from the results: (1) AETD, WCETT and ETX outperform HOP with noticeable improvement even in single radio networks by considering the link quality when making routing decisions; (2) the use of second radio and multiple channels can greatly improve system capacity; (3) the throughput improvement of AETD and WCETT over HOP and ETX has verified the importance of routing metric in MRMC networks. For example, AETD and WCETT achieve more than 102% higher throughput than HOP; (4) As expected, the performances of AETD and WCETT are similar with maximum channel diversity setup (i.e., no adjacent links operate on the same channel). However, when such maximum channel diversity setup is infeasible due to practical reasons such as limited number of non-overlapping channels and high node degree, AETD can achieve better intra-path channel diversity compared to WCETT. This is verified in the random channel assignment experiments.

AETD outperforms WCETT as expected, but with only about 5 percent improvement in throughput. The throughput gain of AETD over WCETT is limited compared to our simulation results in Chapter. 2, mostly due to three reasons: (1) the network density of the testbed is much lower than that in simulation, hence the number of candidate paths between each pair of nodes is greatly reduced; 2) the network size of the testbed is much smaller than that in simulation settings; 3) it is difficult to control the interference range in real world environment. Another important observation is that 802.11a/b/g (2.4/5 GHz mixed) mode achieves the best overall performance by offering more non-overlapping channels and suffering less potential interference.

Next, we compare the four routing metrics' performance by varying the minimum path length, which is controlled by carefully choosing source and destination nodes with different minimum hops in between. We use the 2.4/5 GHz mixed mode in this experiment to provide maximum channel diversity. Note that routing metrics considering link characteristics (e.g. AETD) may select longer path in terms of hop count, however such longer path may have better overall quality. Fig. 4.12 depicts the end-to-end delay and throughput using different routing metrics. The x-axis represents the minimum hop distance between the source and destination, while y-axis represents the average delay and achieved TCP throughput using different metrics. As we can see, by taking into account link quality, ETX outperforms HOP even in single radio networks. As the minimum hop distance between the source and destination nodes increases, AETD and WCETT show significant throughput gain by considering both link quality and channel diversity in multi-hop paths. On the other hand, the links in CyMesh vary a lot in packet loss ratio, delay and throughput. In such scenario, the potential gain by channel diversity is limited by the huge difference in the link quality. This is because the weight factors of channel diversity in AETD and WCETT are much lower than the weight of ETT. In the environments with more uniform link quality, higher node density and larger network size, AETD can be an attractive metric to offer more significant throughput improvement.

4.6 Conclusions

In this chapter, we describe the design and implementation of CyMesh, a wireless mesh network testbed based on IEEE 802.11 devices. We present our experimental results on link characteristics and the effect of routing metrics using CyMesh. We also discuss the issues we met and the lesspns we learned during the design and deployment, which could serve as useful reference and guidance for future wireless network testbed implementations. We highlight the unique features of our testbed that differentiate it from other systems, such as diversity in the link characteristics (indoor/outdoor, LOS/NLOS), flexibility on routing metric selection, limited interference between co-located wireless networks, and capabilities of real-time network visualization, remote management, configuration and experiment operation.

Experimental results show that MRMC mesh networks can provide significant capacity gains over

SRSC networks. We also present the important role of routing metric in MRMC networks by extensive experiments, which verifies our analysis and the effectiveness of the proposed routing metric discussed in Chapter 2. In general, routing metrics for MRMC networks must be carefully designed in order to fully exploit the spectrum resource and additional radios to improve system performance.

We also identify some critical issues that limit the capacity of today's WMNs. Firstly, the predominant MAC protocol used in most WMNs is the IEEE 802.11 family of protocols, which originally was not designed for multi-hop networks and hence may limit the WMN capability. Although there have been research approaches to address the issues of CSMA/CA in multi-hop networks [66, 67], novel MAC protocols or cross-layer optimization are desired to increase the system capacity while retaining the basic MAC compatibility with current Wi-Fi devices. Secondly, since TCP is originally designed for wired networks, there exist some issues of TCP over wireless links, such as degraded TCP performance due to mistaking wireless errors for congestion [68, 69]. This issues must be carefully addressed in the design of WMNs. Thirdly, our experiments show that the radio technology used in Wi-Fi could be inefficient in multi-hop WMNs under certain scenarios because of interference induced by the limited number of non-overlapping channels and the omnidirectional transmission nature. Therefore, using directional antennas is naturally an attractive option to improve further spatial and frequency reuse in WMNs.

In summary, as a manageable and affordable wireless network testbed solution, CyMesh can be easily extended and updated with new network protocols and radio technologies to investigate the aforementioned research issues. We expect CyMesh to serve as an open and expendable framework for future research in WMNs.

CHAPTER 5. NETWORK DESIGN AND CAPACITY OPTIMIZATION FOR WMNs

5.1 Literature survey

One of the key design considerations in the design of WMNs is to maximize aggregate system throughput and to provide satisfactory services to clients. In order to achieve these goals, the critical interference issue needs to be carefully addressed. It has been well known that interference among transmissions operating on the same frequency channel could be alleviated by using multiple radios on each mesh node and by assigning different channels to each radio, thus enabling more concurrent transmissions. For example, the routing metric we proposed in Chapter 2 is designed to find the path with high channel diversity and hence less intra-path interference. In addition to the MRMC network architecture, employment of directional antennas on each mesh node could further improve the system throughput via alleviating the interference between nearby nodes thus allowing more concurrent transmissions in the network.

Extensive research has been done to study the network performance optimization problem in WMNs. In [70], the authors present a maximum throughput and fair bandwidth allocation algorithm for MRMC WMNs, where channel assignment is predefined [71] and considered independently. The authors of [72] propose a centralized channel assignment and routing scheme based on heuristic route discovery and traffic load estimation. In [73], a dual-path routing selection metric is proposed to consider both link quality and interference. However, each node performs route selection independently, which leads to sub-optimal solutions.

In [74], tree-based network structure and routing protocol are proposed. Unfortunately, single-path routing in such tree structure cannot fully exploit the parallel transmissions offered by multi-path routing in MRMC WMNs. The authors of [75] formulate the joint routing and channel assignment problem as a Linear Programming (LP) problem to optimize the overall network throughput subject

to fairness constraints on clients. The algorithm begins by solving a network max-flow LP problem, which may violate certain practical constraints, followed by a set of post processing in order to round the LP results to a feasible solution. Moreover, channel assignment is performed after routing has been determined, which may not be optimal. A similar approach is proposed in [76]. Time synchronization is required in both algorithms. In [77], the authors show that the capacity of multi-channel networks exhibits different bounds that are dependent on the ratio between the number of channels and radios.

5.2 Motivation

It is well known that although the MRMC network architecture allows more simultaneous transmissions, it cannot eliminate the interference completely due to limited number of available non-overlapping channels and broadcast nature of the wireless medium. For example, the IEEE 802.11a physical layer (PHY) [2] offers 12 non-overlapping channels while there are only 3 in the IEEE 802.11b PHY [3]. Any radio within the interference range of a radio with omnidirectional antenna (which is approximately a disk centered at the radio) will be affected if they operate on the same frequency channel. In addition to exploiting frequency diversity, improving spatial reuse through antenna directionality in WMNs has been recognized as an attractive solution to further ameliorate the interference problem and increase the network capacity. With the same number of available non-overlapping channels, networks using directional antennas typically allow more parallel transmissions than those using conventional omnidirectional antennas. This motivated us to study the joint routing and channel assignment problem for WMNs with directional antennas.

5.3 System models

5.3.1 Network architecture

We consider a MRMC WMN consisting of stationary mesh nodes at known locations. Each mesh node is equipped with multiple IEEE 802.11 radios using directional antennas. As shown in Fig. 1.1, mesh nodes are connected through wireless links to form the communication backbone of the WMN. Traffic between end users and Internet will be relayed over one or multiple paths through the WMN. In

practice, quantity and locations of mesh nodes vary with the area of deployment, demand of services, and availability of resources.

We assume that all radios operate in half-duplex mode, i.e., a radio can only transmit or receive at any time. We say that there exists a link between two nodes if: (1) they have radios pointing to each other and operating on the same frequency channel, and (2) they are within the transmission range of each other. Two links are called adjacent if they have a node in common. Link capacity is defined as the highest possible data transmission rate over the link. Moreover, we assume symmetric links in the network; hence without loss of generality, we only consider traffics from APs to GNs in this work.

Formally, the WMN under consideration can be modeled as an undirected graph $G = (V, E)$, where each node $v \in V$ is equipped with $d(v)$ radios with directional antennas. We use $\Delta(G)$ to denote the maximum degree of the nodes in G, i.e., $\Delta(G) = \max\{d(v)\big|v \in V\}$. Moreover, we use $e(u, v) \in E$ to represent the bi-directional link between nodes u and v with capacity C_e. K stands for the total number of available non-overlapping frequency channels in the network.

5.3.2 Directional antenna and interference model

With an omnidirectional antenna, the interference range of a radio can be approximately modeled as a disk centered at the radio, and all nodes inside the disk are affected if their radios operate on the same frequency channel. How to improve the throughput by separating transmissions in the frequency domain has been well studied. However, the extent of improvement is strictly limited by the number of available non-overlapping channels. By contrast, usage of directional antennas offers spatial separation between contending transmissions hence may further improve the network performance. In this chapter, we consider mesh nodes equipped with multiple radios and each radio uses a practical low-cost switch-beam directional antenna with a fixed transmitting/receiving direction.

Since the transmit power of a directional antenna focuses in one direction and forms a cone-shape pattern, one can expect better spatial usage compared to an omnidirectional antenna. For example, as shown in Fig. 5.1(a), there is no interference between transmissions M2 $\rightarrow$ T and S $\rightarrow$ M3; hence they may proceed at the same time. However, if node M2 uses an omnidirectional antenna with interference range r, these two transmissions cannot take place at the same time because M3 is within M2's

interference range and their radios work on the same channel.

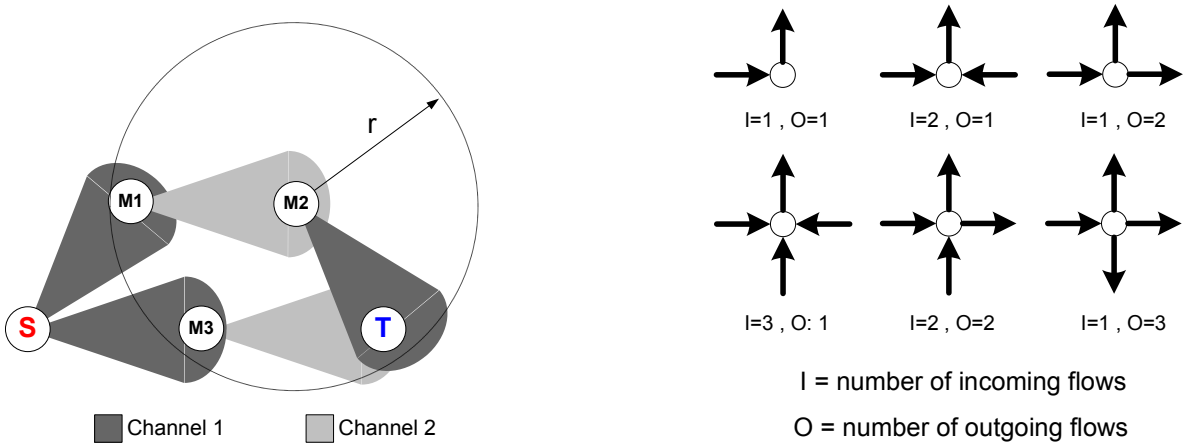

(a) Directional antenna: spatial reuse

(b) Interference patterns in a network with $\Delta(G) = 4$

Figure 5.1 Directional antenna and interference model

Unfortunately, interference cannot be eliminated completely even with directional antennas. Interference occurs if (1) a node is located within the cone-shape area of transmitter's radio, and (2) it has radio(s) operating on the same frequency channel as the transmitter's radio. We assume that the transmit power of each directional antenna is set properly so that they are able to communicate with one-hop neighbors while causing minimal interference to others. Thus, we only consider the interference among adjacent links. Moreover, in order to characterize the severity level of the interference on the common node of adjacent links, we introduce a heuristic *interference factor*, denoted by ϕ. The value of ϕ at a node is determined by the following criteria:

- Each link with non-zero flow will be assigned a channel;
- The number of incoming flows (I) and outgoing flows (O) at a node and the channel assignment are both determined by the MIP solution;
- An increasing number of links (with flow) operating on same frequency channel at a node will result in a higher value of ϕ;
- Interference among incoming flows has greater impact on throughput than that among outgoing flows.

The sum of ϕ of all nodes ($\Phi = \sum_{v \in V} \phi_v$) is a penalty applied to MIP solutions that assign same frequency channel to multiple interfaces on a node. Fig. 5.1(b) illustrates several example interference patterns in a network with maximum degree of 4, where $\phi_d > \phi_e > \phi_b > \phi_f > \phi_c > \phi_a$. In general, a larger ϕ is assigned to an interference pattern with more incoming/outgoing flows operating on the same channel. In practice, ϕ values could be determined by experimental measurements at the initial stage of the WMN deployment.

5.4 Problem statement

5.4.1 Design objectives

The goal of this work is to design a multi-objective algorithm to produce joint decisions on routing and channel assignment in MRMC WMNs. The primary objective is to maximize the aggregate system throughput, which measures the efficiency of network resource utilization. However, simply maximizing the aggregate system throughput may lead to starvation of certain APs. To address this fairness issue, the second objective is to maximize the minimum bandwidth allocation among APs. Further, we add the third objective which is to minimize the total hop count if the first two objectives have been achieved. In other words, if there exist multiple solutions that satisfy the first two objectives, our algorithm picks the one with minimum hop count in order to minimize the network resource utilization.

Most of previous work have proposed to perform channel assignment after the routing decision has been made [50, 70], which may not be optimal. In contrast, our algorithm is designed to consider routing and channel assignment together by solving a joint optimization problem, so as to yield better network performance.

5.4.2 Dual-path routing and one-to-one AP-GN association

Routing in a graph with link capacity limitation is usually formulated and solved as a max-flow problem, which finds a maximum-rate flow in a single-source single-sink network. The max-flow method may also be used in a multi-source multi-sink network by introducing a hyper source (which connects to all sources) and a hyper sink (which connects to all sinks). It has been shown that multi-path routing can significantly improve the end-to-end throughput in MRMC wireless networks [50, 73, 74].

However, such approaches have several inherent limitations in practice. Firstly, in the max-flow problem, each flow is allowed to travel through unlimited number of paths which makes the corresponding routing protocol very complicated. On the other hand, previous work [73, 78, 79] have shown that dual-path routing protocol efficiently exploits the feature of multi-path routing with much lower implementation complexity. For this reason, we add a feasibility constraint in our joint optimization problem: *route selection is limited to dual-path routes*. Simulation results in Chapter 5.6 demonstrate the effectiveness of dual-path routing in MRMC WMNs.

Secondly, in the max-flow problem, there is no restriction on the AP-GN association. One AP may be associated with multiple GNs. From practical implementation point of view, this may be technically challenging because multiple GNs have to cooperate with each other in order to service one AP. Therefore, we add another feasibility constraint in our joint optimization problem: *each AP can only associate with one GN*. This further reduces the complexity of the routing protocol generated by our algorithm.

5.5 Joint routing and channel assignment

We now describe the details of our proposed joint routing and channel assignment scheme. It consists of two steps. Given a network graph G, we construct an auxiliary graph G' to model the following constraints explicitly:

- *General network constraints* that include the general flow constraint, number of radios on each node and total number of available non-overlapping channels, which will be formulated in Chapter 5.5.2;
- *Feasibility constraints* for implementation considerations: dual-path routing and one-to-one AP-GN Association, which were discussed in Chapter 5.4.2 and will be formulated in Chapter 5.5.2.

We formulate the problem of making joint decisions on routing and channel assignment as a Mixed Integer Programming (MIP) problem. The output of the MIP includes (1) the AP-GN associations, (2) the flow rate of each AP-GN pair on each link, which determines the routes and bandwidth allocated to each AP, and (3) the channel assigned to each link.

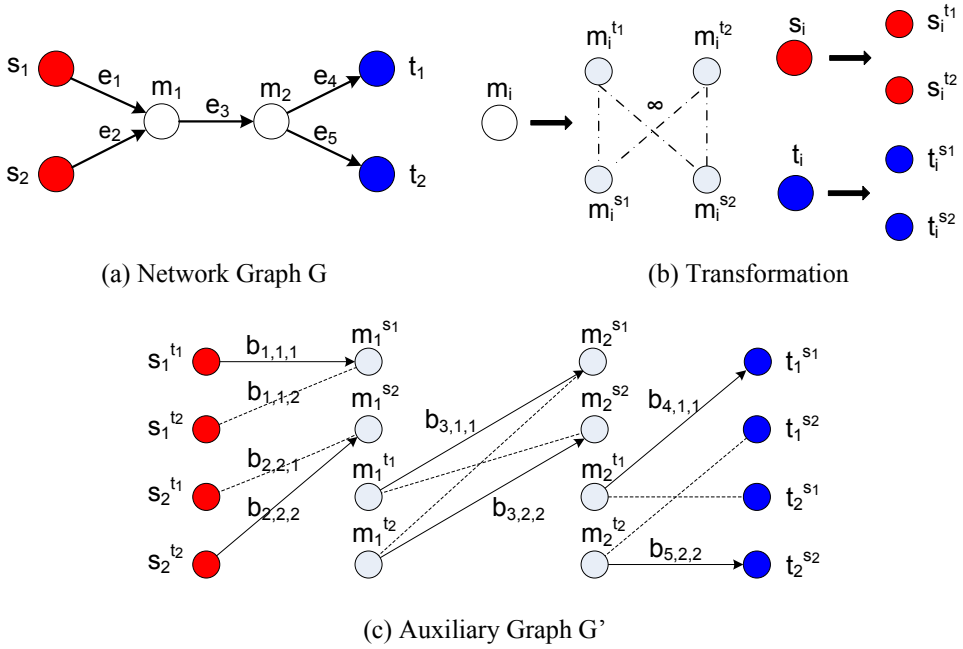

(a) Network Graph G

(b) Transformation

(c) Auxiliary Graph G'

Figure 5.2 An example network graph G and its auxiliary graph G'

5.5.1 Constructing the auxiliary graph

Given a network graph $G = (V, E)$, we construct its auxiliary graph $G' = (V', E')$ in three steps:

- The sets of Access Points (APs), Gateway Nodes (GNs), and Mesh Routers (MRs) in a WMN are denoted by $S = \{s_1, s_2..., s_{|S|}\}$, $T = \{t_1, t_2..., t_{|T|}\}$, and $M = \{m_1, m_2..., m_{|M|}\}$, respectively. For each MR $m \in M$, we create $|S| + |T|$ virtual nodes in G' corresponding to m, namely $m^{s_1}, m^{s_2}, ..., m^{s_{|S|}}$ and $m^{t_1}, m^{t_2}, ..., m^{t_{|T|}}$, and denote this set of virtual notes as M'. All flows coming into m^{s_i} are from AP s_i and all flows going out from m^{t_j} are destined for GN t_j. Similarly, each AP $s \in S$ is mapped to $|T|$ virtual nodes in G' and each GN $t \in T$ is mapped to $|S|$ virtual nodes in G'.

- Secondly, for each MR $m \in M$, $|S| \times |T|$ intra-node links with infinite link capacity (∞) are created in G' which allow traffic to switch between different radios within node m, as shown in Fig. 5.2(b). Note that all intra-node links are omitted in the example G' shown in Fig. 5.2(c) for clarity. Moreover, for each link $e \in E$ between MRs, we create $|S| \times |T|$ virtual links in G', each with capacity C_e. For each link connected to an AP or a GN in G, $|T|$ or $|S|$ virtual links

are created in G'.

- Thirdly, since both G and G' are undirected graphs, the flow on link $e' \in E'$, denoted by $f_{e'}$, is bounded by $[-C_e, C_e]$, meaning that a flow can travel in either direction on a link depending on the algorithm. Note that if multiple flows (from different APs) share a common link, all the flows should follow the same direction on the link.

Fig. 5.2 shows an example of the above procedure. The original network graph G and its auxiliary graph G' are shown in Figs. 5.2(a) and (c), respectively. For instance, a flow in G $s_1 \rightarrow m_1 \rightarrow m_2 \rightarrow t_1$ is mapped to $s_1^{t_1} \rightarrow m_1^{s_1} \rightarrow m_1^{t_1} \rightarrow m_2^{s_1} \rightarrow m_2^{t_1} \rightarrow t_1^{s_1}$ in G', which enables us to model the feasibility constraints explicitly and conveniently.

Table 5.1 Additional notations used in the MIP Formulation

F^{st}	A flow from AP s to GN t
f_{uv}^{st}	Rate of flow F^{st} on link (u, v)
$f^{s\rightarrow}$	Total bandwidth allocated to AP s
$H_{F^{st}}$	Total number of hops of flow F^{st}
$N(v)$	Set of neighbor nodes to v
Φ	Network-level interference factor

5.5.2 MIP formulation

We formulate the problem of making joint decisions on routing and channel assignment as a Mixed Integer Programming (MIP) problem, which is shown in Fig. 5.3.The MIP formulation is presented using notations in G for conceptual clarity only. In order to formulate the problem as a network flow model, all constraints and the objective function are transformed into G' notations when solving the MIP. Other than the notations defined in Chapter 5.3, Table 5.1 summarizes the additional notations used in the MIP formulation.

Our objective is to maximize the aggregate system throughput, to balance the bandwidth allocation among APs, and to minimize the total hop count if the previous two objectives have been achieved. Correspondingly, as shown in Fig. 5.3, three parameters, α, β and γ, are introduced to the MIP objective function to weigh the minimum bandwidth allocation among APs, the total hop count, and the

$$\textbf{maximize} \quad \sum_{s\in S} f^{s\rightarrow} - \gamma \cdot \Phi + \alpha \cdot \min_{s\in S} f^{s\rightarrow} - \beta \cdot \sum_{F} H_F$$

subject to

$$\text{[C1]} \quad \sum_{u\neq v} f_{uv}^{st} = \sum_{v\neq u} f_{vu}^{st}, \qquad \forall v \in M$$

$$\text{[C2]} \quad f^{s\rightarrow} = \sum_{v\in N(s)} f_{sv}^{st}, \qquad \forall s \in S$$

$$\text{[C3]} \quad \sum_{v\in N(s)} f_{sv}^{st} = \sum_{w\in N(t)} f_{wt}^{st}, \quad \forall s \in S,\ v, w \in M$$

$$\text{[C4]} \quad -C_e \leq \sum_{s\in S} f_e^{st} \leq C_e, \qquad \forall e \in E$$

$$\text{[C5]} \quad H_{F^{s_i t_j}} = \sum_{e_k} b_{k,i,j}, \qquad \forall e_k \in F^{s_i t_j}$$

$$\text{[C6]} \quad \Phi = \sum_{v} \phi_v, \qquad \forall v \in V$$

$$\text{[C7]} \quad \sum_{t_j\in T} b_{k,i,j} = 1, \qquad \forall e_k \in E, s_i \in S$$

$$\text{[C8]} \quad p_{s,t} \leqslant 2, \qquad \forall s \in S$$

Figure 5.3 The formulated MIP problem

interference level, respectively. These parameters can be adjusted by the network designer to reflect different design considerations.

We now explain the meanings of eight constraints in the MIP formulation.

- [C1] is a general flow constraint for all MRs, which ensures that the sum of incoming flows equals the sum of outgoing flows at each MR.
- [C2] states that the total bandwidth allocated to an AP s equals the sum of its outgoing flows.
- [C3] makes sure that the sum of outgoing flows from an AP s equals the sum of incoming flows to its associated GN t. Note that the AP-GN associations are output by the MIP. By contrast, in the max-flow problem, the solution only guarantees that the sum of outgoing flows from all APs equals the sum of incoming flows to all GNs.
- [C4] ensures that there is no link capacity violation, meaning that the sum of all flow rates on a link does not exceed the capacity of this link.

Before proceeding to explanations for constraints [C5] to [C8], we first describe two integer variables introduced in the MIP formulation for modeling the feasibility constraints.

- For each link $e' \in E'$ corresponding to $e_k \in E$, we assign a binary variable $b_{k,i,j}$ to 1 if a flow from AP s_i to GN t_j goes through link e_k or 0 otherwise. For example, in Fig. 5.2(c), $b_{3,1,1}$ is set to 1 if there is a flow from AP s_1 to GN t_1 going through link e_3 in G.

- In order to limit the number of paths for each flow, we associate an integer variable $p_{i,j}$ to a flow from AP s_i to GN t_j. Specifically, $p_{i,j}$ is initially set to 1 and it increments by 1 each time flow $F^{s_i t_j}$ splits into two flows at AP s_i or an MR.

Now we resume to explain constraints [C5] to [C8].

- [C5] represents the total number of hops of flow F^{st}.

- [C6] is a heuristic measurement of the total interference level in the network. I is the sum of interference factors ϕ of all nodes, where ϕ_v is calculated based on the routing and channel assignment on node v, as described in Chapter 5.3.B.

- [C7] limits each AP to associate with only one GN.

- [C8] characterizes the dual-path routing limitation on all flows, which ensures that a flow cannot split into more than two paths towards the GN.

The solution to this MIP problem (1) maximizes the aggregate system throughput by selecting the best dual-path routes and minimizing the interference; (2) maximizes the minimal bandwidth allocation among all APs; and (3) minimizes the total hop count, while satisfying all the afore-described constraints. Although the MIP problem is known to be NP-hard, our problem can be solved efficiently in a reasonable time using the CPLEX solver [80], thanks to the branch-and-cut technique as well as our application of model optimization and two feasibility constraints, which shrinks the search space of the MIP significantly. This enables our algorithm to dynamically adapt to network condition changes in a timely manner.

5.6 Performance evaluation

We evaluate the effectiveness of the proposed scheme using the QualNet simulator [10].

5.6.1 Simulation setup

In the network we simulated, each mesh node is equipped with multiple radios with directional antennas. IEEE 802.11a MAC and PHY are adopted. We assume that link capacity is determined by the link distance, and each link may transmit at one of the eight available rates: 6, 9, 12, 18, 24, 36, 48, or 54 Mbps. Moreover, since the beam width of commonly available directional antennas ranges from 30° to 60°, we limit the number of radios on each node to 4 to minimize the backlobe and sidelobe effects of directional antennas.

We compare four routing protocols in the simulation: Single-Path; Dual-Path; Triple-Path; and Unlimited-Path which has no restriction on the number of paths from an AP to its associated GN. All routing protocols are generated by the MIP with constraint [C8] adjusted accordingly. We vary the number of available non-overlapping frequency channels (K) from 1 to 4 to study its effect on the network performance. Two types of networks are simulated: Grid Topology and Random Topology.

The parameters in the MIP objective function are set as follows. Recall that α is the weight for fair bandwidth allocation in the objective function. A larger α favors the AP with the minimum allocated bandwidth but may affect the aggregate system throughput. Therefore, we set $\alpha = 1$ since the aggregate system throughput is our primary objective. On the other hand, since the total hop count minimization has the lowest priority in the objective function, we set its weight $\beta = 1/L$ (where L is the total number of links in G), which ensures that the total hop count will be minimized only if the other two objectives have been met. Moreover, since interference plays a critical role in system performance, we set $\gamma = 100$ to penalize the interference on adjacent links. ϕ values for different interference patterns are determined via simulation.

We evaluate the performance of the simulated routing protocols using two metrics: (1) the aggregate system throughput, which is the total bandwidth allocated to all APs, and (2) Jain's fairness index [81]

of the bandwidth allocations among APs, calculated by

$$J = \frac{(\sum x_i)^2}{n \cdot \sum x_i^2}, \tag{5.1}$$

where x_i represents the bandwidth allocated to AP i and n is the number of APs. Jain's fairness index lies in (0, 1] and $J = 1$ corresponds to the best-case scenario when bandwidth is evenly allocated among APs.

5.6.2 Effect of antenna directionality and channel diversity

We present the results from our preliminary studies on (1) the effect of spacial reuse by directional antennas and (2) channel diversity in chain topology with directional antennas.

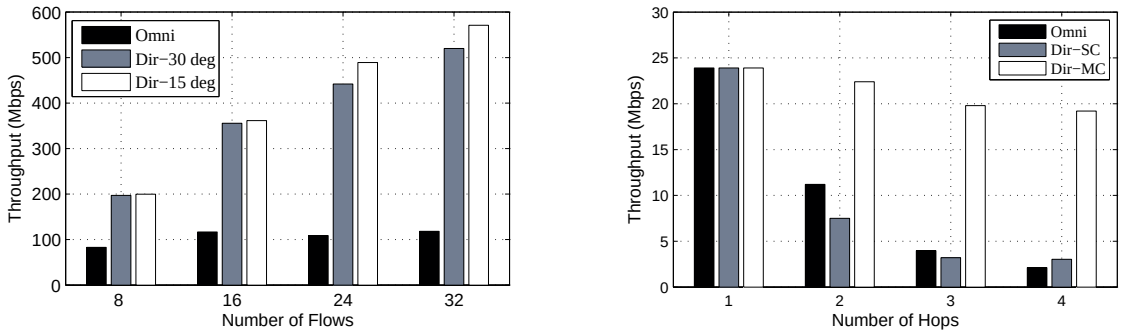

(a) Throughput improvement using directional antenna

(b) Effect of channel diversity with directional antenna

Figure 5.4 Effect of antenna directionality and channel diversity

To study the effect of spatial reuse and potential throughput improvement by using directional antennas, we vary the number of links in a $500m \times 500m$ area. The distance between each pair of nodes is 50 meters. All nodes are equipped with 802.11a radio. In each link Tx transmits CBR traffic to Rx using the highest data rate (54 Mbps). We evaluate three antenna models: omni-directional antenna, directional antenna with 30 degree main-lobe beamwidth, and directional antenna with 15 degree main-lobe beamwidth. The results are plotted in Fig. 5.4(a). It is shown that antenna directionality can significantly improve the aggregate system throughput by effectively exploiting spatial reuse. As expected, the throughput gain becomes more significant with smaller beamwidth which enables more simultaneous transmissions and less collisions.

Next, we study the impact of channel diversity in a chain topology with different antenna models. We create a chain topology where nodes are placed 50 meters apart. We measure the end-to-end throughput of the following configurations: omni-directional antennas with single channel, directional antennas with single channel and directional antennas with multiple channels. As shown in Fig. 5.4(b), with omni-directional, the end-to-end throughput decreases dramatically as number of hop increases because carrier sense prevents simultaneous transmissions. On the other hand, with directional antennas and single channel, links suffers severe interference because transmitters are not aware of other transmissions which may result in high level of interferences in such chain topology, and hence throughput degradation. With directional antennas and multiple channels, it is possible for multiple directional transmissions to operate simultaneously and achieve significantly higher end-to-end throughput.

The preliminary results show that efficient utilization of directional antennas and multiple frequency channels can effectively improve spatial reuse and frequency reuse, which is critical to enhancing the system capacity of WMNs.

5.6.3 Grid topology

We now study a grid-topology network. As shown in Fig. 5.5(a), 49 mesh nodes are uniformly deployed in a $1500m \times 1500m$ area and form a 7×7 grid topology. The distance between neighbor nodes is 250 meters, which corresponds to link capacity of 24 Mbps according to the IEEE 802.11a propagation model in QualNet. We generate 10 scenarios with different AP and GN locations. In each scenario, we randomly selected three nodes as APs and three nodes as GNs. An example scenario is shown in Fig. 5.5(a). Simulation results are shown in Fig. 5.6 where each point is averaged over 10 scenarios.

We have two observations from Fig. 5.6. Firstly, the system throughput increases with the number of available non-overlapping channels (K). The prominent throughput increment is observed when K increases from 1 to 2. However, one can see that the performance improvement is almost negligible when $K \geqslant 3$. This suggests that we can obtain considerable throughput improvement in multi-radio networks with only a small number of non-overlapping channels.

Our second observation is that the proposed dual-path routing protocol can efficiently exploit the

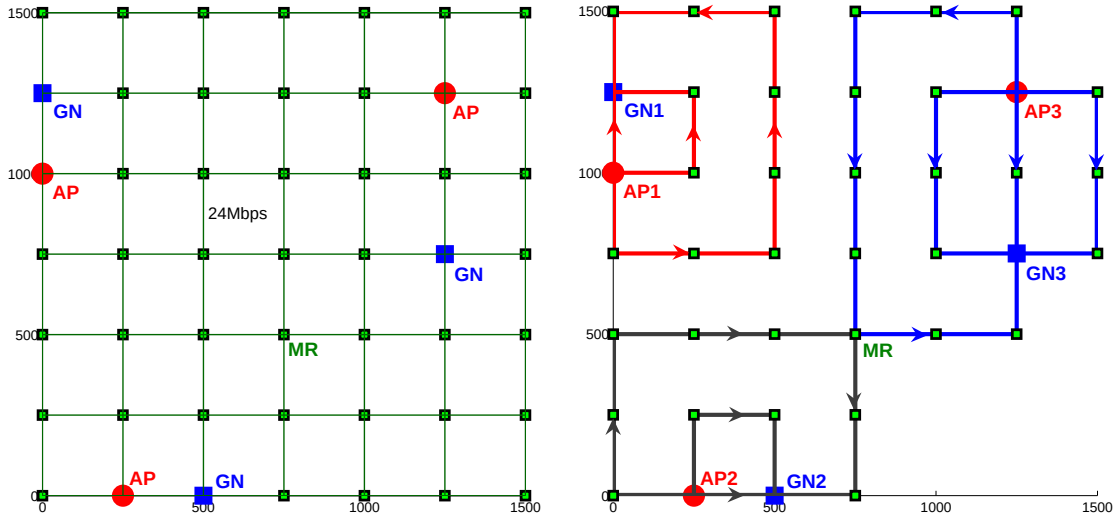

(a) Red circle represents AP, blue square represents GN, and other nodes are MRs

(b) Routing paths in Scenario #7

Figure 5.5 The grid-topology network with 49 nodes

MRMC architecture of the network and achieve significant throughput improvement compared with the single-path routing protocol. Moreover, as shown in Fig. 5.6, the marginal gain obtained by triple-path and unlimited-path routing over dual-path routing are very limited in most scenarios. According to our analysis, in grid-topology networks, triple-path and unlimited-path routing show clear advantage only if (1) an AP can find more than three disjoint paths to its associated GN, and (2) there are at least three available non-overlapping channels.

In order to study the system performance in detail, we plot the simulation results of all 10 scenarios in Fig. 5.7. The cases of $K = 1, 2$ are omitted since the performance difference are less significant due to severe interference. Compared with dual-path routing, unlimited-path routing improves the system throughput by 65.5% at most, which occurs in Scenario #7 as shown in Fig. 5.5(b). In this scenario, both AP1 and AP2 have three disjoint paths to their associated GNs (GN1 and GN2 respectively), and AP3 has four disjoint paths to GN3. Therefore, all the transmissions shown in Fig. 5.5(b) can take place simultaneously when $K = 4$. This agrees with our analysis above. On the other hand, in most of the randomly generated scenarios, there are only small performance differences between dual-path and triple-path/unlimited-path routing. This in turn supports our decision on limiting the route selection to dual-path routes, which strikes a balance between the network performance and the complexity of

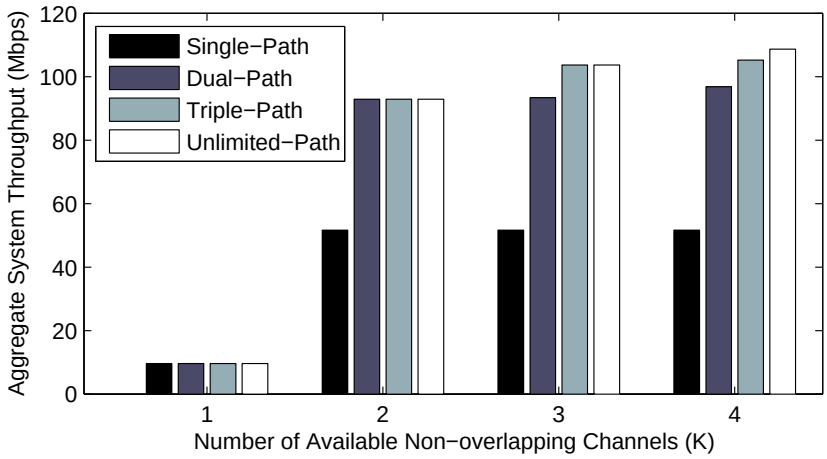

Figure 5.6 Comparison of system throughput in grid-topology networks

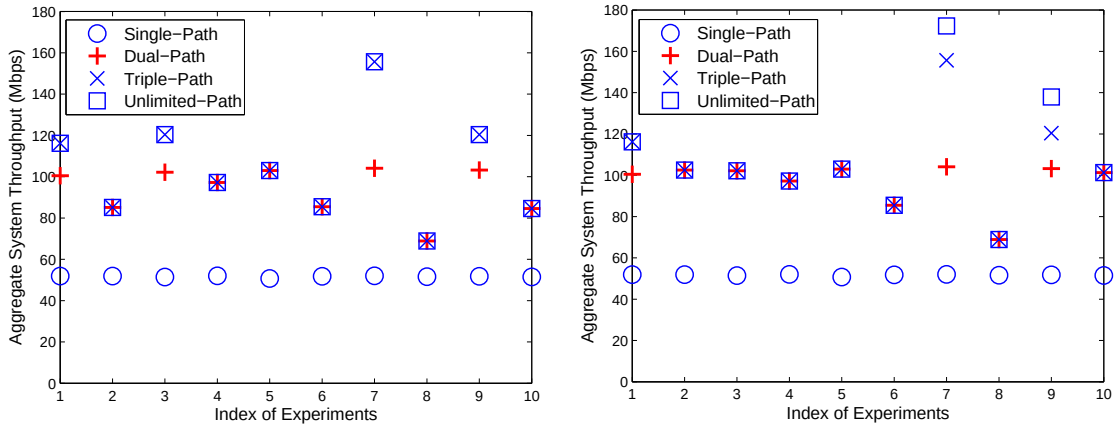

(a) 3 non-overlapping channels (b) 4 non-overlapping channels

Figure 5.7 Results of 10 simulated scenarios in the grid-topology network

system implementation.

The Jain's fairness index of bandwidth allocation in the 10 simulated scenarios are {1, 1, 1, 0.9977, 1, 0.9290, 1, 0.8939, 1, 0.9999} respectively. We observe that even the worst-case scenario yields a fairness index of 0.8939, which proves that the introduction of the fairness component in our objective function can effectively balance the bandwidth allocation and avoid starvation on some of the APs.

5.6.4 Random topology

We next consider random-topology networks where 49 mesh nodes are uniformly randomly placed in a $1500m \times 1500m$ area. We assume that the network is a planar graph with maximum degree of 4. Link capacity is only dependent on the link distance. An example random topology is shown in Fig. 5.8(a), where the number along each link represents the link capacity (in Mbps). Again, three APs and three GNs are randomly selected in each scenario. Simulation results are plotted in Fig. 5.9 where each point is averaged over 10 scenarios.

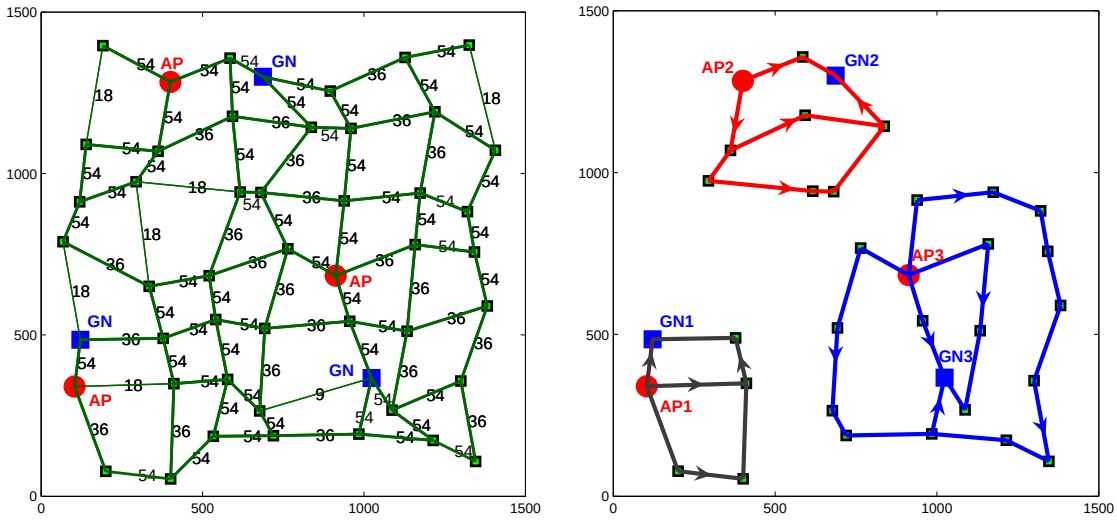

(a) An example network with the number along each link representing the link capacity (in Mbps)

(b) Routing paths in Scenario #3

Figure 5.8 Random-topology networks with 49 nodes

Compared with that in the grid-topology network, the performance gain of multi-path routing over single-path routing is less significant in random-topology networks. The reason is that, due to the link capacity diversity in random-topology networks, there may exist bottleneck regions where even multi-path routing cannot detour around or find better paths.

Another observation in Fig. 5.9 is that the performance gap between dual-path routing and triple-path/unlimited-path routing is even more narrowed than that in the grid-topology network. One explanation for this phenomenon is that the interference problem becomes more severe as the number of routing paths increases, especially in random-topology networks where two links that are more than two hops away may still interfere with each other. Note that, though we assume that the transmit power

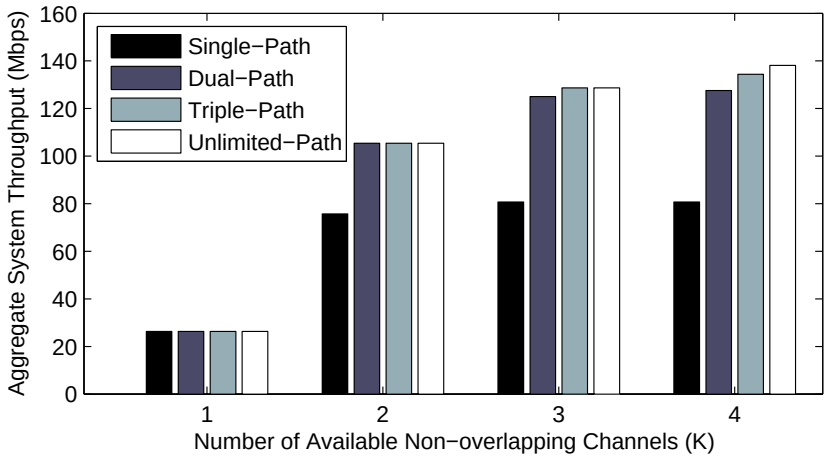

Figure 5.9 Comparison of system throughput in random-topology networks

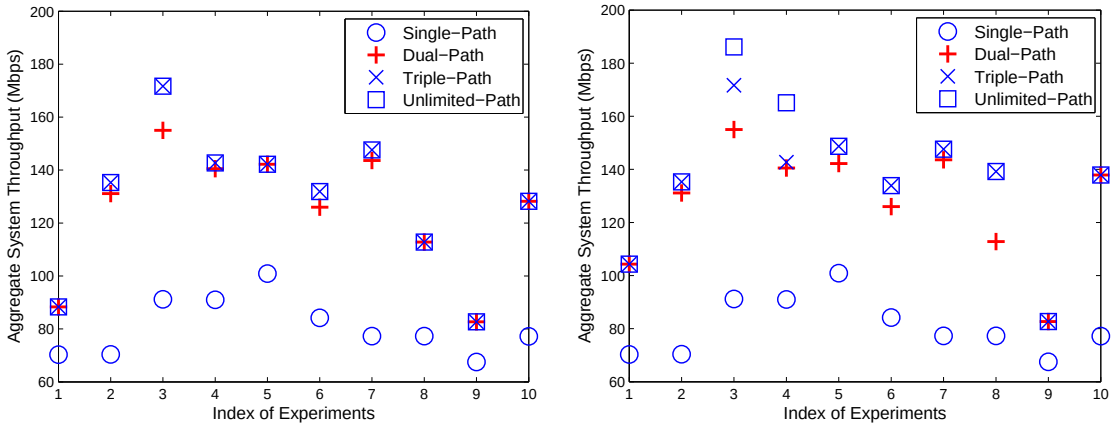

(a) 3 non-overlapping channels (b) 4 non-overlapping channels

Figure 5.10 Results of 10 simulated scenarios in random-topology networks

of each directional antenna has been adjusted properly, the interference pattern is still difficult to predict when mesh nodes are randomly placed.

In order to show insight of the performance difference of simulated routing protocols in random-topology networks, we plot the simulation results of all the 10 simulated scenarios in Fig. 5.10. We can see that single-path routing performs differently in 10 scenarios, mainly due to non-uniform link capacities and unpredictable bottlenecks along routing paths. In contrast, triple-path and unlimited-path routing are more likely to achieve higher throughput. Fig. 5.8(b) shows the routing paths when unlimited-path routing is used in Scenario #3, which yields significantly higher throughput than dual-

path routing because there exist more than two fully or partially disjoint paths from each AP to its associated GN. However, the performance gain of triple-path or unlimited-path routing over dual-path routing is limited on average.

The Jain's fairness index of bandwidth allocation in the 10 simulated scenarios are {0.9996, 0.9886, 0.9953, 0.9863, 0.9957, 0.9511, 0.9327, 0.9154, 0.9980, 0.9703} respectively. Clearly, the bandwidth is almost evenly distributed to all APs in most scenarios despite the link capacity diversity in random-topology networks. These results again convincingly confirm the effectiveness of the proposed scheme which achieves high aggregate system throughput while maintaining fairness among APs, both of them are highly desirable in WMN applications.

5.7 A heuristic approach to the joint routing and channel assignment problem

The proposed centralized MIP-based algorithm is designed to find the optimal solution to the joint problem. Since the search space of such NP-hard problem could be very large, the computational complexity is high and hence finding the optimal solutions of the MIP is time consuming, which is the main drawback of the MIP algorithm. Therefore, a heuristic approach is desired to balance the tradeoff between optimality and implementation complexity. Moreover, a simple, fast heuristic algorithm can adapt to varying network conditions (e.g., link quality fluctuation and topology changes) and handle node join/leave events easily. Hence, we propose two heuristic algorithms as alternate solutions to the MIP-based algorithm with the following requirements:

- Performs in a distributed manner.
- Converges to a stable solution within much less time than the centralized algorithm.
- Yield reasonable performance with the same constraints and objective function.

Table 5.2 summarizes the characteristics of the two proposed heuristic algorithms:

5.7.1 Distributed algorithm 1

In this section, we describe the Distributed Algorithm 1 (DA-1) in details. The operation of DA-1 includes two steps:

Table 5.2 Summary of the two heuristic algorithms

	DA-1	DA-2
Operation	Find best route(s) for each AP; Then assign channels to each route accordingly to minimize interference	Assign channels to all links; Then decide best route(s) for each AP
Pros	Channel assignment is optimized according to traffic pattern which can efficiently exploit the frequency resource	Route decision considering channel information can estimate the overall quality of a path more accurately; Newly joined AP will not trigger channel assignment
Cons	May lead to channel conflict and unfairness in channel assignment among APs; Newly joined AP may require channel assignment	Links with flows may not be able to efficiently exploit the frequency resource comparing to DA-1
Routing Complexity	$O((E+V\cdot\log V)\cdot No.ofGN)$	$O((E+V\cdot\log V)\cdot No.ofGN)$

1. Route discovery - each AP calculates the best routes to each GN and associate with the GN with lowest routing cost.

2. Channel assignment - once routing decision is made, channel assignment is performed in a way that interference is minimized.

In route discovery, all radios operate on a common channel in route discovery mode. Each GN broadcasts its routing announcement messages with an advised channel sequence periodically, which are propagated to all mesh nodes along with link and route cost information; link and node status change will be updated in nodes routing table, which may trigger route change. Each node keeps tracking the route cost to all GNs, and calculates two best link-disjoint routes (if applicable) to the GN that minimizes the given path metric using a modified Dijkstra's algorithm. Each AP uses the best and second-best route (to the selected GN) for data forwarding. Once route discovery is completed, traffic pattern in the network will be determined and GNs can share the load information of all APs. Channel assignment will be performed and optimized for the selected routes based on the order of APs loads.

During channel assignment, each GN initializes the channel assignment procedure by advising a unique channel sequence to each route. The route to the AP with highest load will perform channel assignment first, then the AP with next highest load, so on so forth. All nodes along a route follow the advised channel sequence and switch to assigned channels to minimize intra-path interference. If there exists a channel conflict on a link (e.g., a link is shared by multiple routes with different channel sequences), the link will switch to a new channel different from the advertised two - if the new channel does not incur intra-path interference in both routes. If such a new channel does not exist, the link uses the previously assigned channel. Note that this may lead to sub-optimal channel assignment, however it ensures that the protocol can converge in a short period of time.

5.7.2 Distributed algorithm 2

We now describe the Distributed Algorithm 2 (DA-2) in details. The operation of DA-2 includes two steps:

1. Channel assignment - a simple, distributed channel assignment algorithm is applied to minimize the interference among multiple radios at each node.

2. Route discovery - each AP calculates the best route to each GN (routing metric accounts for link quality and channel diversity) and select the GN with lowest routing cost to associate with.

Although one can model and solve it as a classic node-coloring problem in a conflict graph, it is time consuming for such distributed protocol. In this proposed heuristic, we try to assign different channels to links that are adjacent to the same node to minimize interference. Specifically, each GN assigns different channels to adjacent links by sending an advertised channel messages to its neighbors. GNs and nodes closer to GN (measured by hop count) have higher priority when assigning channels. Each neighbor node follows the advertised channel, and try to assign different channels to its other radios; if this is impossible due to limited number of channels, the algorithm favors the link with lower cost. If there exists a conflict (the two radios of a link prefer different channels and there is no 3rd channel available), the algorithm will select a channel randomly.

Once channel is assigned to all links, route discovery will be performed. Nodes compute the route to each GN using Dijkstra's algorithm and select the GN with lowest routing cost. Routing metric accounts for both link quality and channel diversity. If applicable, each node computes a second link-disjoint route to the selected GN. Each AP uses the best and second-best route (to the selected GN) for data forwarding.

5.7.3 Performance evaluation

In this section, we evaluate the performance of DA-1 and DA-2 and compare them with the MIP-based algorithm. We study random topologies where 49 nodes are deployed in a $1500m \times 1500m$ area with a average distance of $250m$. The number of radios on each node is set to 4 and the the number of non-overlapping channel varies from 1 to 4. Same practical constraints are applied which ensures dual-Path routing and 1-to-1 AP-GN association. 3 GN and 3 AP are randomly selected in each run and all results are averaged over 10 randomly generated topologies. All other settings are same as those described in Sec. 5.6.

Three metrics are used to evaluate the performance of three algorithms: system aggregated throughput, throughput fairness of among GNs and time consumed to derive the solution (simulation). The simulation results are shown in Fig.5.11.

Simulation results show that the two proposed distributed algorithms can achieve comparable performance with the MIP while using significantly less time. For example, in 3-channel scenarios, DA-1 and DA-2 yield 93% and 87% of the throughput of MIP, respectively. MIP takes more than 3 hours on average to derive solutions, in comparison, both DA-1 and DA-2 take less than 2 minutes to find the solutions in our simulation (this does not include the distributed protocol overhead). As expected, both DA-1 and DA-2 lead to some unfairness issues as they do not explicitly consider fairness among APs when make routing decisions, while MIP performs well in guaranteeing a certain level of fairness among APs by considering fairness in the objective function.

Fig.5.12 and Fig.5.13 compare the performances of all algorithms with different traffic load (i.e., number of flows) and number of non-overlapping channels in the network. We have the following observations:

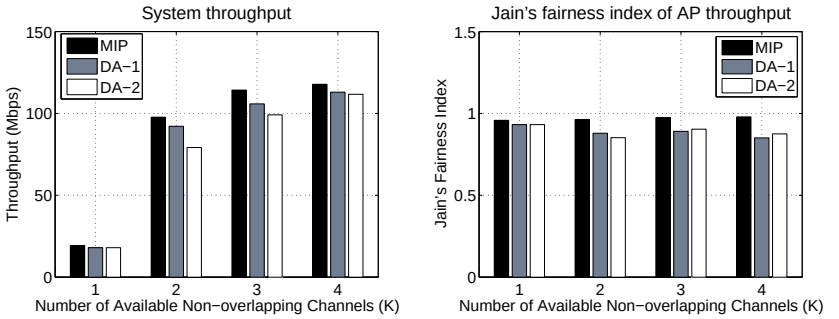

(a) System throughput vs Number of channels (b) Jain's fairness index vs Number of channels

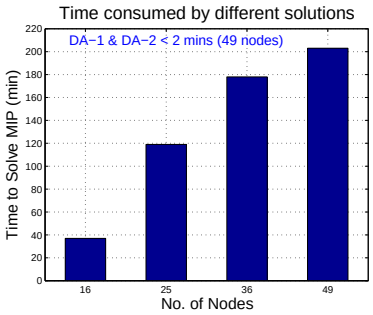

(c) Time consumed vs Number of nodes

Figure 5.11 Performance comparison of heuristic algorithms and MIP

- When the number of channels and traffic load are both low, DA-1 could be a better choice since it shows some advantage over DA-2 in throughput and performs similarly to DA-2 in terms of fairness.

- When traffic load is heavy or unpredictable, DA-2 is a better option regardless of the number of channels. This is because, in additional to the advantage of lower implementation complexity, DA-2 yields similar throughput as DA-1 and outperforms DA-1 in terms of fairness since the frequency resource is allocated to all flows more uniformly.

- As the traffic load increases, the MIP solution is less affected in maximizing system throughput, while guaranteeing fairness among APs comparing to DA-1 and DA-2. Therefore, the performance gap between the two heuristics and the MIP-based algorithm will increase especially in terms of fairness provisioning. However, the difference in the computation time will also increase as the number of flows increases, which makes the MIP-based algorithm infeasible to handle frequent node join/leave events or network condition variation.

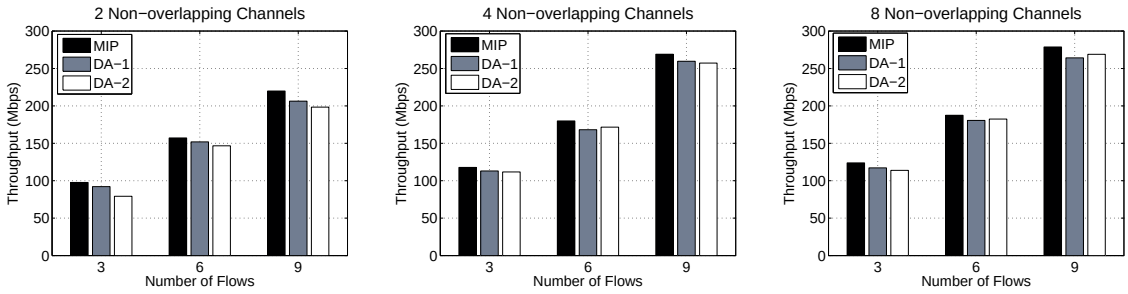

(a) 2 non-overlapping channels (b) 4 non-overlapping channels (c) 8 non-overlapping channels

Figure 5.12 Impact of traffic load and number of channels on system throughput

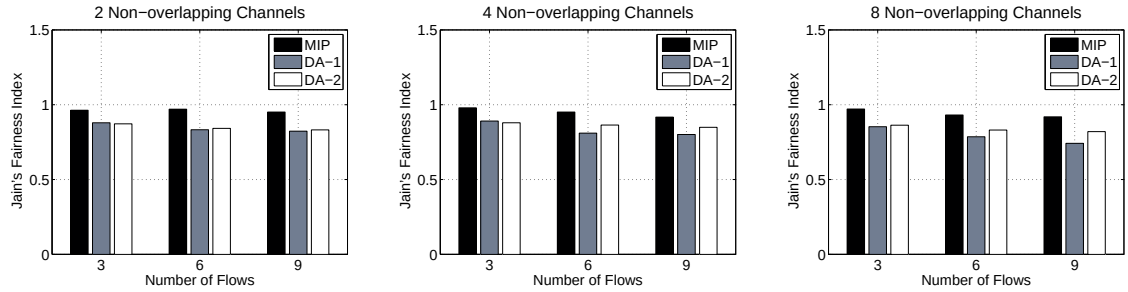

(a) 2 non-overlapping channels (b) 4 non-overlapping channels (c) 8 non-overlapping channels

Figure 5.13 Impact of traffic load and number of channels on fairness

In summary, one may consider DA-1 when the traffic load is light and the number of non-overlapping channels is less than the number of radios on each node, because the channel assignment scheme of DA-1 can efficiently exploit the traffic pattern information and achieve higher throughput. However, in other scenarios, DA-2 is the appropriate choice which can achieve similar or better performance than DA-1 with less implementation and operation complexity. Finally, the MIP solution can be used to provide the throughput and fairness benchmark to evaluate the performances of different heuristic algorithms. We hope the simulation results could provide a preliminary guidance for network designers and administrators to select the most appropriate solution based on the real scenarios.

5.8 Conclusion

In this chapter, we study the problems of system throughput maximization and fair service provisioning in MRMC WMNs with directional antennas. We propose a novel algorithm to produce joint

decisions on routing and channel assignment with practical implementation considerations. Since this problem is known to be NP-hard, we formulate it as a Mixed Integer Programming problem and solve it using the CPLEX optimizer. Through extensive simulation study, we show that our scheme (i.e., the solution to the MIP problem) efficiently exploit the MRMC network architecture and directional antennas in WMNs, which lead to drastically improved aggregate system throughput while maintaining fair bandwidth allocations among APs. Moreover, we translate practical implementation considerations into feasibility constraints in the MIP problem; as a result, our scheme is simple and easy to implement, thus facilitating its deployment with commercial wireless networking devices such as IEEE 802.11 compliant devices.

Furthermore, to seek a balance between optimality and complexity, we propose two simple, easy-to-implement heuristic algorithms as alternatives to the MIP-based centralized algorithm. Simulation results show that the proposed heuristic algorithms yield comparable performances to the MIP-based solution and take much less time to derive the solution. Simulation results could aid network designers to select an appropriate algorithm based on real network conditions, such as the number of available non-overlapping channels and predicated traffic load. Possible extensions include incorporating the routing metric and fairness notion presented in previous chapters into the proposed algorithms, and development of the distributed protocol to implement the proposed heuristic algorithms.

CHAPTER 6. SUMMARY

In this dissertation, we have studied the key issues related to QoS provisioning in WMNs. We propose novel solutions to these issues, and present protocols and schemes specifically designed and optimized for WMNs to achieve efficient radio resource usage and provide cost-efficient Internet access services to clients. Our main contributions are summarized below.

- We propose a new routing metric, called AETD, to find the path with minimal interference and channel contention for high throughput routing in MRMC WMNs. Moreover, AETD can be integrated into existing routing protocols and automatically determine the best path for a source/sink pair through the network.

- We devise a novel fairness notion, called Fulfillment-based Fairness (*FbF*), to address the performance anomaly and association anomaly issues associated with the existing fairness notions. *FbF* seeks a balance between aggregate system throughput and fulfilment-based fairness among clients. In addition, two algorithms are developed to implement *FbF* in different scenarios.

- We design and implement CyMesh, an MRMC WMN testbed using off-the-shelf IEEE 802.11 hardware on the campus of Iowa State University. We discuss the issues, observations and learned lessons during the design and deployment of CyMesh. We demonstrate that the MRMC architecture can significantly improve the capacity of WMNs comparing to the SRSC architecture. Moreover, we evaluate the performance of our proposed routing metric using CyMesh and report the experimental results. Our implementations and feasibility tests have demonstrated enough advantages to motivate further experimenting in MRMC WMNs.

- We develop a centralized, MIP-based joint routing and channel assignment algorithm for WMNs with directional antennas. This joint algorithm is designed to maximize spatial and frequency

reuse simultaneously in WMNs for optimizing network capacity, which considers both practical limitations and implementation complexity issues. Moreover, in order to balance performance optimality and implementation complexity, we propose two simple, fast heuristic algorithms which yield comparable performances to the MIP-based centralized algorithm but requiring much less computational time. These algorithms can serve as a network architecture design and capacity optimization framework in resolving the multi-dimensional QoS provisioning challenges in WMNs.

The simulation and experimental results in this dissertation show that it is possible to deploy cost-efficient, easy-to-deploy and high capacity WMNs with appropriate design and implementation. We believe that the insights and experiences we gained from this dissertation work can stimulate more research in architecture design, protocol optimization and testbed implementation of WMNs in order to provide low-cost, anywhere-anytime Internet access solutions in the near future.

BIBLIOGRAPHY

[1] IEEE 802.11, *Part 11: Wireless LAN Medium Access Control (MAC) and Physical Layer (PHY) Specifications*, Aug. 1999.

[2] IEEE 802.11a, *Part 11: Wireless LAN Medium Access Control (MAC) and Physical Layer (PHY) Specifications: High-speed Physical Layer in the 5 GHz Band, Supplement to IEEE 802.11 Standard*, Aug. 1999.

[3] IEEE 802.11b, *Part 11: Wireless LAN Medium Access Control (MAC) and Physical Layer (PHY) Specifications: High-speed Physical Layer Extension in the 2.4 GHz Band*, Sept. 1999.

[4] P. Kyasanur and N. H. Vaidya, "Routing and interface assignment in multi-channel multi-hop wireless networks with a single transceiver," UIUC, Tech. Rep., Dec. 2004.

[5] ——, "Routing and interface assignment in multi-channel multi-interface wireless networks," in *Proc. IEEE WCNC'05*, 2005.

[6] M. Alicherry, R. Bhatia, and L. Li, "Joint channel assignment and routing for throughput optimization in multi-radio wireless mesh networks," in *Proc. ACM MobiCom'05*, 2005.

[7] M. Kodialam and T. Nandagopal, "Characterizing the capacity region in multi-radio multi-channel wireless mesh networks," in *Proc. ACM MobiCom'05*, 2005.

[8] D. De Couto, D. Aguayo, J. Bicket, and R. Morris, "A high-throughput path metric for multi-hop wireless routing," in *Proc. ACM MobiCom'03*, 2003.

[9] R. Draves, J. Padhye, and B. Zill, "Routing in multi-radio, multi-hop wireless mesh networks," in *Proc. ACM MobiCom'04*, 2004.

[10] QualNet Simulator, http://www.scalable-networks.com/, Online Link.

[11] A. Demers, S. Keshav, and S. Shenker, "Analysis and simulation of a fair-queueing algorithm," in *Proc. ACM SIGCOMM'89*, 1989.

[12] TCP Congestion Control, http://rfc.sunsite.dk/rfc/rfc2581.html, Online Link.

[13] TCP Friendly Rate Control, http://www.ietf.org/rfc/rfc3448.txt, Online Link.

[14] R. Braden, D. Clark, S. Shenker, and J. Wroclawski, "Developing a next-generation internet architecture," *White paper, DARPA*, 2000.

[15] B. Briscoe, "Flow rate fairness: Dismantling a religion," *ACM Computer Communications Review*, vol. 37, no. 2, pp. 63–74, 2007.

[16] T. Nandagopal, T.-E. Kim, X. Guo, and V. Bharghavan, "Achieving mac layer fairness in wireless packet networks," in *Proc. ACM MobiCom'00*, 2000.

[17] L. Tassiulas and S. Sarkar, "Maxmin fair scheduling in wireless networks," in *Proc. IEEE INFOCOM'02*, 2002.

[18] D. Qiao and K. G. Shin, "Achieving efficient channel utilization and weighted fairness for data communications in ieee 802.11 wlan under the dcf," in *Proc. IEEE IWQoS'02*, 2002.

[19] H. Luo, S. Lu, and V. Bharghavan, "A new model for packet scheduling in multihop wireless networks," in *Proc. ACM MobiCom'00*, 2000.

[20] F. Kelly, "Charging and rate control for elastic traffic," *European Transactions on Telecommunications*, vol. 8, no. 1, pp. 33–37, 1997.

[21] B. Sadeghi, V. Kanodia, A. Sabharwal, and E. W. Knightly, "An opportunistic auto-rate media access protocol for ad hoc networks," *Wireless Networks*, vol. 11, no. 1-2, pp. 39–53, 2005.

[22] G. Tan and J. Guttag, "Time-based fairness improves performance in multi-rate wireless lans," in *Proc. USENIX Annual Technical Conference*, 2004.

[23] L. B. Jiang and S. C. Liew, "Proportional fairness in wireless lans and ad hoc networks," in *Proc. IEEE WCNC'05*, 2005.

[24] T. Bu, L. Li, and R. Ramjee, "Generalized proportional fair scheduling in third generation wireless data networks," in *Proc. IEEE INFOCOM'06*, 2006.

[25] L. Li, M. Pal, and Y. R. Yang, "Proportional fairness in multi-rate wireless lans," in *Proc. IEEE INFOCOM'08*, 2008.

[26] Cisco System Inc, http://www.cisco.com/en/US/prod/collateral/wireless.html, Online Link.

[27] M. Balazinska and P. Castro, "Characterizing mobility and network usage in a corporate wireless local-area network," in *Proc. ACM MOBISYS'03*, 2003.

[28] A. Vasan, R. Ramjee, and T. Woo, "Echos: Enhanced capacity 802.11 hotspots," in *Proc. IEEE INFOCOM'05*, 2005.

[29] A. Balachandran, P. Bahl, and G. M. Voelker, "Hot-spot congestion relief in public-area wireless networks," in *Proc. IEEE WMCSA'02*, 2002.

[30] I. Papanikos and M. Logothetis, "A study on dynamic load balance for ieee 802.11b wireless lan." in *Proc. IEEE COMCON'01*, 2001.

[31] Y. Fukuda, T. Abe, and Y. Oie, "Decentralized access point selection architecture for wireless lans," in *Proc. IEEE VTC'04*, 2004.

[32] Y. Bejerano and S.-J. Han, "Cell breathing techniques for load balancing in wireless lans," in *Proc. IEEE INFOCOM'06*, 2006.

[33] P. Bahl, M. T. Hajiaghayi, K. Jain, V. Mirrokni, L. Qiu, and A. Saberi, "Cell breathing in wireless lans: Algorithms and evaluation," *IEEE Transactions on Mobile Computing*, vol. 6, no. 2, pp. 164–178, 2007.

[34] A. Mishra, V. Brik, S. Banerjee, A. Srinivasan, and W. Arbaugh, "A client-driven approach for channel management in wireless lans," in *Proc. IEEE INFOCOM'06*, 2006.

[35] Y. Bejerano, S.-J. Han, and L. E. Li, "Fairness and load balancing in wireless lans using association control," in *Proc. ACM MobiCom'04*, 2004.

[36] MIT Roofnet, http://pdos.csail.mit.edu/roofnet/doku.php, Online Link.

[37] GaTech Wireless Mesh Networks, http://www.ece.gatech.edu/research/labs/bwn/mesh/index.html, Online Link.

[38] D. Raychaudhuri, I. Seskar, M. Ott, S. Ganu, K. Ramachandran, H. Kremo, R. Siracusa, H. Liu, and M. Singh, "Overview of the orbit radio grid testbed for evaluation of next-generation wireless network protocols," in *Proc. IEEE WCNC'05*, 2005.

[39] Technology For All (TFA) Rice Wireless Mesh Network, http://tfa.rice.edu/, Online Link.

[40] UCSB MeshNet, http://moment.cs.ucsb.edu/meshnet/, Online Link.

[41] MAP - Mesh At Purdue, https://engineering.purdue.edu/MESH, Online Link.

[42] Carleton University Wireless Mesh Networking, http://kunzpc.sce.carleton.ca/MESH/index.htm, Online Link.

[43] J. Robinson, K. Papagiannaki, C. Diot, X. Guo, and L. Krishnamurthy, "Experimenting with a multiradio mesh networking testbed," in *Proc. IEEE WiNMee'05*, 2005.

[44] K. Papagiannaki, M. Yarvis, and W. S. Conner, "Experimental characterization of home wireless networks and design implications," in *Proc. IEEE INFOCOM'06*, 2006.

[45] Microsoft Mesh Networking Academic Resource Toolkit, http://research.microsoft.com/netres/kit/index.htm, Online Link.

[46] V. Nitin, B. Jennifer, V. Veeravalli, R. Kumar, and R. Iyer, "Illinois wireless wind tunnel: a testbed for experimental evaluation of wireless networks," in *Proc. ACM SIGCOMM'05*, 2005.

[47] R. Curtmola and C. Nita-Rotaru, "Bsmr: Byzantine-resilient secure multicast in multi-hop wireless networks," in *Proc. IEEE SECON'07*, 2007.

[48] J. Broch, D. Maltz, D. Johnson, Y. C. Hu, and J. Jetcheva, "A performance comparison of multi-hop wireless ad hoc network routing protocols," in *Proc. ACM MobiCom'98*, 1998.

[49] B. Li, "End-to-end fair bandwidth allocation in multi-hop wireless ad hoc networks," in *Proc. IEEE ICDCS'98*, 1998.

[50] I. Akyildiz, X. Wang, and W. Wang, "Wireless mesh networks: a survey," *Computer Networks*, vol. 47, no. 4, pp. 445–487, 2005.

[51] S. Shakkottai, T. Rappaport, and P. Karlsson, "Cross-layer design for wireless networks," *IEEE Communications Magazine*, vol. 41, no. 2, pp. 17–23, 2003.

[52] Simple Network Management Protocol, http://www.ietf.org/rfc/rfc1157.txt, Online Link.

[53] Cisco Mesh Products, http://www.cisco.com/en/US/netsol/ns703/, Online Link.

[54] Order One Networks Mesh Networking Products, http://www.orderonenetworks.com, Online Link.

[55] A. Jardosh, P.Suwannatat, T. Hollerer, E. Belding, and K. Almeroth, "Scuba: Focus and context for real-time mesh network health diagnosis," in *Proc. IEEE PAM'08*, 2008.

[56] K. N. Ramachandran, E. M. Belding-Royer, and K. C. AImeroth, "Damon: a distributed architecture for monitoring multi-hop mobile networks," in *Proc. IEEE SECON'04*, 2004.

[57] K. N. Ramachandran, "Design, deployment, and management of high-capacity large-scale wireless networks," Ph.D. dissertation, University of California Santa Barbara, 2007.

[58] D. M. N. Scalabrino, R. Riggio and I. Chlamtac, "Janus: A framework for distributed management of wireless mesh networks," in *Proc. IEEE TRIDNC'07*, 2007.

[59] A. Rowstron and P. Druschel, "Pastry: Scalable, distributed object location and routing for largescale peer-to-peer systems," in *Proc. IFIP/ACM ICDSP'01*, 2001.

[60] S. Kaul, M. Gruteser, , and I. Seskar, "Creating wireless multi-hop topologies on space-constrained indoor testbeds through noise injection," in *Proc. IEEE Tridentcom'06*, 2006.

[61] D. B. Johnson, D. A. Maltz, and J. Broch, "Dsr: The dynamic source routing protocol for multi-hop wireless ad hoc networks," *Ad Hoc Networking*, vol. 2, no. 1, pp. 139–172, 2001.

[62] R. de Oliveira and T. Braun, "A smart tcp acknowledgment approach for multihop wireless networks," *IEEE Transactions on Mobile Computing*, vol. 6, no. 2, pp. 192–205, 2007.

[63] I. Sheriff and E. Belding-Royer, "Multipath selection in multi-radio mesh networks," in *Proc. IEEE Broadnets'06*, 2006.

[64] Penton Media Inc., http://www.infosec.co.uk/ExhibitorLibrary/316/WirelessProtectforMobile20.pdf, Online Link.

[65] Aruba Radio, https://airheads.arubanetworks.com/article/aruba-radio-corner-making-sense-rssi, Online Link.

[66] S. Xu and T. Saadawi, "Does the ieee 802.11 mac protocol work well in multihop wireless ad hoc networks?" *IEEE Communications Magazine*, vol. 39, no. 6, pp. 130–137, 2001.

[67] A. R. Nasipuri, J. Zhuang, and S. Das, "A multichannel csma mac protocol for multihop wireless networks," in *Proc. IEEE WCNC'99*, 1999.

[68] M. Gerla, K. Tang, and R. Bagrodia, "Tcp performance in wireless multi-hop networks," in *Proc. IEEE WMCSA'99*, 1999.

[69] G. Xylomenos and G. Polyzos, "Tcp performance issues over wireless links," *IEEE Communications Magazine*, vol. 39, no. 2, pp. 52–58, 2001.

[70] J. Tang, G. Xue, and W. Zhan, "Maximum throughput and fair bandwidth. allocation in multi-channel wireless mesh networks," in *Proc. IEEE INFOCOM'06*, 2006.

[71] J. Tang, G. Xue, and W. Zhang, "Interference-aware topology control and qos routing in multi-channel wireless mesh networks," in *Proc. ACM MobiHoc'05*, 2005.

[72] A. Raniwala, K. Gopalan, and T.-C. Chiueh, "Centralized channel assignment and routing algorithms for multi-channel wireless mesh networks," *SIGMOBILE Mobile Computing and Communications Review*, vol. 8, no. 2, pp. 50–65, 2004.

[73] W.-H. Tam and Y.-C. Tseng, "Joint multi-channel link layer and multi-path routing design for wireless mesh networks," in *Proc. IEEE INFOCOM'07*, 2007.

[74] A. Raniwala and T.-C. Chiueh, "Architecture and algorithms for an ieee 802.11-based multi-channel wireless mesh network," in *Proc. IEEE INFOCOM'05*, 2005.

[75] M. Alicherry, R. Bhatia, and L. Li, "Joint channel assignment and routing for throughput optimization in multi-radio wireless mesh networks," in *Proc. ACM MobiCom'05*, 2005.

[76] M. Kodialam and T. Nandagopal, "Characterizing the capacity region in multi-radio multi-channel wireless mesh networks," in *Proc. ACM MobiCom'05*, 2005.

[77] P. Kyasanur and N. Vaidya, "Capacity of multi-channel wireless networks: Impact of channels and interfaces," in *Proc. ACM MobiCom'05*, 2005.

[78] S. Bandyopadhyay, S. Roy, T. Ueda, and K. Hasuike, "Multipath routing in ad hoc wireless networks with directional antenna," in *Proc. PWC'02*, 2002.

[79] E. Gabrielyan and R. Hersch, "Reliable multi-path routing schemes for real-time streaming," in *Proc. ICDT'06*, 2006.

[80] ILOG CPLEX, http://www.ilog.com/products/cplex/, Online Link.

[81] R. Jain, D. Chiu, and W. Hawe, "A quantitative measure of fairness and discrimination for resource allocation in shared computer systems," DEC-TR-301, Digital Equipment Corporation, Tech. Rep., 1984.